2015

BEDROCK GEOLOGIC MAPPING AND STRUCTURAL ANALYSIS OF THE WESTERN HALF OF THE PETERSHAM QUADRANGLE, CENTRAL MASSACHUSETTS: FURTHER TESTS OF THE MODEL FOR MIDDLE TO LATE PALEOZOIC DUCTILE TRANSPRESSION, VERTICAL EXTRUSION, AND LATERAL ESCAPE IN THE NORTHERN APPALACHIANS

Lucas P. Rohrer
University of Kentucky, lucas.rohrer@caldwell.kyschools.us

STUDENT AGREEMENT:

I represent that my thesis or dissertation and abstract are my original work. Proper attribution has been given to all outside sources. I understand that I am solely responsible for obtaining any needed copyright permissions. I have obtained needed written permission statement(s) from the owner(s) of each third-party copyrighted matter to be included in my work, allowing electronic distribution (if such use is not permitted by the fair use doctrine) which will be submitted to UKnowledge as Additional File.

I hereby grant to The University of Kentucky and its agents the irrevocable, non-exclusive, and royalty-free license to archive and make accessible my work in whole or in part in all forms of media, now or hereafter known. I agree that the document mentioned above may be made available immediately for worldwide access unless an embargo applies.

I retain all other ownership rights to the copyright of my work. I also retain the right to use in future works (such as articles or books) all or part of my work. I understand that I am free to register the copyright to my work.

REVIEW, APPROVAL AND ACCEPTANCE

The document mentioned above has been reviewed and accepted by the student's advisor, on behalf of the advisory committee, and by the Director of Graduate Studies (DGS), on behalf of the program; we verify that this is the final, approved version of the student's thesis including all changes required by the advisory committee. The undersigned agree to abide by the statements above.

Lucas P. Rohrer, Student

Dr. David Moecher, Major Professor

Dr. Edward Woolery, Director of Graduate Studies

BEDROCK GEOLOGIC MAPPING AND STRUCTURAL ANALYSIS OF THE WESTERN HALF OF THE PETERSHAM QUADRANGLE, CENTRAL MASSACHUSETTS: FURTHER TESTS OF THE MODEL FOR MIDDLE TO LATE PALEOZOIC DUCTILE TRANSPRESSION, VERTICAL EXTRUSION, AND LATERAL ESCAPE IN THE NORTHERN APPALACHIANS

THESIS

A thesis submitted in partial fulfillment of the requirements for the degree of Master of Science in the College of Arts and Sciences at the University of Kentucky

by

Lucas Pettit Rohrer

Lexington, KY

Director: David P. Moecher, Professor of Geology

Lexington, KY

2015

ABSTRACT OF THESIS

BEDROCK GEOLOGIC MAPPING AND STRUCTURAL ANALYSIS OF THE WESTERN HALF OF THE PETERSHAM QUADRANGLE, CENTRAL MASSACHUSETTS: FURTHER TESTS OF THE MODEL FOR MIDDLE TO LATE PALEOZOIC DUCTILE TRANSPRESSION, VERTICAL EXTRUSION, AND LATERAL ESCAPE IN THE NORTHERN APPALACHIANS

Bedrock mapping, structural analysis, and geochronology reveal the distribution of lithologies and timing of metamorphism and deformation in the western half of the Petersham 7.5' quadrangle, western Massachusetts. Underlying lithologies are: (from west to east) the Ordovician Monson granitic orthogneiss, Silurian Rangeley migmatitic paragneiss, and Late Devonian (357 Ma) Hardwick tonalitic orthogneiss. Their tightly folded contacts strike north to south. The 361 Ma, unfoliated, strike-parallel Nichewaug quartz-diorite (10-100 m wide) intrusion spans the map area within the Rangeley. Evidence for vertical and lateral extrusion/escape of the Monson orthogneiss, as observed in the Palmer MA area, is absent. Instead, petrofabrics (foliations and lineations) indicate E-W shortening and N-S stretching concentrated within the Rangeley Fm. and orthogneiss margins. Asymmetric structures at the Rangeley-Hardwick contact indicate localized sinistral displacement parallel to unit boundaries and tectonic fabrics. U-Th-Pb chemical age dating of Rangeley monazite revealed three precise age populations (1 = 344 Ma; 3 = 377 Ma; 4 = 405 Ma) and one broad population divided into two subpopulations: 2b (~370 Ma) and 2a (~ 360 Ma). The similarity in age between tonalitic/dioritic magmatism and monazite growth in the Rangeley suggests regional metamorphism was driven by magmatic heat input from latest Devonian/earliest Carboniferous plutonism.

KEYWORDS: New England, Massachusetts, Appalachian, Petersham, transpression, metamorphism

Lucas Pettit Rohrer
November 4, 2015

BEDROCK GEOLOGIC MAPPING AND STRUCTURAL ANALYSIS OF THE WESTERN HALF OF THE PETERSHAM QUADRANGLE, CENTRAL MASSACHUSETTS: FURTHER TESTS OF THE MODEL FOR MIDDLE TO LATE PALEOZOIC DUCTILE TRANSPRESSION, VERTICAL EXTRUSION, AND LATERAL ESCAPE IN THE NORTHERN APPALACHIANS

by

Lucas Pettit Rohrer

David P. Moecher
Director of Thesis

Edward Woolery
Director of Graduate Studies

November 4, 2015

ACKNOWLEDGEMENTS

First I would like to thank my advisor, Dr. Moecher, for his guidance and support on this project. I would not have been able complete a mapping project without his help in the field. I would also like to thank Dr. Matt Massey for being available to answer questions and for completing the bulk of the work that went into processing data and making figures for the geochronology work on the Hardwick tonalite and Nichewaug Sill. Last but not least, I would like to thank my wife, Lilly, for providing unending support and even accompanying me in the field on a few occasions. Funding was provided by USGS EDMAP grant G13AC00100, the Ferm Fund and Brown-McFarlan Fund of the UK Department of Earth and Environmental Sciences, and a student research grant from the Geological Society of America. Mr. Paul Lyons of the Quabbin Reservoir Authority (Massachusetts) provided the means to access the eastern Quabbin Reservation.

TABLE OF CONTENTS

LIST OF FIGURES

CHAPTER I. INTRODUCTION AND PURPOSE

A series of early to late Paleozoic oblique collisions between the modified Laurentian continental margin and various composite arc/microcontinental terranes resulted in widespread dextral transcurrent and compressional tectonics (transpression) throughout east-central New England. These are documented in various places throughout New England from Maine to Connecticut (Swanson, 1999; Solar and Brown, 2001; Growden et al., 2006; Massey and Moecher, 2008b, 2013). In this study, geologic bedrock mapping, structural analysis, and geochronology within the western half of the Petersham quadrangle in central Massachusetts (Fig. 1.1) will be carried out to: (1) to delineate the distribution of lithologic units within the study area, (2) do determine the deformational styles within the map area in the context of regional dextral transpression, (3) to determine the timing of deformation within the map area, and (4) to relate the findings within the study area to those of previous studies in central Massachusetts (especially Massey and Moecher, 2008, 2013).

A. Tectonic History of New England

The distribution of metamorphic isograds (Fig. 1.2) and style of deformation across the New England Appalachians is principally the expression of three orogenic pulses, from earliest to latest: the Taconian, the Acadian, and the Alleghanian (Robinson et al., 1998). Taconian (Middle Ordovician) metamorphism is expressed mostly within the Berkshire-Green Mountain, Rowe-Hawley, Connecticut Valley, and Bronson Hill Terranes (Robinson and Hall 1980; Robinson, 1983) and predates the accretion of the rocks within the area of proposed study (Fig. 1.1) in south-central New England.

From Late Silurian to Middle Devonian time (ca. 423-382 Ma: Robinson et al., 1998), Acadian orogenesis marked the final closure of the Iapetus Ocean (Soper et al., 1992; van Staal, 2006) and the accretion of the composite Avalon microcontinent to the Taconic-modified Laurentian margin. The Acadian deformation front swept ~240 km northwestward across New England over a period of ~50 m.y. (Bradley et al., 2000; Solar and Brown, 2001; Wintsch et al., 2003) as the leading edge of the composite Avalonian Terrane was thrust beneath rocks of the Bronson Hill Arc on the margin of Laurentia (Wintsch et al., 2003). In south-central New England, Acadian metamorphism reached granulite facies (Fig. 1.2) and is associated with extreme shortening and tonalitic to granitic intrusive magmatism (Robinson et al., 1998; Bradley et al., 2000).

The Acadian orogeny is considered the dominant tectonic event in New England (Robinson et al., 1998; Hatcher, 2010). Metamorphic mineral assemblages and fabrics associated with Acadian metamorphism predominate in rocks of the Merrimack, Central Maine, Bronson Hill, Connecticut Valley, and Putnam-Nashoba (Eastern Acadian boundary) Terranes in eastern and central New England (Fig. 1.1: Robinson and Hall 1980; Robinson, 1983; Eusden and Barriero, 1988; Robison, 1998; Moecher, 1999; Wintsch et al., 2003).

The Neo-Acadian orogeny describes Late Devonian to Early Carboniferous (ca. 366-345 Ma) deformation and metamorphism in southern New England (Robinson et al., 1998). Its expression is marked by tonalitic to granitic magmatism and up to granulite facies metamorphism that is most intense in central Massachusetts and Connecticut (Robinson et al., 1998). Neo-Acadian orogenesis is correlated with dextral-oblique

accretion of the Meguma terrane to Laurentia, an event that was much more significant in Canada (van Staal, 2006).

The subsequent collision of Gondwana with Laurentia to form Pangea was accompanied by Alleghanian orogenesis, which is characterized by up to sillimanite grade metamorphism ranging in age from Late Pennsylvanian to Early Permian (Robinson et al., 1998; Wintsch et al., 2003; van Staal, 2006). Though Alleghanian metamorphism was originally thought to be constrained mostly to the more southeasterly Avalon Composite Terrane, studies such as those by Moecher et al. (1997), Robinson et al. (1998), Moecher (1999), and Wintsch et al. (2003) have identified Alleghanian metamorphism as far west as the southern Connecticut Valley terrane in Connecticut.

Avalon's approach from the southeast caused Late Silurian compressional and initial sinistral transcurrent tectonics. Soon afterward, a shift in plate motion caused dextral transcurrent tectonics to prevail from Early Devonian through the Carboniferous, likely resulting (indirectly) from the approach of northward drifting Gondwana (Soper et al., 1992; Holdsworth, 1994). Since the later Neoacadian and Alleghanian orogenic events also involved dextral oblique collisions, the resulting metamorphism and deformation would have amplified pre-existing Acadian structures (Massey and Moecher, 2008b). Though evidence for orogen parallel, dextral transpressive and transcurrent tectonics is documented in various places throughout New England from Maine to Connecticut (Swanson, 1999; Solar and Brown, 2001; Growden et al., 2006, Massey and Moecher, 2008b), the extent, distribution, and mechanisms still require assessment (Massey and Moecher, 2008).

The goal of this study is to (1) to delineate the distribution of lithologic units within the study area, (2) to assess the significance of dominant fabrics and structures in the study area in the context of regional dextral transpression, (3) to determine the timing of deformation within the map area, and (4) to relate the findings within the study area to those of previous studies in central Massachusetts (especially Massey and Moecher, 2008, 2013).

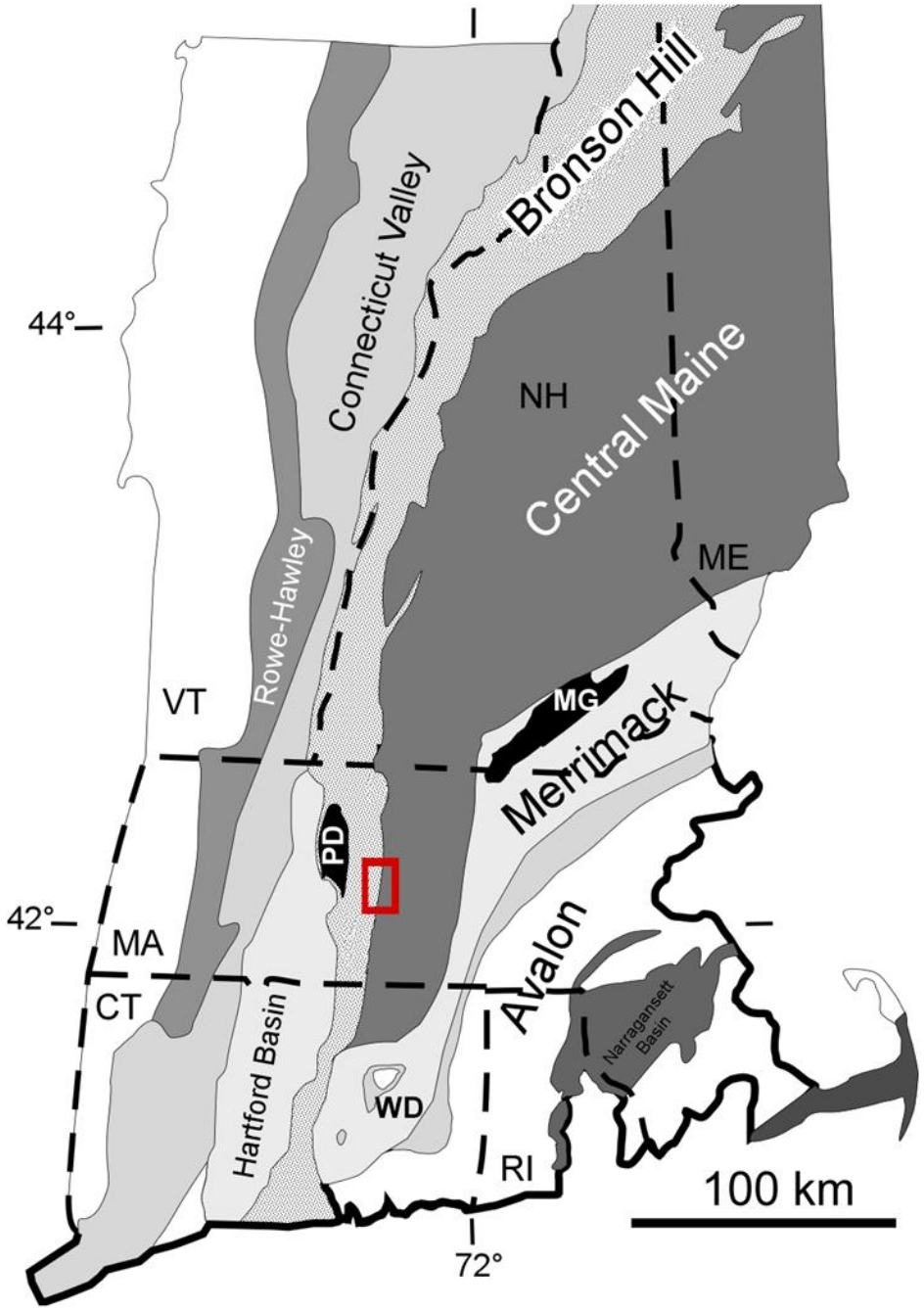

Figure 1.1: Map of central New England with lithotectonic zones. The Petersham quadrangle is outlined in red. Figure after Moecher (1999).

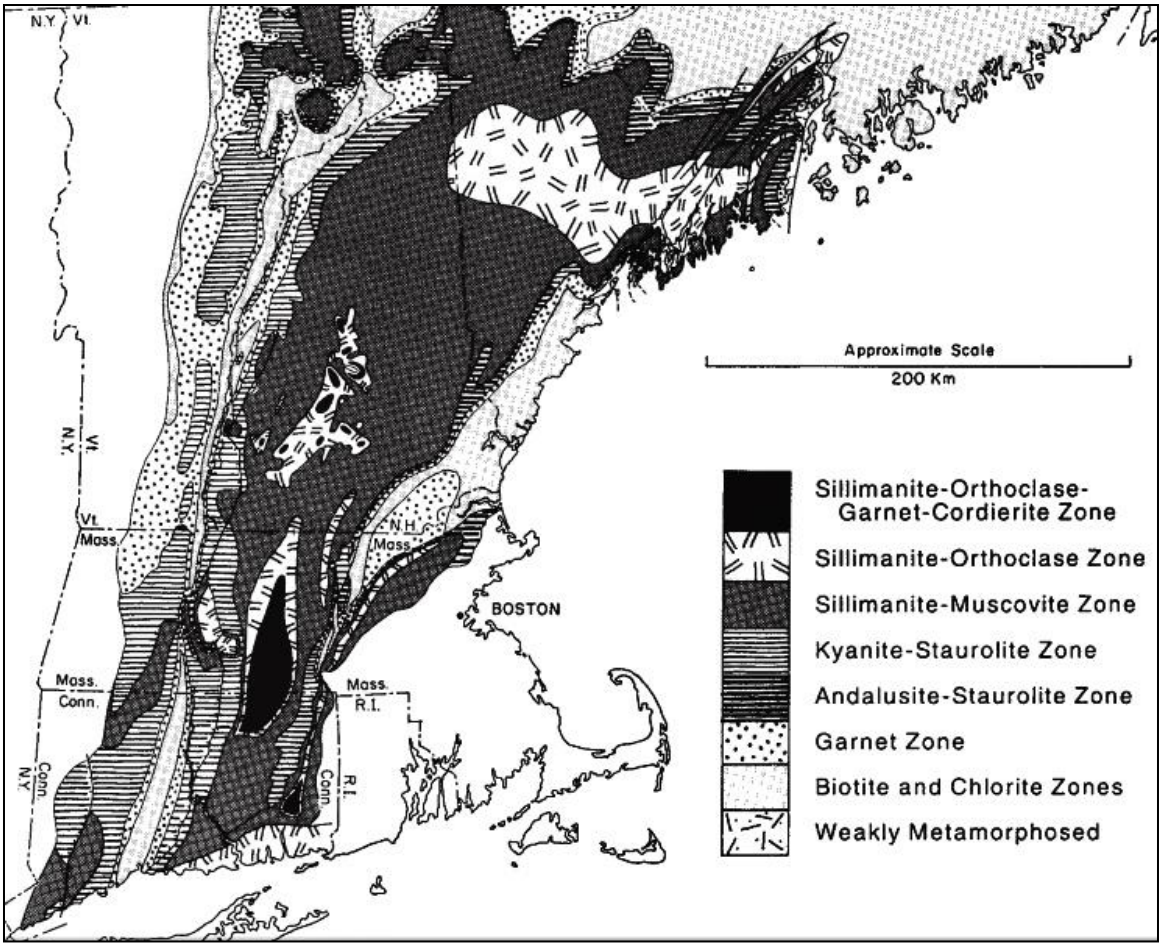

Figure 1.2. Map of south-central New England showing the distribution "Acadian" metamorphic intensities (modified from Robinson et al., 1998).

CHAPTER II. GEOLOGIC SETTING

The study area for this thesis (Fig. 1.1) is the western half of the Petersham 7.5-minute quadrangle in central Massachusetts. This area straddles two major lithotectonic zones in the internides of the New England Appalachian orogen: the Bronson Hill and Central Maine zones. In south-central Massachusetts, this boundary region is comprised of a dextral, reverse (top to east), ductile high strain zone named the Conant Brook Shear Zone (Peterson, 1992b; Peterson and Robinson, 1993), which correlates with the proposed Brennan Hill thrust to the north (Robinson and Elbert, 1992) and the Bonemill Brook ductile high strain zone to the south in Connecticut (Pease, 1982).

Within the field area, competency contrasts between metaplutonic and metasedimentary lithologic units at lithologic boundaries control the expression of the major dextral transpression regime that is the northern Appalachians. These boundaries are the north-south striking contacts between the Monson orthogneiss, Rangeley Formation, and Hardwick orthogneiss, listed as they occur from west to east. Furthermore, the rheological contrast between granitic orthogneisses and metasedimentary rocks provides structural anisotropies that result in local and regional variations in three-dimensional deformational patterns (Massey and Moecher, 2013).

The Petersham quadrangle in central MA (Fig. 1.1) has been selected for this study because of its strategic location. The fact that it is both superimposed over the aforementioned lithologic and tectonic interfaces and positioned along strike of the recently discovered zone of partitioned transpression, extrusion, and lateral escape of Massey and Moecher (2013) gives the study area an added significance. Bedrock mapping, structural analysis, and geochronologic age determinations will provide

valuable spatial and temporal information concerning the northward (along strike) continuation/evolution of the deformation zone of Massey and Moecher (2013). This should in turn provide a broader understanding of regional scale deformational patterns that occurred among contrasting rheologies at the terrane boundary.

A. The Bronson Hill Zone (BHZ)

The Bronson Hill zone (BHZ: Fig. 1.1) is a north-trending belt of approximately 20 ellipsoidal to elongate structural domes that stretches from northern New Hampshire to Long Island Sound (Hollocher et al., 2002). In the cores of these domes are gneisses of the late Ordovician "Oliverian Magma Series" of Billings (1937), who named individual domes by geography (e.g. Monson dome; Leo, 1991; Hollocher et al., 2002).

These dome gneisses are interpreted as the metamorphosed plutonic roots (a composite batholith) of a late Taconian volcanic arc (e.g., Thompson et al., 1968; Chapple, 1973; Osberg, 1978; Robinson and Hall, 1980; Rowley and Kidd, 1981; Hall and Robinson, 1982; Lyons et al., 1982; Stanley and Ratcliffe, 1985; Leo, 1991; Hollocher et al., 2002). Evidence supporting this interpretation includes: (1) the narrow, elongate map pattern of the BHZ, (2) the geochemical island arc affinity of the dome gneisses and mantling volcanics (Leo, 1991; Hollocher et al., 2002) (3) the middle to late Ordovician (Taconian) ages of the dome gneisses and mantling volcanics (Tucker and Robinson, 1990; Moench et al., 1995); and (4) the position of the BHZ east of and parallel to the axes of the Taconian foreland basins and deformation belt in western New England (Hollocher et al., 2002).

Varied compositions among the gneisses suggest that they were produced from a variety of source rocks (Leo, 1991; Hollocher et al., 2002). Dome gneisses north of and including the Mascoma dome are typically homogeneous, calc-alkaline, and predominantly granitic. These were derived from an intermediate or felsic, igneous crustal source rock, probably the remains of older continental crust on which this portion of the arc was built (Tucker and Robinson, 1990; Leo, 1991; Moench and Aleinikoff, 2003). The dome gneisses farther south (e.g. Monson, Fourmile, and Swanzey gneisses) are the compositionally layered, tonalitic to granodioritic, quartz-plagioclase gneisses of Thompson et al. (1968). These gneisses were derived from more mafic (predominantly basaltic) crustal source (Leo, 1991), suggesting that the southern portion of the arc was built on oceanic crust.

Zartman and Leo (1985) assigned the BHZ dome gneisses a group age of 444 ± 8 Ma based on U-Pb ID-TIMS zircon dates from several domes. More precise zircon ages reported by Tucker and Robinson (1990) for dome gneisses in the central BHZ (Pelham, Monson, Warwick, and Keene domes) range from 454 ± 3 to 442 ± 2 Ma. Moench et al. (1995) report the ages of several dome gneisses in northern New Hampshire (northern BHZ) that range from 456 ± 3 to 441 ± 5 Ma.

Taconian orogenesis spanned tens of millions of years causing extensive metamorphism and contraction of Laurentian basement and sedimentary cover during collision (e.g., Rowley and Kidd, 1981; Stanley and Ratcliffe, 1985; Sutter et al., 1985; Drake et al., 1989; Tremblay, 1992; Cawood et al., 1995). Radiometric and biostratigraphic constraints indicate that advancement of the Taconian composite arc onto Laurentia ceased between latest Ordovician and earliest Silurian (449 Ma and 443 Ma).

This puts emplacement of the BHZ dome gneisses (456–441 Ma) toward the end of subduction, making them the youngest igneous rocks of the Taconian arc proper (Hollocher et al., 2002).

The Bronson Hill dome gneisses are mantled by a structural/stratigraphic sequence of metavolcanic and metasedimentary units described by Billings (1937, 1956), Robinson (1967), and Thompson et al. (1968). These include, from structurally and stratigraphically lowest to highest: the Ordovician Ammonoosuc tholeitic to mostly calc-alkaline volcanics, Silurian Partridge sulfidic pelitic schist and felsic volcanics, Clough quartzite, and Devonian Littleton Fm. pelitic schist and metapsammite (Leo, 1991; Massey and Moecher, 2013).

Widely varying interpretations concerning the contact between the Ammonoosuc volcanics with the underlying dome gneisses claim that it is unconformable (Robinson, 1979; Schumacher, 1988), intrusive (Leo et al., 1984; Leo, 1985, 1991), or a fault (Robinson and Tucker, 1996; Kohn and Spear, 1999). The dome gneisses are juxtaposed against rocks of the Central Maine zone (CMZ). In western Massachusetts, the Monson gneiss of the Monson dome (Fig. 2.1) is in direct contact with rocks of the CMZ that constitute the Conant Brook shear zone (CBSZ).

B. The Central Maine Zone (CMZ)

The Central Maine zone (Fig. 1.1), originally the Merrimack synclinorium of Billings (1956), is an extensive middle Paleozoic depositional basin in the internides of New England, Quebec, and New Brunswick (Williams, 1978; Rankin, 1994; Rankin et al., 2007) that resulted from a period of extension following the Taconian orogeny (van

Staal and de Roo, 1995; Karabinos, 1998; Bourque et al, 2000; Moench andAleinikoff, 2002; Tremblay and Pinet, 2005; Rankin et al., 2007**)**. The CMZ strikes northeast from Connecticut to Maine and is bounded by the Bronson Hill zone to the west and the Norumbega-Nonesuch River fault zone to the east (Lyons et al., 1982 in Dykstra et al., 1987).

Circa 20 m.y. after Taconian subduction was complete, continental collision between the irregular margins of Laurentia and the composite Avalon terrane continued in Newfoundland (Rankin et al., 2007). This resulted in an episode of crustal extension in New England to the south (Pinet, 2005, in Rankin, 2007), most likely caused by hinge retreat of a northwest-directed Brunswick subduction complex in the late Llandovery ca. 444-428 Ma (van Staal and de Roo1995, Van Staal et al., 1998, Van Staal et al., 2003; Rankin et al., 2007). Subsequent lithospheric delamination would have resulted in upwelling of hot asthenospheric mantle, producing partial melting of the crust, Silurian magmatism, and continued (thermally driven) crustal extension (van Staal and de Roo, 2005; Rankin et al, 2007).

While the Central Maine basin was forming, the Bronson Hill arc was a topographic high (Hibbard et al., 2006). Sedimentation began in the western CMZ in the Llandovery (Moench and Pankiwsky, 1988) as sediment from the Taconic highlands of New England was shed eastward into the CMZ basin (Zen (1991) in Rankin et al., 2007; Moench and Pankiwskj, 1988; Hanson et al., 1993).

Sediments within the CMZ constitute a single stratigraphic package that begins near the Bronson Hill Arc with Early Silurian clastic wedges of the Rangeley Formation (Eusden et al., 1987). The sediments transition eastward into more distal, turbiditic shales

and quartz wackes until they are cut off by the Nonesuch River Fault (Hatch al., 1983; Eusden et al., 1987). This transition represents a shift in depositional environment from continental shelf to slope, a stratigraphic pattern that persists through the Silurian (Eusden et al., 1987; Osberg, 1988; Rankin et al., 2007). Devonian rocks in the upper part of the section may originate from an easterly-derived source (Hanson and Sauchuk, 1986; Eusden et al., 1987). Sediments filling the Central Maine basin are collectively named the Rangeley, Maine section (Moench and Boudette, 1970; Nielson, 1981; Hatch et al., 1983; Thompson, 1983, 1984; Chamberlain, 1984; Moench et al., 1984; Moench, 1984; Eusden et al., 1984 in Eusden et al., 1987), which includes (from oldest to youngest) the Silurian Rangeley, Perry Mountain, Smalls Falls, and Madrid Formations and the Devonian Littleton Formation (Eusden et al., 1987).

C. The Hardwick Pluton

The Hardwick Tonalite (originally interpreted as a southern extension of the Acadian New Hampshire Plutonic Series of Billings, 1956) is the largest pluton in Massachusetts, intruding the Silurian and Devonian clastic sedimentary rocks that filled the CMZ basin (Shearer, 1983). The Hardwick pluton is situated in the Acadian metamorphic high, where it forms an irregular, west-dipping, purportedly syntectonic sheet that strikes north-south extending from the Mt. Monadnock 15-minute quadrangle in New Hampshire into south-central Massachusetts (Shearer, 1983). Robinson et al. (1998) reported U-Pb ID-TIMS zircon ages for the Hardwick tonalite of 360 ± 1 Ma (hornblende tonalite) and 361 ± 2 Ma (microcline porphyry). U-Pb SIMS ages on zircon

for samples of the Hardwick taken in this study yielded a weighted mean age of 357 ± 4 Ma (see geochonology section below).

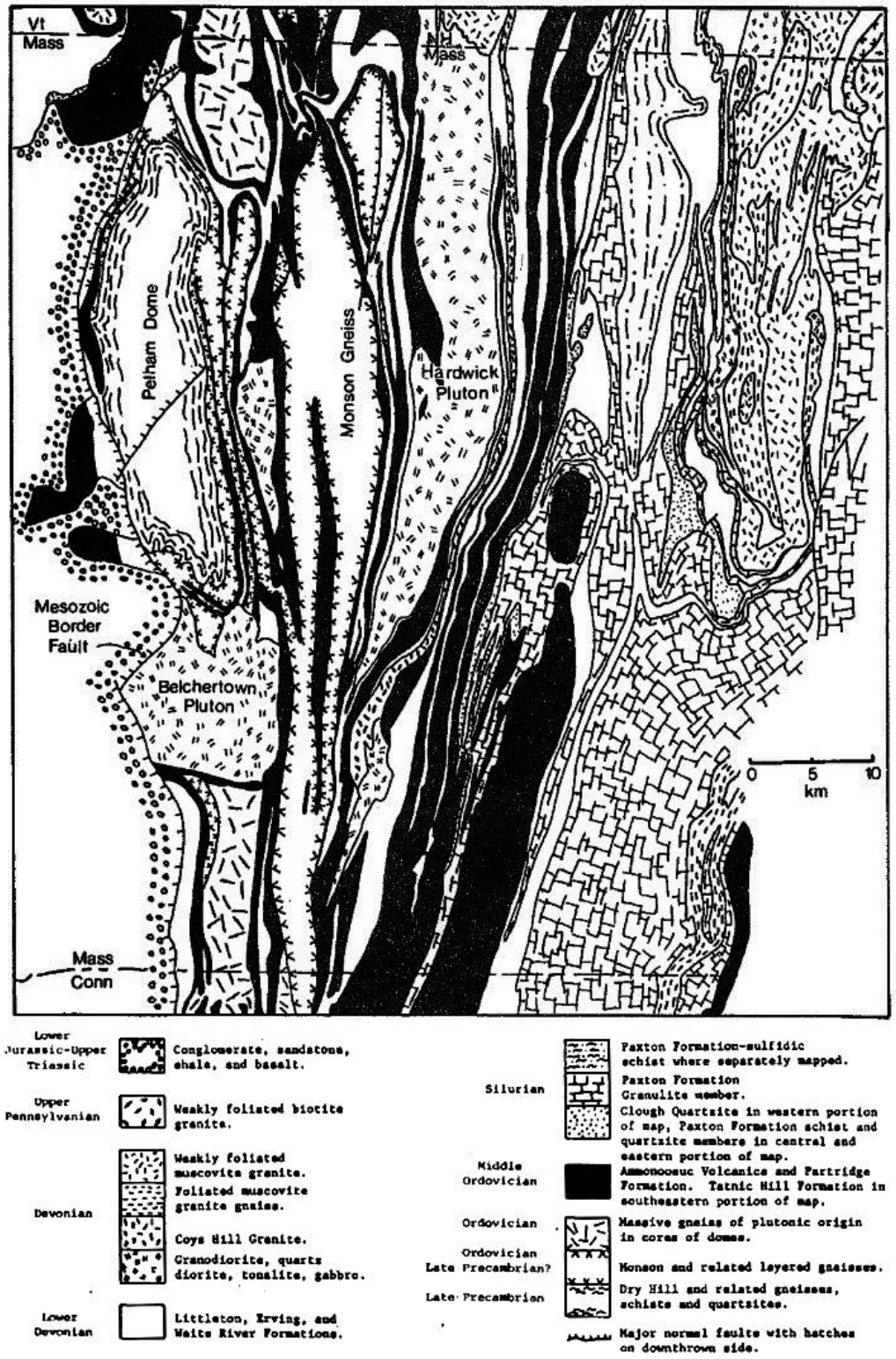

Figure 2.1. Map of central Massachusetts from Shearer (1983) showing major plutons and stratigraphic units. Map shows original interpretation in which sedimentary rocks east of the Monson gneiss are mapped as members of the Bronson Hill arc stratigraphic sequence. These rocks are now mapped as part of the Rangeley Maine sequence.

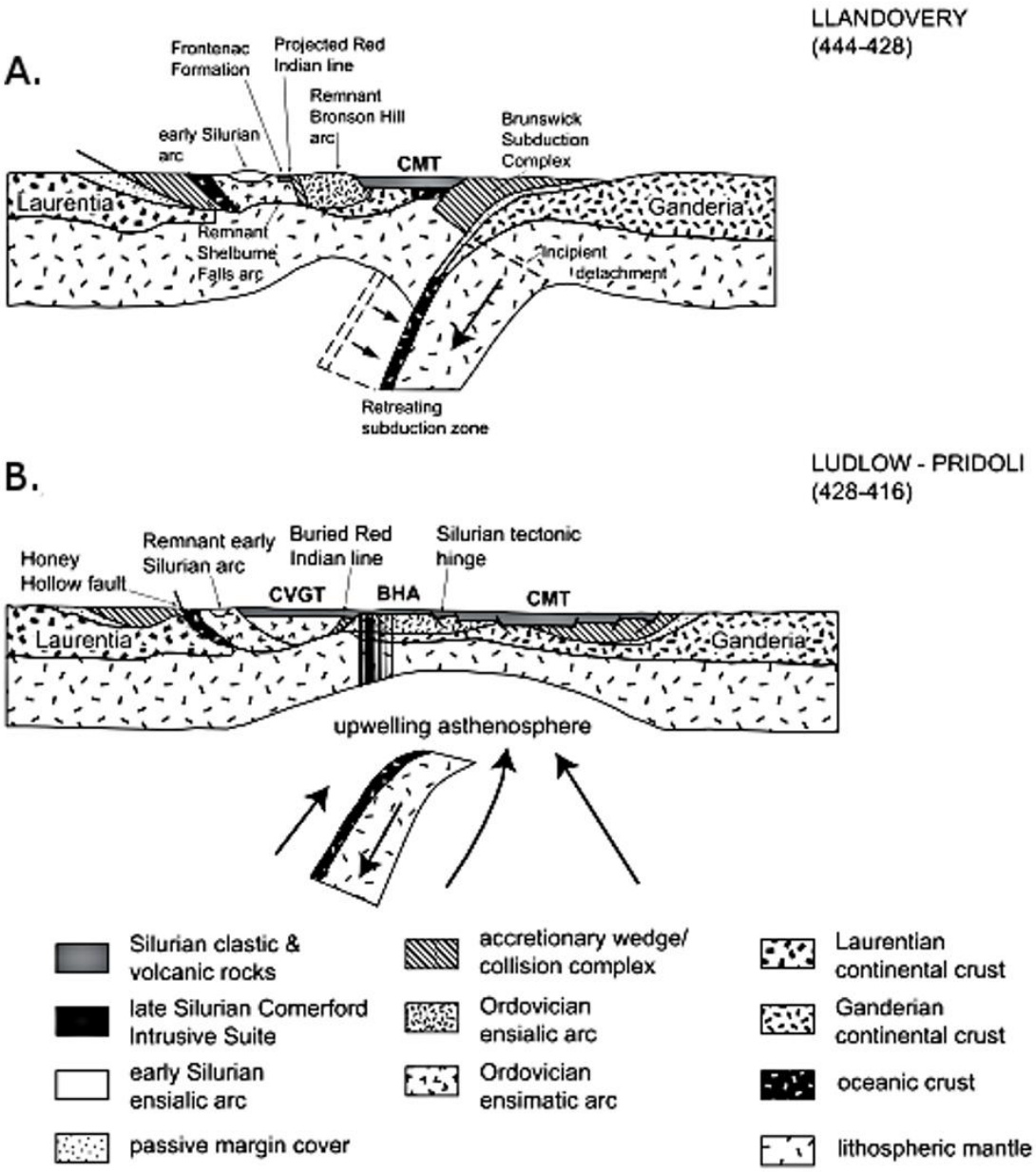

Figure 2.2. A tectonic reconstruction depicting Silurian extension resulting from hinge retreat of the Brunswick Subduction Complex. B. Extension leads to formation of the Central Main trough, which was filled with sediment from the weathering of the Taconian highlands. Modified from Rankin et al. (2007).

CHAPTER III. TRANSPRESSION

The term transpression is used to describe the combination of non-coaxial and coaxial strains resulting from the incomplete segregation of ideal simple shear and pure shear end member components in obliquely convergent domains (Holdsworth et al., 2002). Oblique convergence of tectonic plates/blocks is defined by a non-orthogonal angle (α) between the horizontal far-field plate/block motion vectors and the orientation of the boundary or deformation zone that exists between them (Tikoff and Teyssier, 1994; Dewey et al., 1998). Dewey et al. (1998) define transpression as *"strike-slip deformations that deviate from simple shear because of a component of shortening orthogonal to the deformation zone".* All transpression zones are three-dimensional and contain non-coaxial strains and they are often vertical or steeply dipping (Dewey et al., 1998). Transpression may occur on a wide variety of scales and in a number of tectonic settings including oblique continental plate convergence, oblique subduction margins, restraining bends of transform and other strike-slip displacement zones, slate belts, or in any curvilinear or irregular zone of compression (Dewey, 1975; Dewey et al., 1998).

A. Transpression Models

Theoretical strain models (e.g. Ramberg, 1975; Sanderson and Marchini, 1984; Fossen and Tikoff, 1993; Tikoff and Teyssier, 1994; Dias and Ribeiro, 1994; Robin and Cruden, 1994; and Jones et al., 1997) based on either finite and incremental strain or strain rate have proven to be an important tool for the analysis of three-dimensional, transpressional deformation zones. Traditionally, stress has been considered the primary controlling factor of crustal deformation (Dewey et al., 1998). Numerical analysis of

transpression zones has, however, demonstrated that strain, compelled by boundary conditions, controls the development of most geological structures during deformation of the crustal lithosphere (e.g. Molnar 1992; Tikoff and Teyssier, 1994, Dewey et al., 1998). Consequently, the relationship between large-scale deformation structures and stress is indirect (Dewey et al., 1998).

The first and most basic model (Fig. 3.1) of Sanderson and Marchini (1984) and other similar early models (e.g. Fossen and Tikoff, 1993) describe a constant volume, vertical zone of homogeneous, orthogonal horizontal shortening and vertical stretch. Subsequent models (Fig. 3.1) have included modifications that add levels of complexity and more closely represent a broader range of naturally occurring examples of transpression. In doing so, these models lack requirements for ideal, and somewhat unrealistic, boundary conditions (e.g., Robin and Cruden, 1994; Dutton, 1997; Jiang and Williams, 1998; Jones and Holdsworth, 1998; Lin et al., 1998; Jiang et al., 2001; Jones et al., 2004; Jiang, 2007; Fernandez and Diaz-Azpiroz, 2009). Such models accommodate volume change (Fossen and Tikoff, 1993), lateral extrusion (Fig. 1c; Dias and Ribeiro, 1994; Jones et al., 1997), and oblique simple shear (Robin and Cruden, 1994; Jones et al, 1997).

Models of transpression accompanied with strain partitioning, have the potential to support the contemporaneous formation of geologic structures, previously thought to have formed at different times in changing stress regimes (Massey and Moecher, 2013). While numerical and analogue modeling have enhanced our understanding of the evolution of natural processes, mapping and structural analyses are still necessary in order to constrain boundary conditions and direct future exploration. Furthermore, as

considerable effort is being spent on the development of transpression models (e.g. Holdsworth et al., 1998 and references therein; Czeck and Hudleston, 2003; Giorgis et al., 2005; Sullivan and Law, 2007), it has become progressively more important to test their validity with natural examples observed in the field.

B. Strain Types

A Flinn Diagram (Fig. 3.2: Dewey et al., 1998) representing finite strains and strain paths for the basic constant volume, vertical stretch model of Sanderson and Marchini (1984) illustrate that transpression generates flattening ($k < 1$) bulk strains, while transtension generates constrictional bulk strains. This is also the case for constant volume deformation zones that incorporate lateral extrusion, oblique simple shear, or heterogeneous transpression (Dewey et al., 1998). However, where there is a component of lateral stretch and vertical shortening or volume loss, it is possible to generate constrictional (prolate) strains in zones of transpression (Fossen and Tikoff, 1993; Dias and Ribiero, 1994).

C. Strain partitioning

Crustal deformation in convergent domains is inherently three-dimensional due to the curved nature of Earth's surface (Dewey et al., 1998). A number of features, including orogenic thickening and strike-slip faults, anastomosing shear zones, and porphyroblast-matrix relationships, demonstrate that deformation partitioning is a ubiquitous, fundamental, and scale-independent process for accommodating three-

dimensional deformation (Bell, 1981; Massey and Moecher, 2013 and references therein).

In continental orogens, strain is generally concentrated in complex zones of high strain (ductile) or displacement (brittle) bounding more resistant, less deformed blocks on various scales (Dewey et al., 1998). A plastic rheological model demonstrates that partitioning of strains into thrust and strike-slip components is stronger at lower angles of convergence, especially at < 20° (Tikoff and Teyssier 1994; Teyssier et al., 1995). Hamilton's Principle, which states that a system chooses a configuration that minimizes work done by the system, determines whether strain is partitioned in a particular system, and if so, in what way it is partitioned (Dewey et al., 1998).

D. Lateral Extrusion and Escape

All models of transpression accommodate shortening across the deforming zone by the extrusion (stretch) of material outside of the zone's boundaries (Massey and Moecher, 2013). In most models, extrusion is vertical (e.g., Sanderson and Marchini, 1984), but models have been proposed that incorporate both lateral (Dias and Ribeiro, 1994; Jones et al., 1997) and non-vertical (Czeck and Hudleston, 2003, 2004; Fernandez and Diaz-Azpiroz, 2009) extrusion. Lateral extrusion is a horizontal, along-strike mass movement of material toward the end (or ends) of the deformation zone relative to the zone margins (Jones et al., 1997). Heterogeneous extrusion can be boundary wall compatible if a strain gradient exists across the deformation zone. In this case, extrusion volume will be much smaller. Homogeneous lateral extrusion requires slippage along zone margins, which varies along strike (Dewey et al., 1998). The term "escape" is used

when this latter type of extrusion is accommodated predominantly by slip along less competent bounding zones (e.g. Massey and Moecher, 2013).

In the upper crust, strain compatibility problems are resolved by altering Earth's free surface (vertical extrusion). In the middle crust where no free surface is available, or in any transpression zone where extrusion is non-vertical, compatibility problems at the ends of the zone must be resolved by the creation of space (Ramsay and Graham, 1970; Harland, 1971; Ramsay and Huber, 1987; Dewey et al., 1998; Hudleston, 1999). Due to this and other kinematic requirements, lateral extrusion is unlikely at the plate-boundary scale. Nonetheless, it is possible in some transpressional settings at smaller scales where geometric and mechanical boundary conditions and internal rheologies are favorable (Dewey et al., 1998).

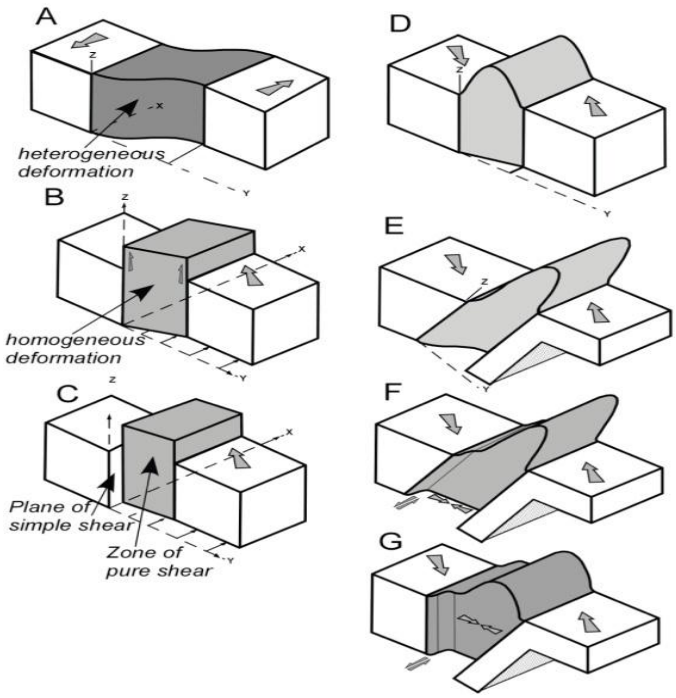

Figure 3.1. Block diagrams for models of transpression from Sanderson and Marchini (1984), Jones and Tanner (1995), and Jones et al. (2005); compiled by Massey and Moecher (2008b).

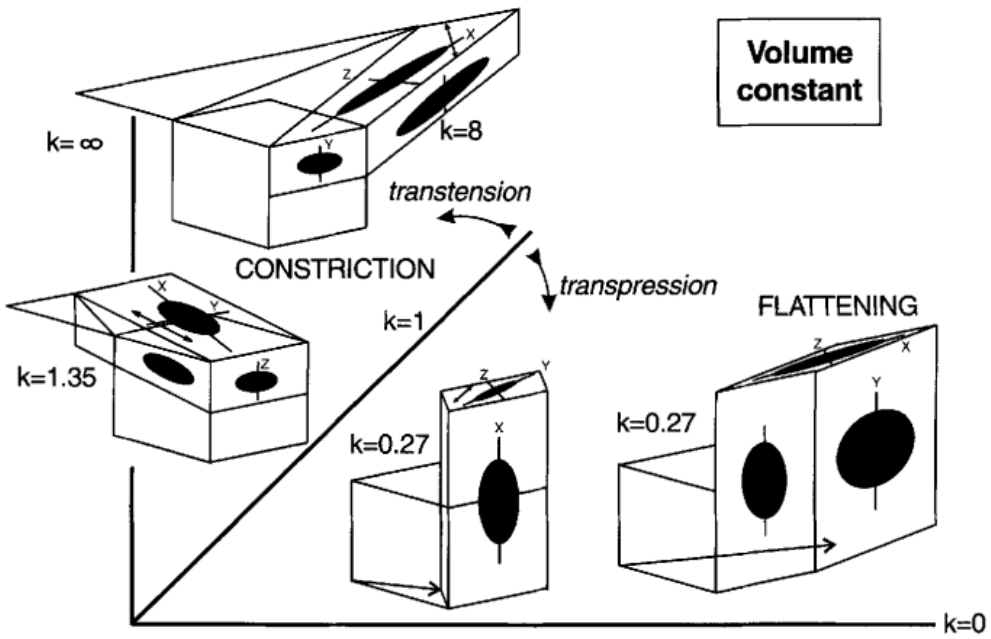

Figure 3.2. Flinn diagram showing finite strains and strain paths using the basic transpression model of Sanderson and Marchini (1984), which demonstrate transpressional flattening and transtensional constriction. Double-headed arrows show incremental stretching directions (modified from Dewey et al., 1998).

CHAPTER IV. PREVIOUS WORK

A. Zen et al. (1983)

The Massachusetts Bedrock Geologic Map (Zen et al., 1983) summarizes the geology of the Petersham quadrangle at 1:250,000 scale (Fig. 4.1). Revealed are three main lithologic units striking N-S, which are described from west to east. The Monson orthogneiss (Omo) of the Bronson Hill zone is a ca. 443-454 Ma (Tucker and Robinson, 1990), highly attenuated pluton(s) representing a portion of the north-northeast trending Bronson Hill Zone (BHZ)—proposed to be the exposed roots of a Late Ordivician, Taconian volcanic arc (Hollacher et al., 2002). The Rangeley formation (Sr) is a Silurian aged metapelitic, porphyroclastic, leucosome- and pegmatite-rich pargneiss. It is a high-grade analog of the sedimentary sequence that filled the CMZ basin (Massey and Moecher, 2008b). The Hardwick Tonalite (Dh) is a ca. 360 Ma (Tucker and Robinson, 1995) pluton that intruded the stratigraphic sequence of the CMZ in the Devonian. The general strike of all contacts is approximately north-south.

Rocks in many parts of the CMZ were originally mapped as the Ordovician Partridge and Devonian Littleton formations (e.g. Zen et al., 1983). These rocks have since been subdivided by Eusden and others (1984) into five lithostratigraphic units (S1, S2, S3, S4, and D4) and correlated with the Rangeley, Maine section (Moench and Boudette, 1970; Nielson, 1981; Hatch et al., 1983; Thompson, 1983, 1984; Chamberlain, 1984; Moench et al., 1984; Moench, 1984; Eusden et al., 1984). In this study, rocks that were previously mapped as the Partridge and Littleton formations are now considered to be part of the Rangeley formation.

B. Hall and Robinson (1982)

Thompson (1954) introduced the first deformational model for southern New England based on an interpretation of stratigraphic relationships in the Skitchewaug Mountain area of southeastern New Hampshire (see also: Thompson, 1956). This model, initially composed of a single massive recumbent fold nappe, was developed into the Alpine-inspired nappe-backfold-dome stage model of Hall and Robinson (1982). This model eventually included four massive fold nappes spanning the area from central Vermont and New Hampshire to southern Massachusetts (Robinson et al., 1991) and three separate deformational stages— nappe, backfold, and dome—in order to explain the spatial arrangement of lithotectonic units across southern New England and into Massachusetts (Hall and Robinson, 1982). Figure 4.2 is a cross-section showing a geologic interpretation across central MA based on the nappe-backfold-dome stage model.

C. Peterson (1992, 1993), Peterson and Robinson (1993)

Peterson (1992a) conducted a mapping and structural study of portions of the Palmer, Monson, Warren, and Wales quadrangles (Massachusetts-Connecticut) that straddle the boundary between rocks of the Bronson Hill (Monson orthogneiss) and Central Maine (Rangeley Fm.) zones. The results describe a dextral, reverse (top to east), ductile high strain zone denoted the Conant Brook Shear Zone (Peterson, 1992b; Peterson and Robinson, 1993), which correlates with the proposed pre-metamorphic Brennan Hill thrust to the north (Robinson and Elbert, 1992). Within this zone, two mineral lineations defined by quartz, feldspar, and sillimanite are present within the same outcrops and

foliation surfaces. The two lineations are indistinguishable other than by orientation; one is steep and west-plunging while the other is shallow and plunges shallowly to the SSW (Peterson 1992b, Peterson and Robinson, 1993). Peterson and Robinson (1993) explained the presence of these lineations within the context of the nappe-backfold-dome stage model, wherein the shallow SSW-plunging lineation is correlated with orogen-parallel transport during the dome-stage, and the steep west-plunging lineation is correlated with backfold-stage deformation. Therefore, as interpreted by the nappe-backfold-dome stage model, the formation of these two lineations was partitioned temporally between two separate deformational stages.

D. Massey and Moecher (2008, 2013), Massey (2010)

An alternative interpretation of the deformational style and history of southern New England was prompted by evidence documented from 1:24,000 scale mapping (Massey and Moecher, 2008) and structural analysis of the Palmer quadrangle and surrounding areas in central MA. The fabrics observed record a range of apparent finite strains with contrasting kinematics. Petrographic evidence, however, indicates coeval development (Massey and Moecher, 2013). The observed fabrics and structures led to the development of a new tectonic model for Late Paleozoic (360 to 300 Ma) deformation within the Palmer area. This model proposes a north-south striking zone of mid-crustal, coeval, partitioned dextral transpression, vertical extrusion, and north-directed lateral escape (Massey and Moecher, 2008; Massey and Moecher, 2013) between the obliquely converging Bronson Hill and Central Maine zones.

In the resulting model (Fig. 4.3: Massey and Moecher, 2013), shortening is accommodated within a relatively broad, subvertical slab of granitic Monson orthogneiss which constitutes a central zone of transpression and vertical extrusion (Massey and Moecher, 2006; Moecher and Massey 2007). In the Palmer area, the Monson is characteristically a steeply dipping S>L tectonite with strongly planar foliations, mineral stretching lineations subparallel to dip, zones of mylonite, closed to isoclinal folds, and dextral/reverse kinematics (Massey and Moecher, 2013). Vertical extrusion and lateral (northward) escape of the Monson was accommodated by a conjugate pair of relatively thin bounding zones of metastratified rocks, the Conant Brook shear zone (CBSZ) and Mount Dumplin high strain zone (MDHSZ), into which transcurrent motion was partitioned (Massey and Moecher, 2013). Kinematics in the CBSZ are dextral and reverse while those in the MDHSZ are sinistral and normal. In the Palmer area, the east-bounding CBSZ typically bears a steeply dipping mylonitic foliation and bimodal, foliation-parallel lineation (Massey and Moecher, 2013). The MDHSZ bears similarly steep dipping mylonitic foliations, but lineations tend to be only subhorizontal. Although the kinematics of the MDHSZ are somewhat unexpected in a dextral transpressional context, structural relationships and geochronology tie them in with the local deformational system (Massey and Moecher, 2013).

The zone of transpression and bounding zones of high strain were further divided into structural subdomains that can be more adequately simulated by pre-existing models (Massey and Moecher, 2013). Scale dependent mechanisms of strain partitioning are responsible for both the deformation pattern observed in the Palmer area and for resolving compatibility problems between the different deformational domains and

subdomains. At the regional to outcrop scale, partitioning results from rheological contrasts between lithologies. Coaxial strains are partitioned into orthogneiss bodies while noncoaxial strain is partitioned into well-foliated metastratified rocks (Massey and Moecher, 2013). At smaller scales, partitioning results from complex processes associated with maintaining compatibility between adjacent structures and subdomains which are inherent to simultaneous vertical extrusion and lateral escape at depth (Massey and Moecher, 2013).

Evidence for simultaneous lateral escape and vertical extrusion of the Monson Orthogneiss and opposite shear sense of the bounding zones of high strain includes the orientation and distribution of foliations and mineral lineations, asymmetric fabrics and folds, other kinematic indicators, and the absence of overprinting relationships (Massey and Moecher, 2008b, 2013). Massey and Moecher (2008b) identified the same lineations described by Peterson and Robinson (1993), but interpreted the two lineations as having formed contemporaneously due to strain partitioning, an interpretation that is simpler and more probable since it does not require two separate deformational stages of the exact same metamorphic grade showing ambiguous overprinting relationships.

Current evidence suggests the zone of transpression extends $\geq$ 10 km eastward into the Central Maine zone (Walker, 2011), southward into central Connecticut, and northward possibly as far as southern New Hampshire (Massey and Moecher, 2008b; O'Brien, 2009). Geochronologic constraints indicate that this episode of regional transpression, extrusion, and escape persisted from at least 360 to 300 Ma (Massey and Moecher, 2013; Massey pers. comm. 2015). Mapping and structural analysis in adjacent areas is required in order to determine the spatial extent and evolution of the deforming

zone along strike to the north and south. Furthermore, additional geochronology is necessary in order to establish basic assumptions of timing throughout the system. These issues are partially addressed by the findings of this thesis.

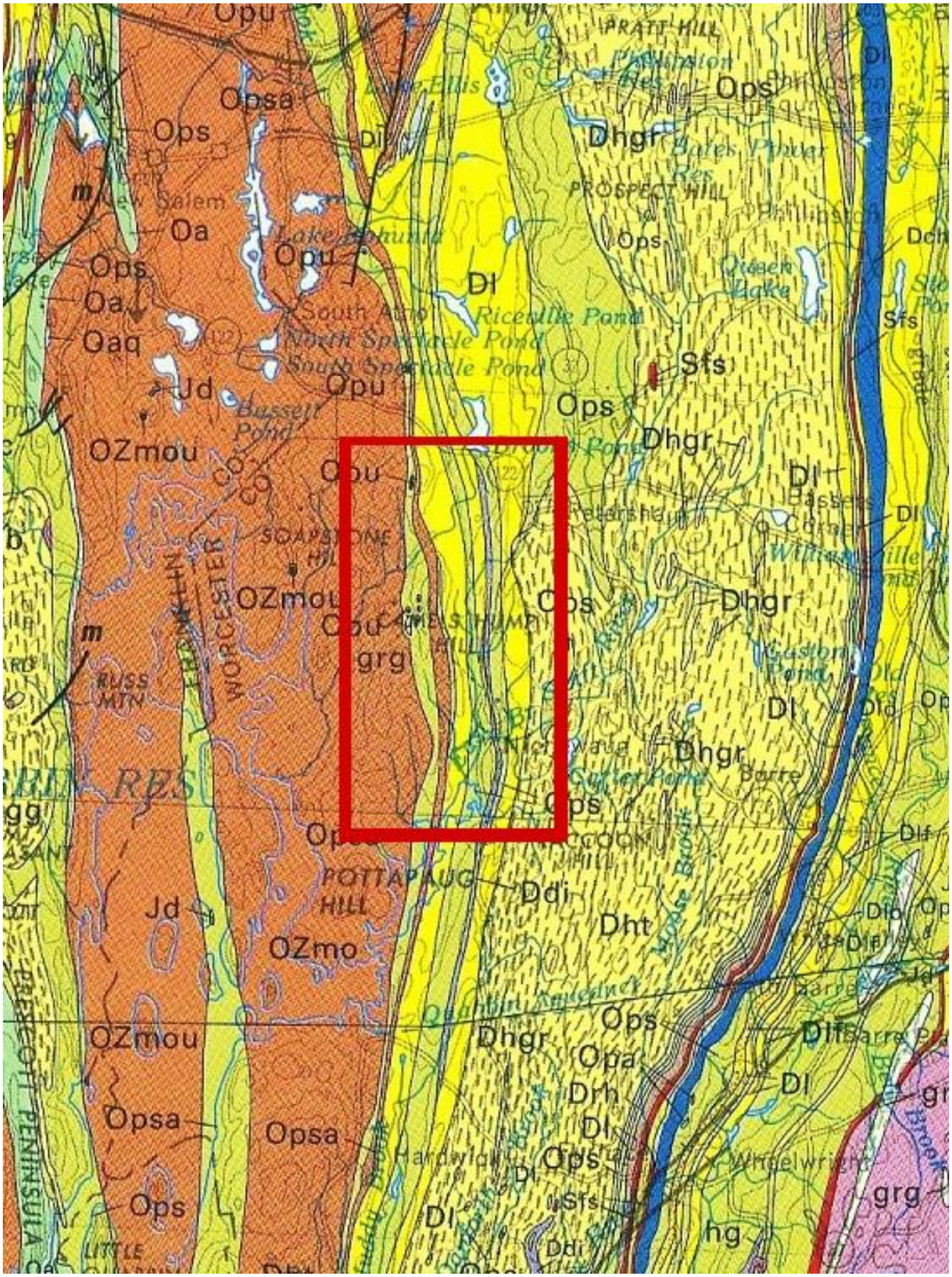

Figure 4.1. A section of the Massachusetts bedrock geologic map (Zen et al., 1983). The study area is outlined in red. Rocks that are now interpreted as Silurian Rangeley formation were mapped as the Ordovician Partridge (Op) and Devonian Littleton Formations (Dl).

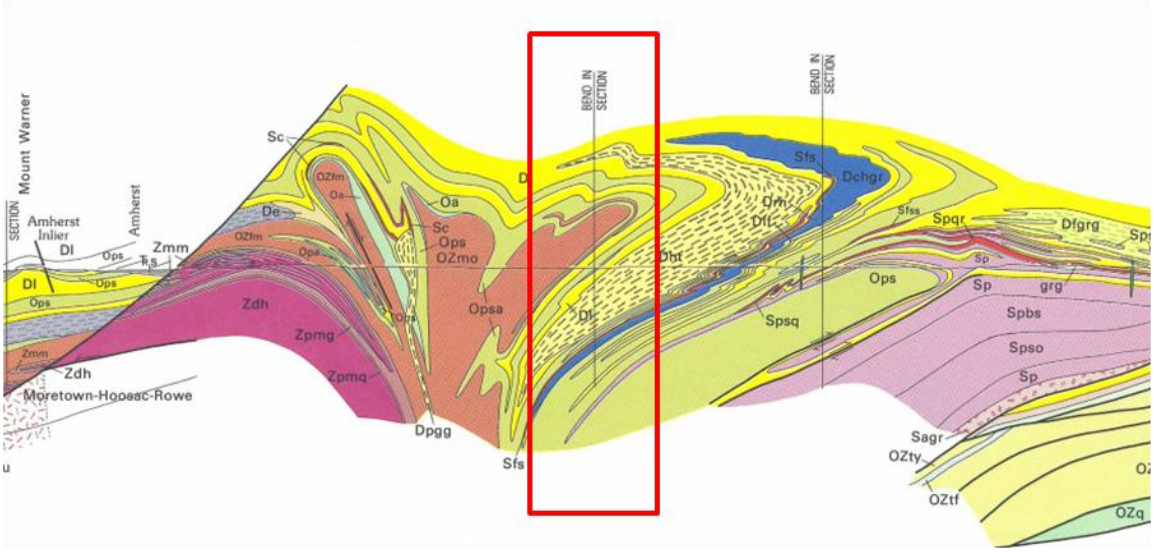

Figure 4.2. Partial cross section from Massachusetts state bedrock geologic map (Zen et al., 1983) with approximate location of the study area outlined in red.

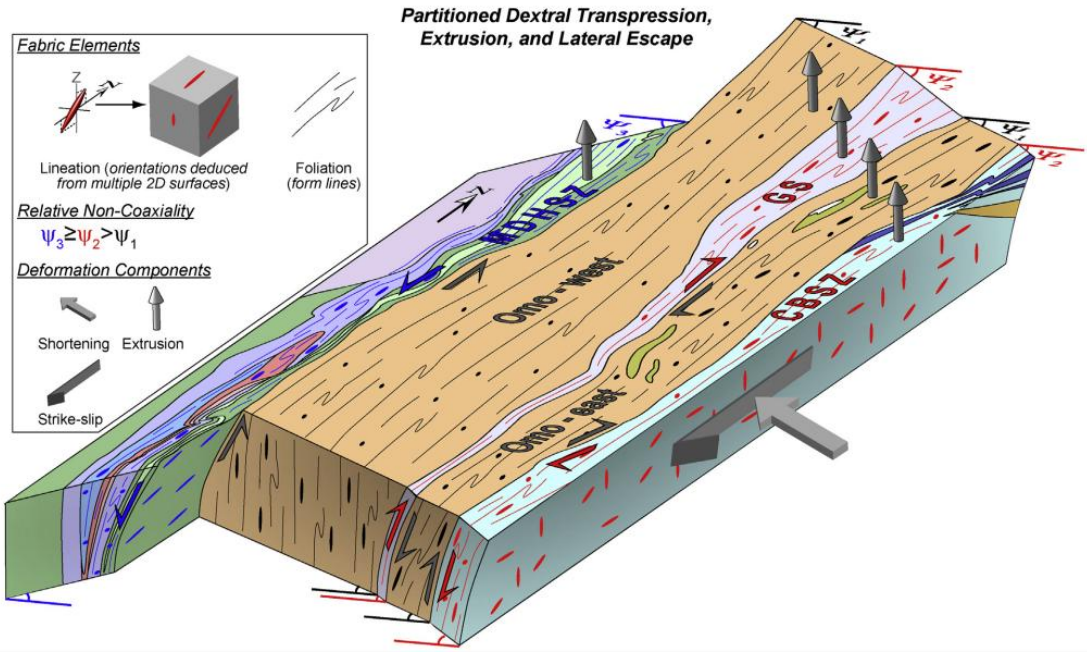

Figure 4.3. Three-dimensional, kinematic block model for the Palmer area showing orientation of foliation surfaces and lineations (blue, black, and red). From Massey and Moecher (2013).

CHAPTER V. DESCRIPTION OF MAP UNITS

A. Monson Orthogneiss (Omo)

The Monson orthogneiss (Fig 2.1) is one of the plagioclase gneisses of Thompson et al. (1968). Its map pattern is a highly attenuated north-south trending belt that extends from northern Massachusetts to the southern tip of the BHZ in Connecticut and occupies the entire core of the purported Monson Dome (Leo, 1991; Leo et al., 1984; Hollocher et al., 2002). The Monson "batholith" is broadly granitic but includes lithologies ranging from intermediate to felsic with a major mafic component and rare ultramafic units (Hollocher et al., 2002).

In the Petersham quadrangle the Monson (Fig 5.1 and Fig. 5.2) is generally layered at the centimeter to meter scale but also appears as homogeneous bodies of amphibolite, or more often granitic gneiss, for more than 100 meters across strike. The dominant lithology is a light to medium gray-weathering, medium- to coarse-grained, mildly to moderately foliated, tonalitic to granodioritic biotite ± hornblende ± muscovite ± garnet orthogneiss. In outcrop, the Monson gneiss varies in appearance as either a distinctively interlayered granitic gneiss and amphibolite, a mildly to moderately foliated biotite or hornblende streaked gneiss, or a massive-looking, homogeneous, leucocratic rock.

B. Monson Amphibolite (Omoa)

Map-scale bodies of massive to moderately foliated (slabby) hornblende-plagioclase ± biotite ± augite amphibolite (Fig 5.3) are lithologically identical to but thicker than layers present within Omo. Monson amphibolite occurs in the Petersham

quadrangle as centimeter to map-scale layers or boudins within the felsic rocks. The amphibolite is more competent than granitic Monson.

The outcrop appearance of Monson amphibolite varies from dark grey to black or mottled. The texture is typically massive but locally appears slabby (foliated) or strongly lineated as defined by hornblende needles and feldspar streaks that are visible in outcrop. Foliated varieties sometimes have thin planar bands of leucocratic plagioclase + quartz.

C. The Rangeley Formation (Sr)

The Silurian Rangeley Formation comprises the cover lithology for a large portion of the western CMZ including the Petersham quadrangle in central Massachusetts. The Rangeley Fm., which was originally identified and described by Moench (1971) at its type locality in the Rangeley quadrangle in southwestern Maine, has since been reported as far south as south-central Connecticut (Hatch et al., 1983; Thompson, 1985; Berry 1989; Massey, 2008b; O'Brien, 2009, Walker, 2011).

In the Petersham quadrangle, the Rangeley Fm. occurs as a gray to rusty weathering, medium-grained, mildly to strongly foliated and/or lineated, quartz-plagioclase-biotite-K-feldspar ± garnet ± sillimanite ± muscovite paragneiss to paraschist. In some areas muscovite has replaced sillimanite and garnet is absent.

Pronounced mineral lineations and an L- or L>S-tectonite to mylonite texture have developed in high strain zones at contacts with the other lithologies. The schistosity and foliation are defined by oriented mica flakes and flattened leucosome (Fig 5.4). The lineation is most commonly defined by coarse-grained acicular sillimanite but may also be defined by feldspar streaks and elongated quartz. Folds are evident in flattened and

folded leucosome. Fold hinge lines are parallel to the mineral lineation.

Layered or irregular (often highly deformed) leucosome and coarse grained plagioclase and K-feldspar porphyroclasts are common. The Rangeley Fm. is almost invariably intruded by massive to mildly foliated centimeter to meter scale leucopegmatite masses that are often deformed into boudins and wrapped by foliation of the enclosing Rangeley (Fig 5.5). Gray-weathering layers of K-feldspar-quartz-plagioclase-biotite-sillimanite-garnet ± muscovite granofels appear locally.

D. The Hardwick Tonalite (Dh)

A modal QAP ternary plot from Shearer (1983: Fig. 58) shows that rocks of the Hardwick pluton are predominantly tonalite with subordinate quartz diorite and granodiorite. On an AFM plot of whole rock compositions (Shearer, 1983: Fig. 59), the trend of the Hardwick is distinctively calc-alkaline in nature. The Hardwick tonalite can be subdivided into four petrographic types: hornblende-biotite, biotite, biotite-muscovite, and biotite-garnet tonalite (Fig. 5.6). Biotite tonalite is the dominant type. The distribution of petrographic types defines a mineralogical zoning (interior to exterior of the pluton) of metaluminous hornblende-biotite and biotite tonalites to peraluminous biotite-muscovite and biotite-garnet tonalites. Contacts between tonalite types are gradational (Shearer 1983), suggesting that the units collectively represent a single intrusive episode.

Partial melting of a heterogeneous crustal source region resulted in the compositional variability among the varieties of tonalite (Shearer, 1983). The source rocks consisted of two interlayered end members within the Acadian subduction

complex. The first is a metaluminous, oxidized, I-type source consistent with an oxidized, altered basalt or andesite. The second is a peraluminous, reduced, S-type source consistent with a greywacke-argillite sequence. Source material assignments as S- and I-types are from Chappell and White (1974). Formation of the biotite-garnet tonalite along the margins of the pluton is attributed to *in situ* contamination by local metamorphic rocks. A large inclusion of the Rangeley formation is present within the Hardwick in the southern portion of the map area (Fig. 6.1). These are reported throughout the Hardwick pluton by Shearer (1983).

Shearer (1983) concluded that the well-developed foliation, development of mylonite in the tonalite, and the character of the regional metamorphic isograds, suggests an early Acadian intrusive age for the Hardwick Tonalite (Shearer, 1983). However, U-Pb zircon ages reported by Robinson et al. (1998) were 360 ± 1 Ma and 361 ± 2 Ma, too young for Acadian metamorphism. A Late Devonian to early Carboniferous age is corroborated by geochronology of this study.

The Hardwick tonalite occurs in the Petersham quadrangle (Fig. 5.7) as a massive to moderately foliated, light to dark grey, biotite-hornblende tonalite to granodiorite. Light grey varieties are locally porphyritic with 1-2 cm K-feldspar phenocrysts (Fig. 5.8). Strongly foliated examples in contact with the Silurian Rangeley typically include mm-cm scale layers of leucosome and quartz veins.

E. Nichewaug Sill of Shearer, 1983

The latest Devonian (361 ± 8 Ma; see results of geochronology below) quartz-Nichewaug diorite is a massive to mildly foliated, medium-grained, biotite-clinopyroxene

± hornblende ± orthopyroxene quartz-diorite sheet intruded into the Rangeley gneiss (Fig. 5.9). It strikes north to south and spans nearly the entire distance through the map area. It ranges in width across strike from slightly more than 100 meters down to 10 meters. In outcrop it is typically a dark grey to black, equigranular, medium grained, massive diorite. In some locations Dpd is mildly foliated and more biotite rich within 1 m of the contact with the Rangeley.

F. Leucopegmatite (lp)

Medium- to very coarse-grained feldspar-quartz ± biotite ± hornblende ± muscovite ± garnet leucopegmatite (Fig. 5.10) occurs in the map area as layers, boudins (Fig. 5.4), or irregular bodies within other units. Leucopegmatite also occurs in map-scale 10-100 m wide ridges that may be >1 to 20+ meters high which are indicated on the geologic map (Fig. 6.1 and Fig. 5.11). These map-scale lecuopegmatite bodies are most commonly found within the Rangeley but may also occur within the Monson and are more common in contact zones where strain is concentrated. Outcrop appearance of leucopegmatite is most often massive with >1-10% fine to coarse grained mafic minerals. It may have a mild to moderate foliation defined by flattened quartz, feldspar streaks, aligned mica grains, and narrow planar 1-2 mm bands of mafic minerals.

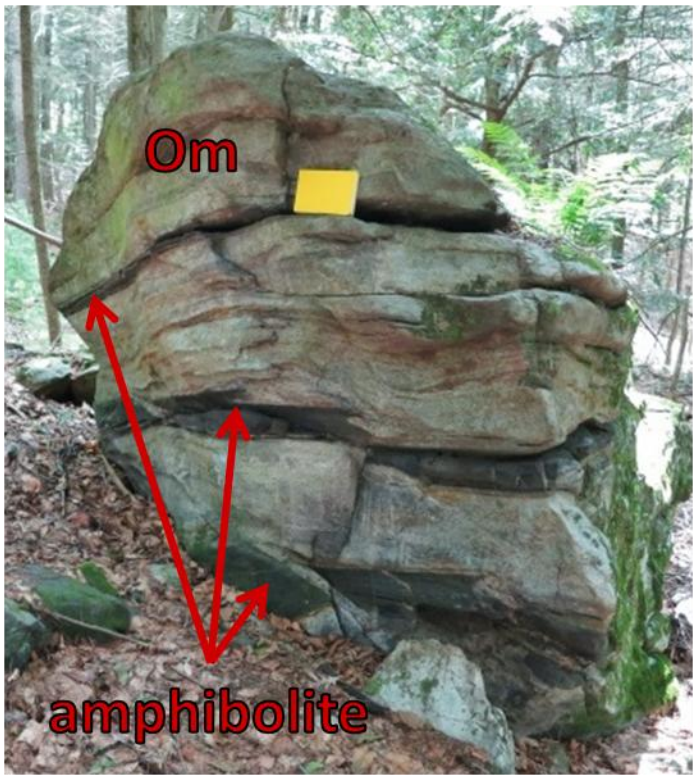

Figure 5.1. Outcrop of mildly foliated granitic Monson gneiss (Om) with cm-scale layers of amphibolite.


Figure 5.2. Sawn slab of interlayered Monson orthogneiss and amphibolite.

Figure 5.3. Outcrop of Monson amphibolite (Omoa) with subordinate layers of Monson gneiss (Om) at Pottapaug Pond recreation area, Quabbin Reservoir.


Figure 5.4. Rangeley outcrop exhibiting typical foliation defined in outcrop by flattened leucosome.

Figure 5.5. Foliated Rangeley Formation wrapping a 2-meter wide pegmatite boudin.

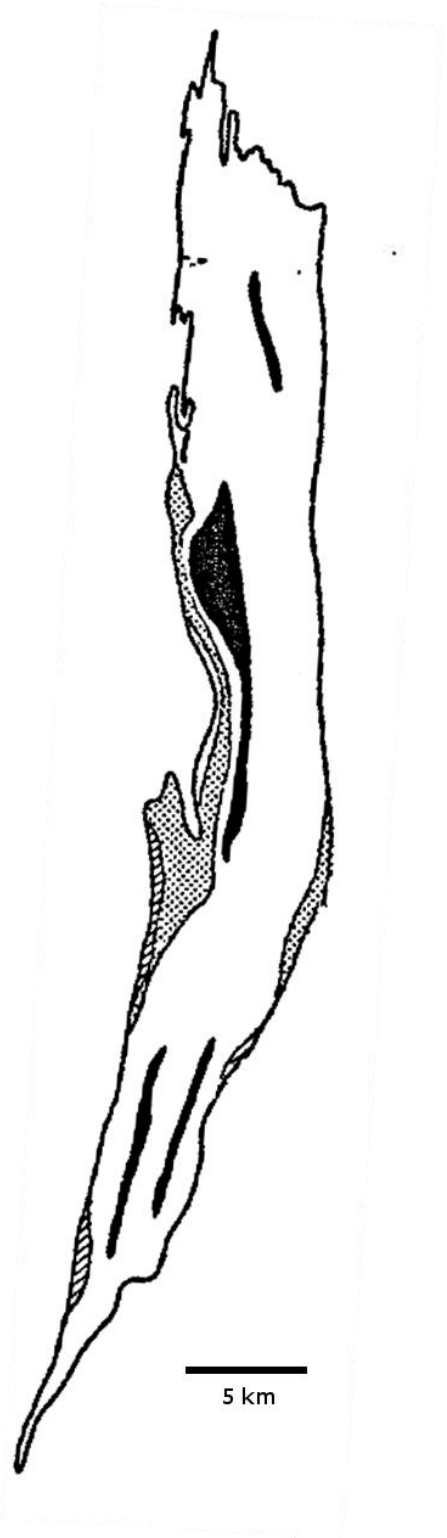

Figure 5.6. Figure 7 of Shearer (1983) showing the distribution of rock types within the Hardwick Tonalite. Honblende-biotite tonalite (black), biotite tonalite (white), biotite-mucovite tonalite (dotted), and biotite-garnet tonalite (striped).

Figure 5.7. Sawn slab of typical appearance of unfoliated, medium grained Hardwick biotite hornblende tonalite.

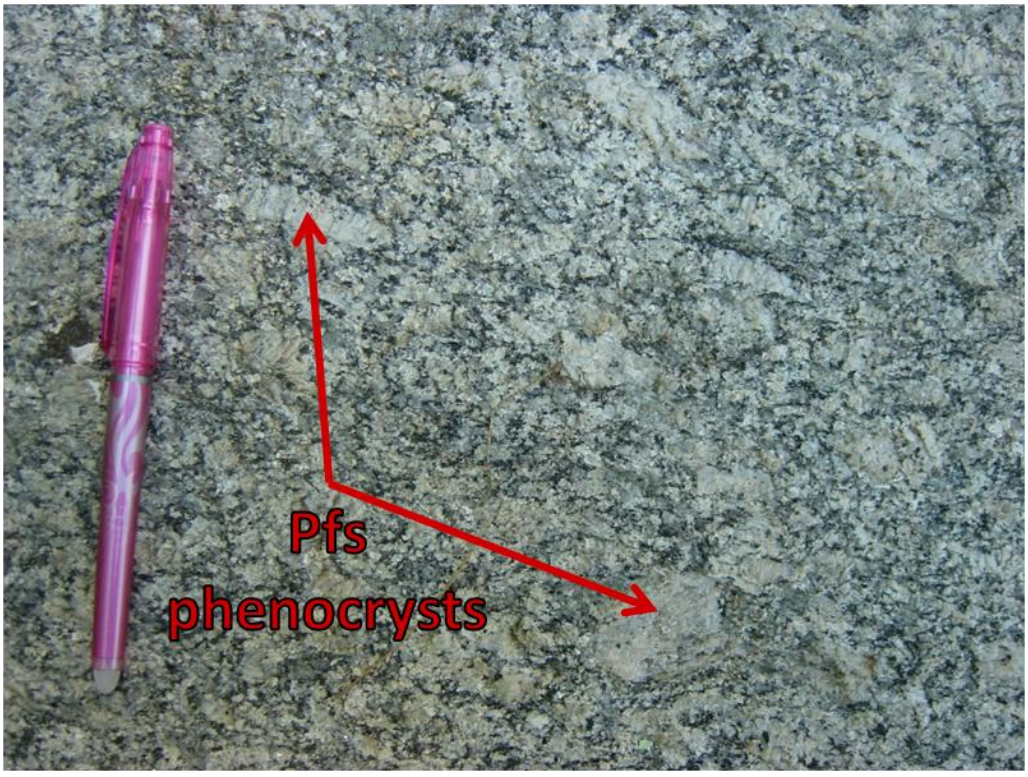

Figure 5.8. Outcrop photo of Hardwick biotite tonalite bearing 1-2 cm plagioclase phenocrysts.

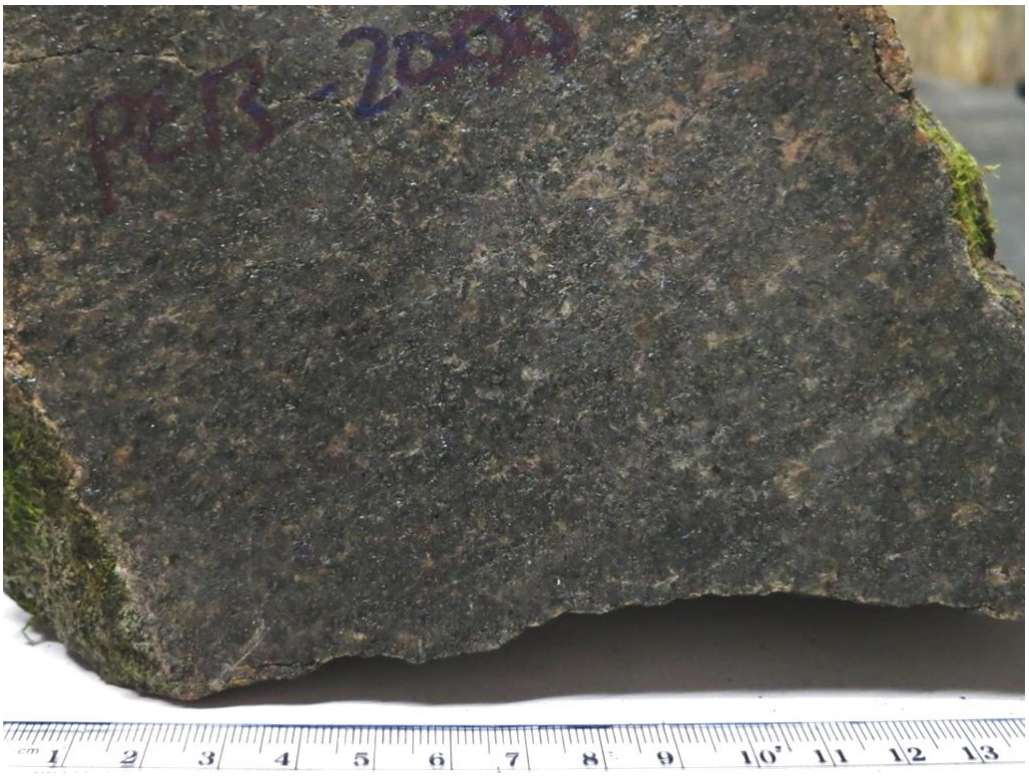

Figure 5.9. Sawn slab of the Nichewaug quartz diorite.

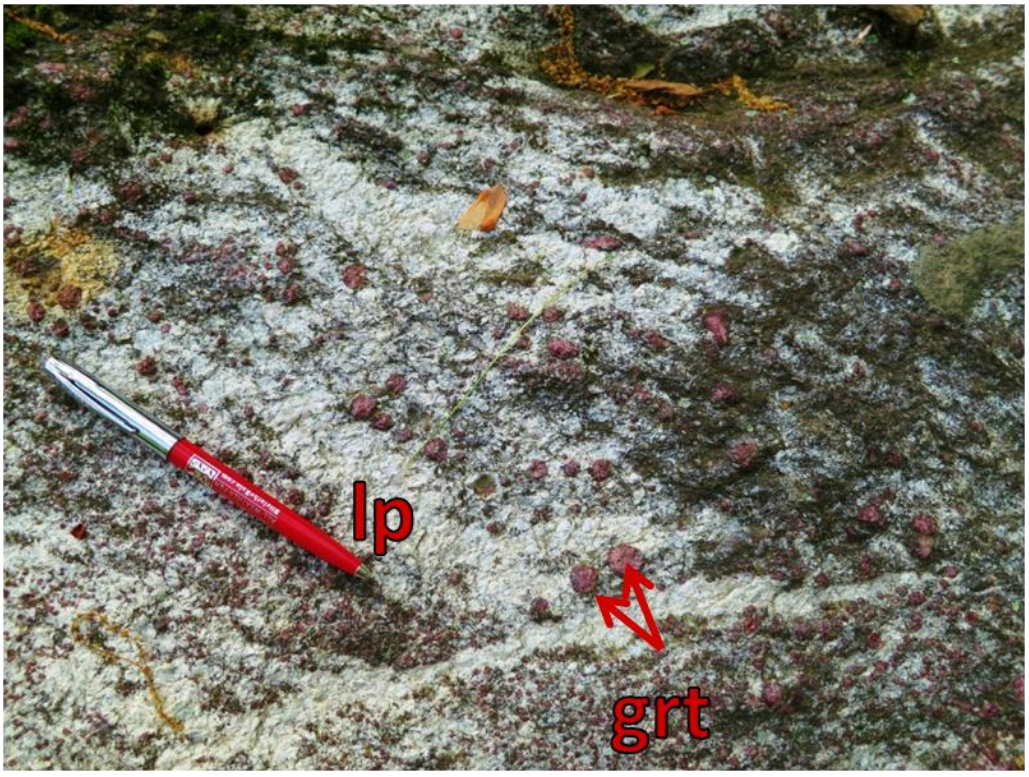

Figure 5.10. Leucopegmatite body within the Monson, bearing 1-cm garnet.

Figure 5.11. East-facing outcrop of typical leucopegmatite on eastern side of Bald hill illustrating the thickness that can be achieved by such bodies. Enclosing rocks are Rangeley gneiss

CHAPTER VI. GENERAL MAP PATTERN

The geologic bedrock map produced for this study and shown in Plate 1 reveals the distribution of lithologic units in the western half of the Petersham 7.5' quadrangle. All but one of the contacts between units trends generally north-south. Contacts are interpreted to dip moderately to the west along with the west-dipping foliation (average orientation is 181/39W) and compositional layering in the Monson. All contacts in the field area are between the more competent meta-intrusive rocks and the less competent metasedimentary Rangeley formation; this is a major factor in defining the deformation styles in the area. Those contacts that exist between the major units (i.e. not involving the Ddi) are interfolded at the 10-meter scale. A thin layer of the Rangeley formation trends through the northern half of the map area within the eastern margin of the Monson pluton. This is interpreted as a larger scale expression of the folds that are found in the boundary zones but are too small to include on the map.

Smaller visible features include map scale bodies of amphibolite within the Monson and a xenolith of the Rangeley Formation within the margin of the Hardwick at the southern end of the map area. Country rock inclusions such as this are reported to occur throughout the Hardwick pluton (Shearer, 1983), but are mapped as the Partridge Formation in previous works (e.g., Zen et al., 1983).

The contact regions between the Rangeley and both orthogneisses are complexly interfolded. Alternating lithologic units on the map that include a thin band of Rangeley within the Monson to the west and in the Hardwick to the east are interpreted as map-scale folds (Fig. 6.2) similar to those observed in a south-facing outcrop of Rangeley at the Hill next to Carter Road (described below). The result, in the case of the Hardwick, is

a very irregular map pattern that is unusual for the region where contacts are typically relatively straight and run N-S or NE-SW. The thin band of Rangeley that projects into the Hardwick is interpreted to be the result of map-scale folding that is likely similar to the folding found in a vertical E-W face of Rangeley in the Carter Road area.

One distinctive map feature that is typical of New England geology is the presence of single ridges or even large areas where plagioclase-quartz ± K-feldspar ± biotite ± hornblende leucopegmatite comprises greater than 90% of the rock volume. These areas are indicated on the map. Leucopegmatite is concentrated in contact regions and is often found as inclusions in the Monson and Rangeley. Thin and shredded or wispy inclusions or rafts of the Rangeley or Monson are locally present within the pegmatite bodies in contact zones.

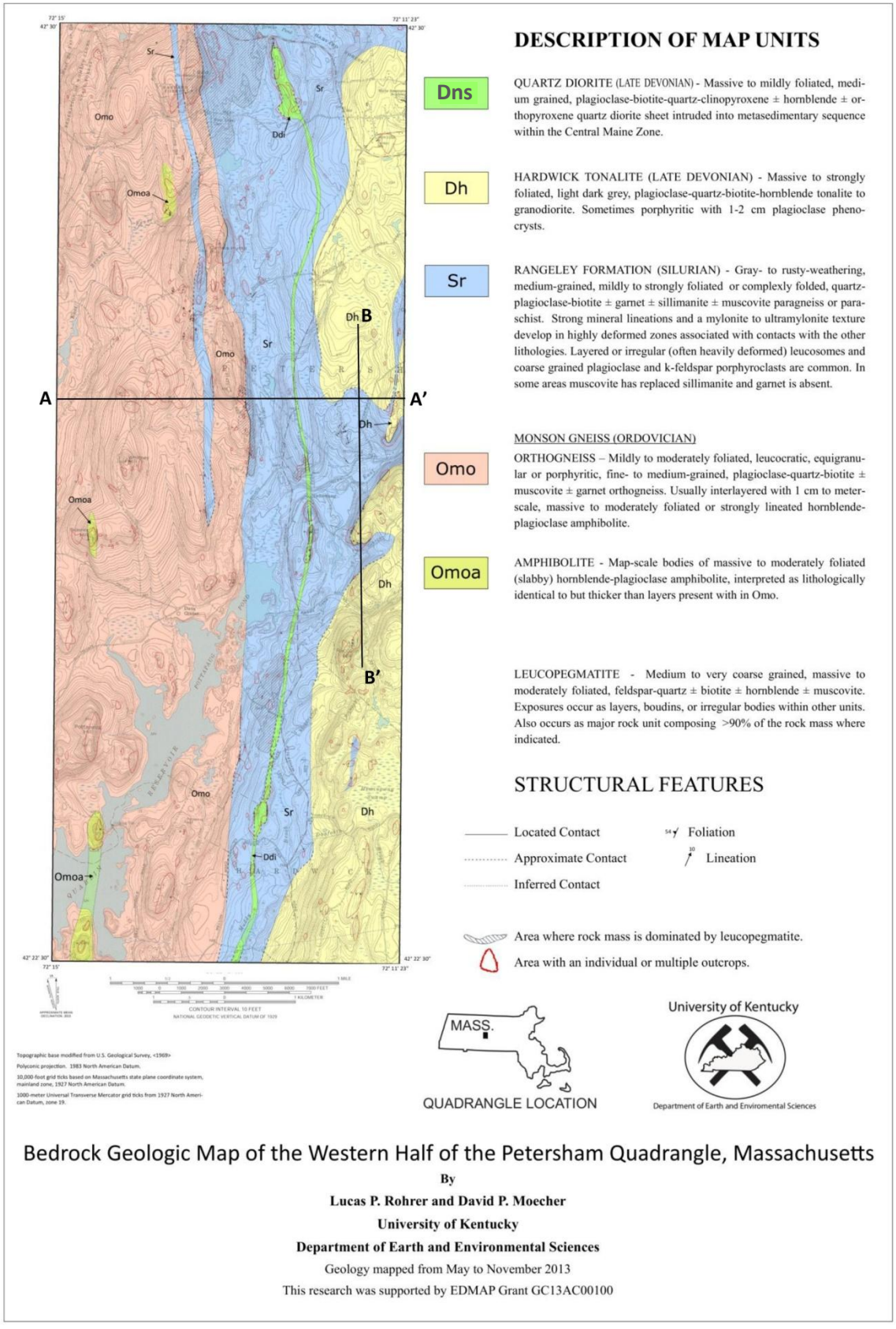

Figure 6.1: Geologic bedrock map of the western half of the Petersham 7.5' quadrangle.

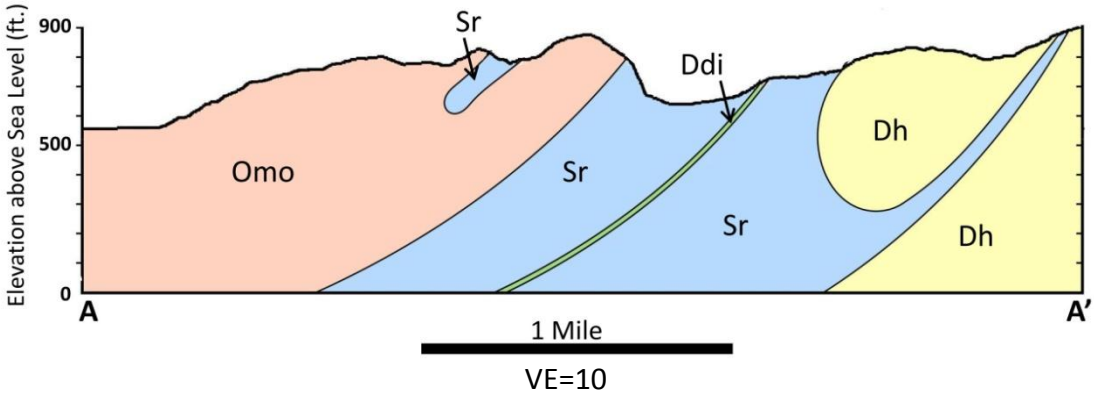

Figure 6.2. Cross section (A-A') showing alternating lithologies across strike.

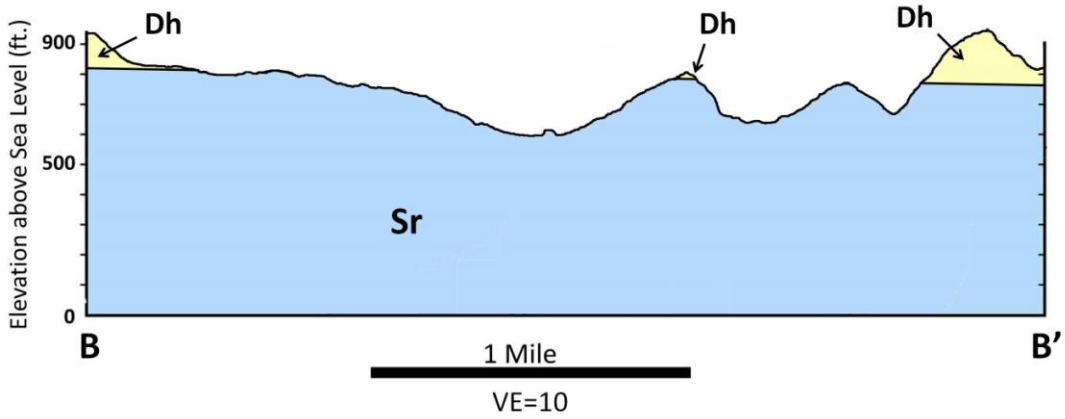

Figure 6.3. Cross section (B-B') demonstrating topographic influence surface bedrock lithology and map pattern.

CHAPTER VII. MESOSCOPIC STRUCTURES

A. Foliations

A SSW-NNE striking and west-dipping foliation (Fig. 7.1) is pervasive in the map area and throughout central Massachusetts (e.g. Zen et al., 1983; Peterson and Robinson, 1993; O'Brien, 2009; Walker, 2011; Massey and Moecher, 2013). In the Monson orthogneiss this foliation dips shallowly to moderately to the west (parallel to bimodal layering), is of mild to moderate intensity, and is planar but is locally deflected around more competent amphibolite bodies. Foliations in Monson amphibolite are apparent in outcrop by leucocratic banding (Fig. 7.3) and a slabby fracture (7.2).

In the Hardwick, the intensity of the foliation varies widely from strong to weak or is absent entirely. Its dip is similar to that in the Monson, shallow to moderately west. Mica grains and flattened quartz define the foliation in both the Monson orthogneiss and the Hardwick. Foliations in the Rangeley are similar in orientation and may be strong or absent. These foliations are defined by mica grains, porphyroclasts, and flattened leucosome (Fig. 5.4 and Fig. 7.4).

B. Folds

In only two locations, one in contact with Dpd and another in contact with the Hardwick tonalite, adjacent to Carter Road, are two generations of folds observed in vertical E-W faces of the Rangeley (Fig. 7.5). The first generation (F_1) is tight to isoclinal with axial planes dipping steeply to the east. These folds have been refolded by more open (F_2) folds with axial planes dipping shallowly to the west. Asymmetrically folded leucosome also appears at these locations demonstrating sinistral kinematics (Fig. 7.6)

Evidence of fold hinges is scarce elsewhere in the quadrangle. Rare folds in the Hardwick are recumbent and open. Their hinge lines dip shallowly to the north. Though fold hinges do not crop out in the field area, the bimodal layering in the Monson (Fig. 5.2) is interpreted to result from high amplitude isoclinal folding.

C. Lineations

According to Goodwin and Tikoff (2002), stretching lineations form most readily within the least competent lithology. Structural analysis within the present map area supports this assertion. The predominant mineral lineation (Fig. 7.9) that occurs in the Petersham quadrangle and surrounding areas is defined by coarse-grained sillimanite needles within the Rangeley Formation (Fig. 7.7). This lineation strikes SSW-NNE and dips shallowly to the north or south. A similarly striking lineation, defined by hornblende needles and feldspar streaks, occurs locally within the Monson amphibolite (Fig. 7.8). This lineation is only visible in two locations in the map area, both of which are at the eastern margin of the Monson orthogneiss near the Monson-Rangeley contact.

D. Leucopegmatite

Leucopegmatite is ubiquitous in the field area and often appears as boudins or irregular masses associated with the Monson and Rangeley. Pegmatite boudins, which are commonly mildly to moderately foliated, tend to be focussed near lithologic contacts. Pegmatites played an important role in the mapping and structural analysis of the Petersham quadrangle. Pegmatite bodies are often the only reason for bringing outcrop of the less resistant Rangeley formation to the surface. Pegmatites also provide the best

(most visible) evidence of the expression of the predominant deformation pattern (north-south elongation) that is created by lithologic units of alternating competency within the map area. Pegmatite bodies also bear inclusions of country rock (Fig. 7.10). These inclusions helped to guide mapping in places where other lithologies were otherwise undetectable.

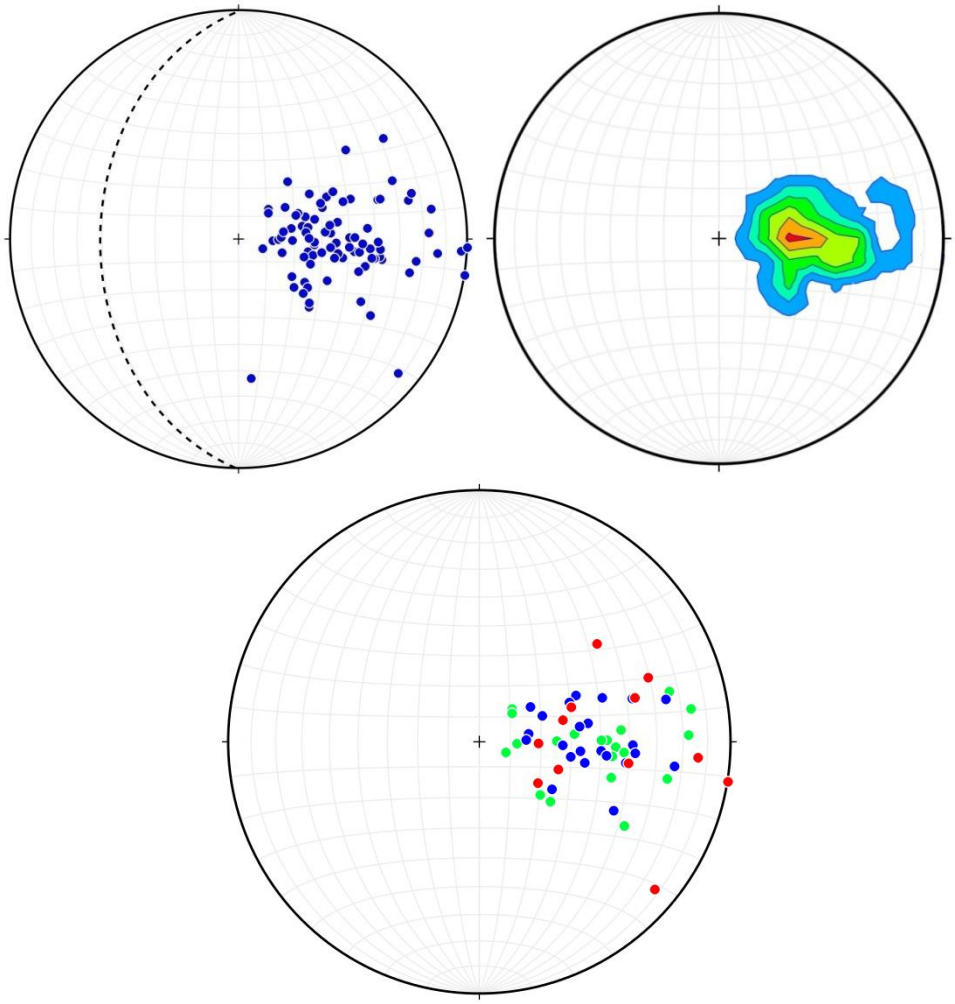

Figure 7.1. Stereonets (equal area, lower hemisphere) showing foliation data recorded from the map area. Figure on left shows poles to foliation (blue dots) and average foliation plane (dotted line). within the map area. Figure on right shows 3% area contours of poles to foliation. The lower stereonet shows poles to foliation color coded by lithology. Blue, red, and green dots indicate poles to foliation measured within the Monson Orthogneiss, Rangeley paragneiss/paraschist, and Hardwick Tonalite respectively.

Figure 7.2. Outcrop of Monson amphibolite demonstrating foliation-induced slabby outcrop character.

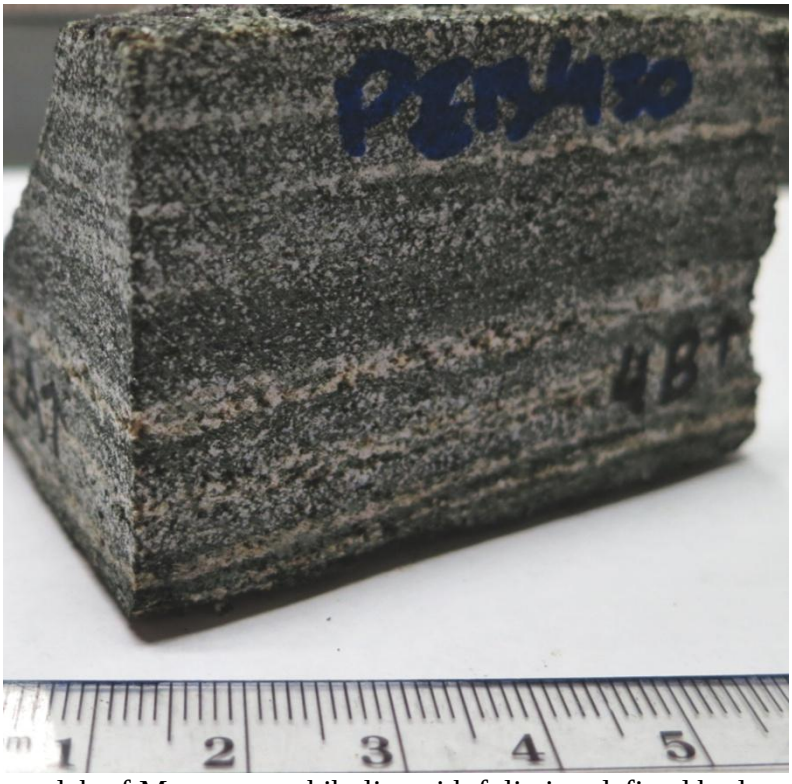

Figure 7.3. Sawn slab of Monson amphibolite with foliation defined by leucocratic plag ± qtz banding.

Figure 7.4.East-west oriented vertical outcrop face of Rangeley Fm. at Carter Hill. Red lines trace folded leucosomes. Yellow dashed lines represent axial surfaces of F_1 folds and green dashed lines represent axial surfaces of F_2 folds.

Figure 7.5. A sinistrally (east side north) folded leucosome on outcrop pavement within the Rangeley Fm. This face is perpendicular to that shown in Fig. 7.5.

Figure 7.6. Coarse grained sillimanite needles within the Rangeley Formation defining a N-S striking mineral lineation.

Figure 7.7. Cut sample of Monson amphibolite showing mineral lineation defined by hornblende needles and feldspar streaks. Left face is perpendicular to foliation and parallel to lineation. Right face is perpendicular to lination.

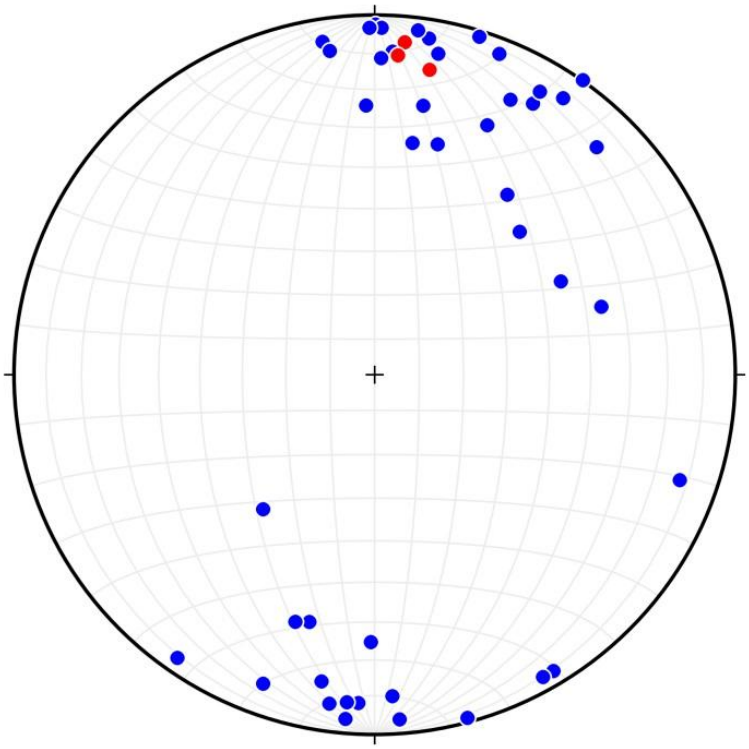

Figure 7.8 Stereonet (equal area, lower hemisphere) showing the orientation of mineral lineations (blue dots) and fold hinge lines (red dots) within the map area.

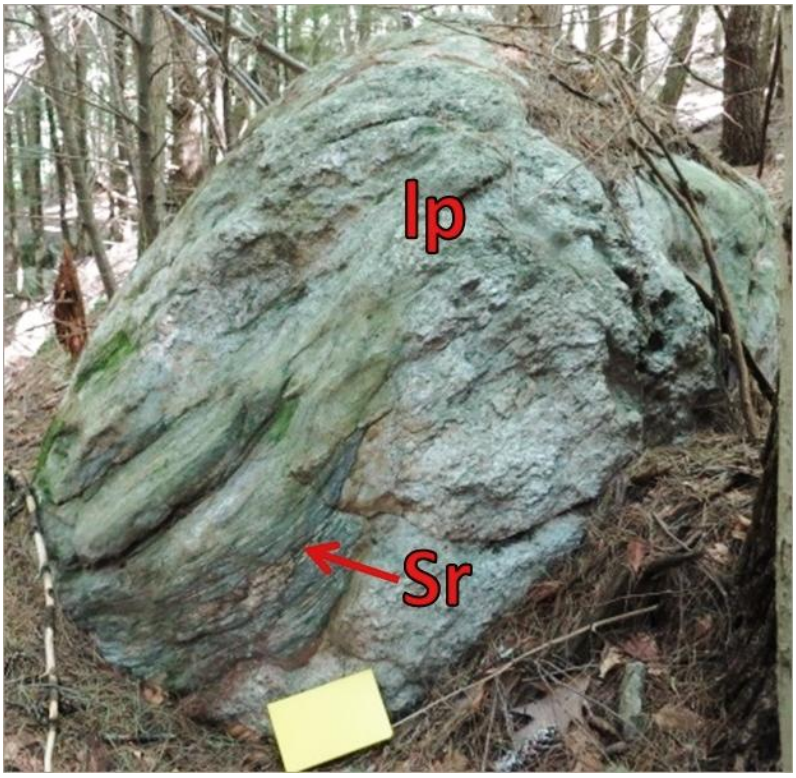

Figure 7.9. Pegmatite boudin with a Silurian Rangeley raft. Outcrop is on east side of Camel's Hump Hill.

CHAPTER VIII. MICROSTRUCTURES

A. Monson Orthogneiss

Monson orthogneiss (Fig. 8.1) typically exhibits an equigranular, medium grained, hypidiomorphic texture and a mild foliation defined by flattened quartz grains and biotite streaks. Plagioclase typically occurs as subhedral, equant grains with long axes parallel to the planar fabric. Biotite and/or anhedral hornblende is often concentrated in narrow bands that also contain quartz ribbons. These bands define 1-2 mm-thick zones where flattening strain is concentrated. Highly fractured and partially disaggregated garnet, when present, is found only within or adjacent to these bands of high strain. Fine to medium grained, anhedral, opaque phases are also concentrated in these bands. K-feldspar is rare.

More highly deformed rocks show high temperature microstructures. These have a seriate texture and moderate foliation defined by fine to medium grained biotite ± muscovite and quartz ribbons which sometimes include feldspars. K-feldspar is by far more abundant than plagioclase and occurs as myrmekite rimmed porphyroclasts or in large polycrystalline patches. Interstitial fine-grained quartz and feldspars (predominantly plagioclase), along with minor mica and zones of myrmekite fill spaces between porphyroclasts and feldspar patches. Feldspar grains that are elongate are oriented parallel to the planar fabric.

B. Monson Amphibolite

Monson amphibolite (Fig. 8.2) is typically medium grained (1-3 mm), relatively undeformed, and massive with polygonal hornblende and plagioclase ± biotite, quartz,

and augite. Rocks with significant biotite tend to be foliated (contributing to a slabby appearance in outcrop). The foliation is defined by oriented biotite, feldspar, and hornblende grains and/or alternating quartzofeldspathic and mafic mineral bearing bands. Plagioclase porphyroclasts are sometimes present in foliated varieties. These have symmetric quartz strain shadows that are aligned parallel to foliation. Medium to coarse-grained quatzofeldspathic aggregates are also aligned with the foliation. Locally, Monson amphibolite is strongly lineated as defined by acicular hornblende and elongate feldspar grains (Fig. 7.8).

The accessory mineral assemblage is the same within both Monson lithologies. Primary accessory minerals include ilmenite, apatite, and titanite. Secondary accessory minerals include sericite, chlorite, and epidote.

C. Rangeley

The Rangeley Fm. (Fig. 8.3) is a metasedimentary unit composed of quartz + biotite + plagioclase + K-feldspar ± sillimanite ± garnet ± muscovite. Composition and texture of the Rangeley Fm. vary widely. Most often the Rangeley is medium-grained, containing both sillimanite and garnet but not muscovite. Sillimanite may be fine-grained, occurring in flattened aggregates intergrown with quartz, or coarse-grained fractured and stretched, defining a mineral stretching lineation manifested by grains that are broken and transported parallel to their long axis (Fig. 8.3C). Flattened quartz aggregates and quartz ribbons are also prevalent. Medium- to coarse-grained biotite, and muscovite when present, are aligned with the predominant fabric. Plagioclase and K-feldspar porphyroclasts and garnet have quartz + mica tails that are usually symmetric,

but in some localities show sinistral (east side north) asymmetry. Garnet, which contains biotite and quartz inclusions, is occasionally disaggregated and transported along foliation surfaces. Meter-scale lenses of quartz + feldspspar ± garnet granofels are present within the main Rangeley lithology.

Sillimanite-poor Rangeley is composed of alternating bands of quartz and mica that wrap around feldspar porphyroclasts. The porphyroclasts sometimes have myrmekite rims. Garnet may be present or absent. This Rangeley type often contains retrograde muscovite replacing sillimanite. Evidence for this is seen within a few medium-grained sillimanite needles remaining within a matrix of fine-grained muscovite (PE12-29-1A: Fig. 8.3F).

In a few locations near the contact with the Hardwick, protomylonitic Rangeley contains an abundance of feldspar + quartz leucosomes. A strong fabric is mostly defined by medium-fine grained quartz ribbons, garnet strain shadows, and mica grain orientation.

D. Hardwick

The texture of the Hardwick (Fig. 8.4) is widely variable. Farther east, away from its margin, the Hardwick is typically massive or weakly foliated and hypidiomorphic. Hornblende bearing varieties tend to be coarse grained, massive and equigranular, while biotite-tonalites are medium grained, mildly foliated, and may be porphyritic with plagioclase and subordinate microcline phenocrysts. These phenocrysts are surrounded by a matrix of medium-grained quartz + biotite + opaque phases. Zones of myrmekite

have formed near the margins of some of the coarse- and medium-grained plagioclase crystals.

Primary accessory minerals in Hardwick tonalites include sphene, allanite, zircon, apatite, magnetite, ilmenite, pyrite, and pyrrhotite. Secondary accessory minerals are muscovite, chlorite, clinozoisite, sphene, and calcite

Closer to the western margin of the pluton, the Hardwick typically exhibits a mild to moderate foliation and seriate texture. The foliation is defined by alternating quartz ribbons and bands of medium grained biotite ± hornblende ± muscovite. Strain is concentrated into narrow (1-2 mm) biotite layers. Medium to coarse-grained feldspar porphyroclasts have tails that are aligned with the foliation. These tails are typically symmetric, but in a few locations show sinistral (east side north) kinematics.

E. Nichewaug Sill

The quartz-diorite Nichewaug Sill is typically equigranular with medium- to coarse-grained plagioclase + biotite + clinopyroxene + orthopyroxene ± hornblende. Subhedral feldspar grains are the largest and may occur as solitary grains or in randomly oriented and intergrown clusters of 3 to 4 grains (Fig. 8.5). Biotite and hornblende are subhedral to anhedral and are intergrown with fine-grained quartz. Pyroxenes are subhedral. In some cases, the quartz-diorite forms a glomeroporphyritic texture in which a mosaic of fine grained, interstitial and equant quartz, biotite, clinopyroxene, plagioclase, and opaques fill spaces between aggregates of the coarser grained minerals mentioned above.

The Nichewaug quartz diorite is typically massive but locally exhibits a very mild foliation defined by inconsistent and incomplete preferential alignment of elongate biotite and plagioclase grains within 1 meter of the Nichewaug Sill-Rangeley contact. Myrmekite forms partial rims around some of the coarse-grained plagioclase and exists in equant zones indicating complete replacement of smaller plagioclase grains.

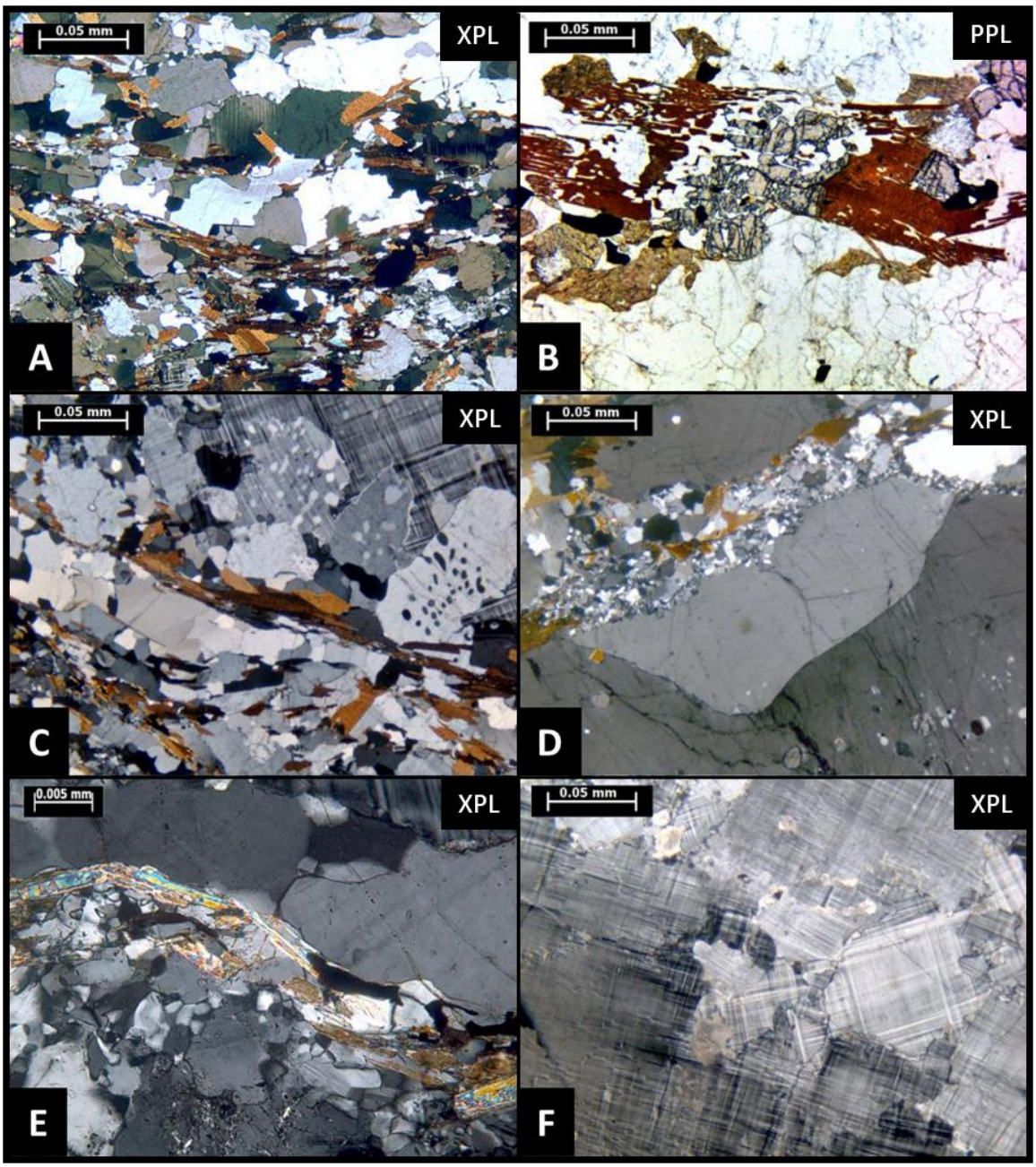

Figure 8.1. Representative photomicrographs of the Monson granitic orthogneiss (Omo). (A) Foliated Omo with flattened quartz and oriented biotite. (B) Thin, concentrated band of mafic minerals within leucocratic (qtz + fs) Omo consisting of biotite, partially resorbed and disaggregated garnet, and opaque phases. (C) Omo foliation bending around a mermekite rimmed microcline phenocryst. (D) Interstitial qtz + fs + bt between coarse grained plagioclase. (E) Thin band of muscovite defining foliation between otherwise equant qtz + pfs. (F) Coarse grained polycrystalline patch of microcline.

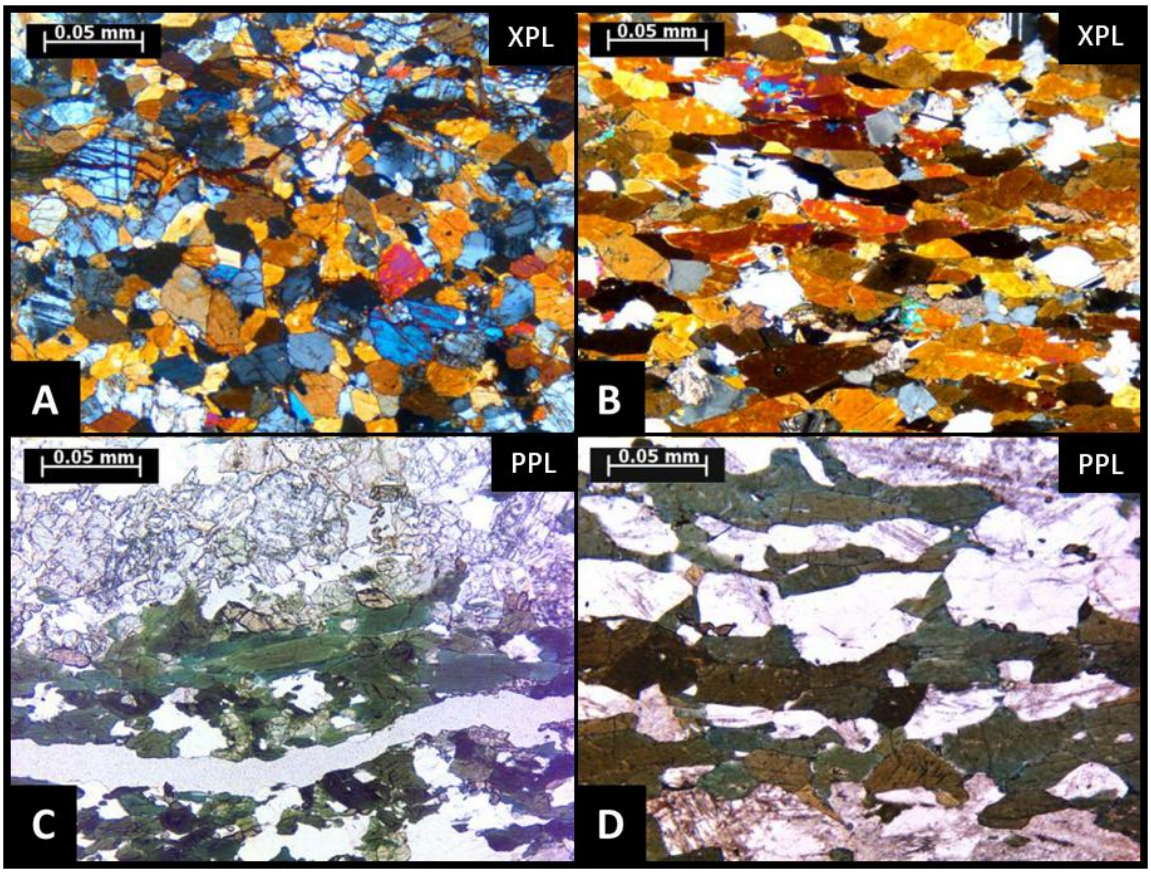

Figure 8.2. Representative photomicrographs of the Monson amphibolite. (A) Unfoliated, medium-grained amphibolite with prismatic hbl + pfs + cpx. (B) Amphibolite foliation defined by oriented hbl, bt, and anhedral opaque phases. (C) Amphibolite sample from Carter Pond hill showing a quartz vein and foliation defined by oriented hbl. (D) Strongly lineated amphibolite. Lineation is defined by oriented hbl and pfs.

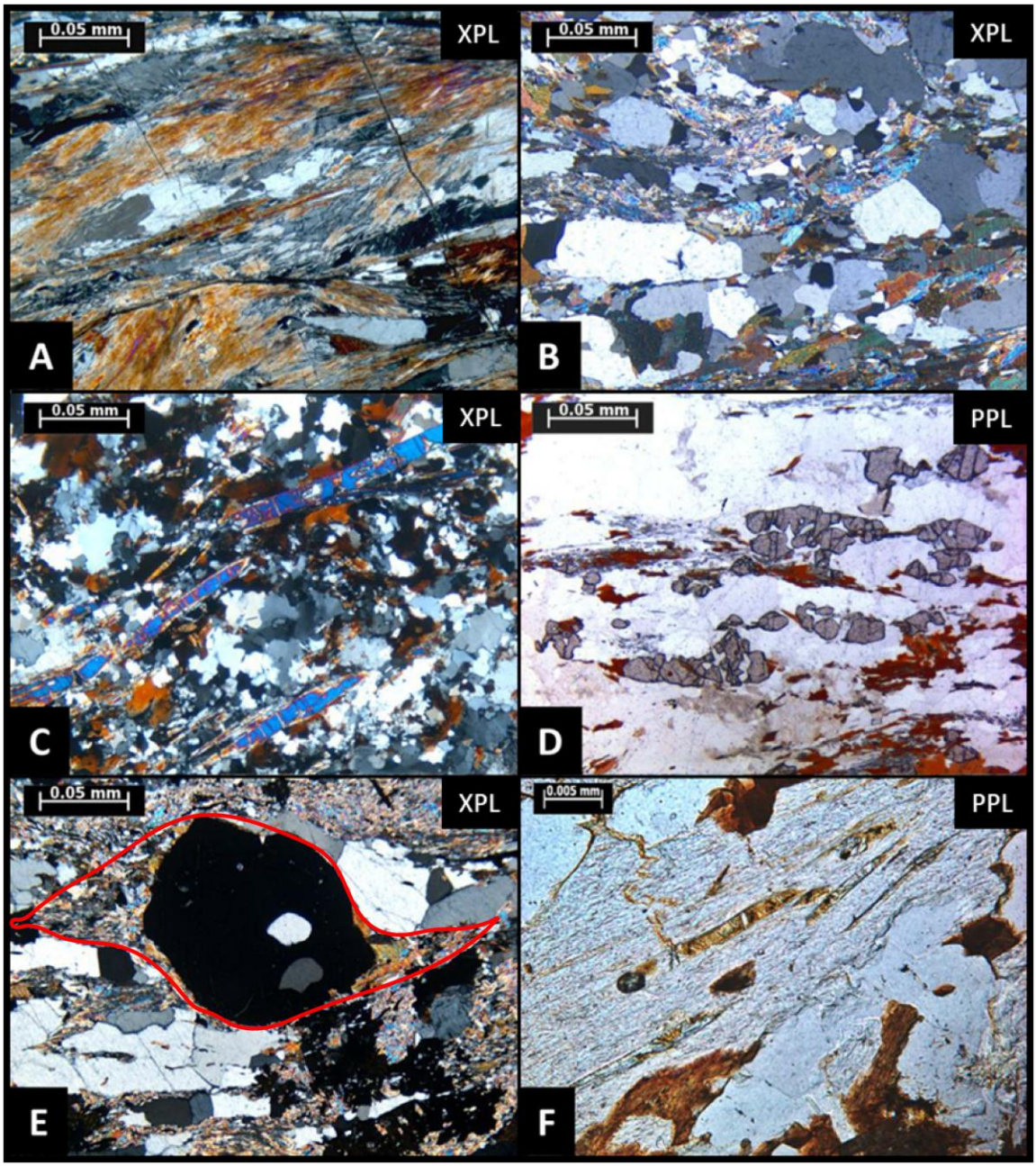

Figure 8.3. Representative photomicrographs of the Rangeley. (A) Symmetric lenses of fine-grained sillimanite interlayered with flattened quartz. (B) Foliation defined by alternating layers of mica and quartz. (C) Coarse grained sillimanite broken and transported along its axis to define stretching direction. (D) Disaggregated garnet transported along foliation surfaces defined by biotite and quartz. (E) Asymmetric strain shadows on either side of garnet showing sinistral kinematics. (F) Sillimanite surrounded by microcrystalline muscovite (evidence for retrograde breakdown of sillimanite into muscovite).

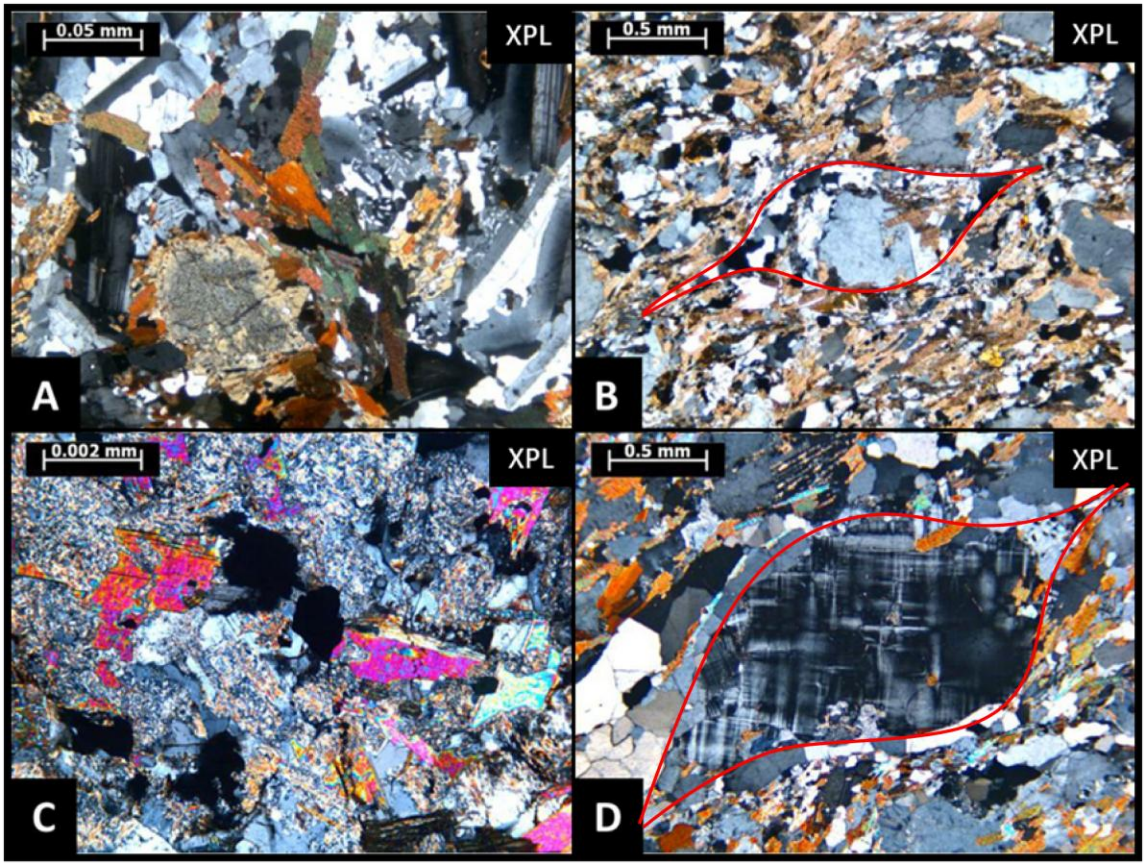

Figure 8.4. Representative photomicrographs of the Hardwick. (A) Medium-grained rock showing typical mineral assemblage of pfs+hbl+bt+opx+qtz. (B) Foliated Hardwick showing pfs porphyroclast with symmetric tails. (C) Sample showing accessory mineral assemblage of opaques+clinozoisite+titanite+sericite. (D) Microcline porphyroclast with sinistral (east to north [left]) asymmetry wrapped by qtz+bt foliation.

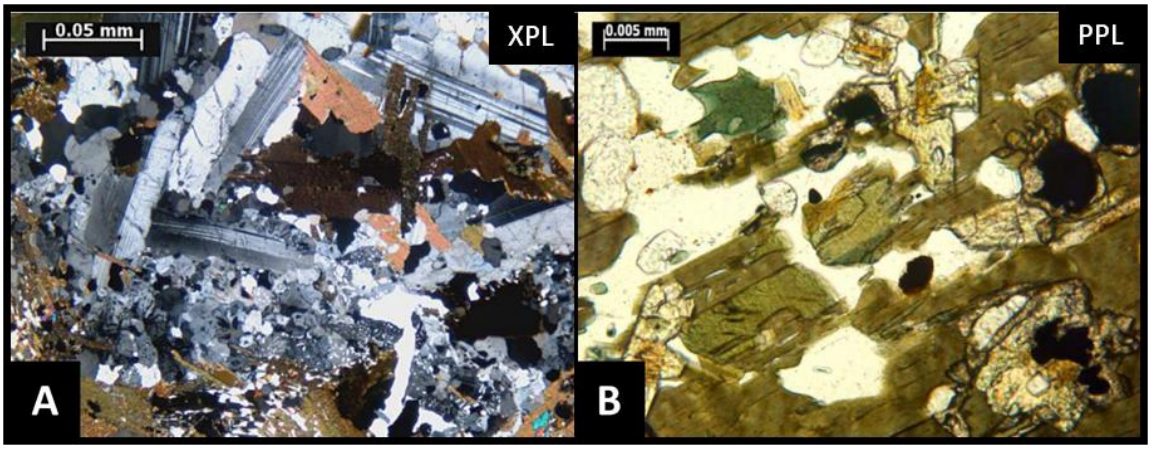

Figure 8.5. Representative photomicrographs of the Nichewaug Sill. (A) Randomly oriented, medium-grained pfs and bt with interstitial fine-grained qtz + pfs. (B) Medium-grained sample showing slight preferential orientation of hbl + qtz with subordinate cpx + opaques + apatite + epidote.

CHAPTER IX. GEOCHRONOLOGY

A. Rangeley U-Th-Pb electron microprobe chemical age dating

1. Methods

Thin sections from three samples of the Rangeley Fm. that exhibit diagnostic mineral assemblages and fabrics were analyzed via monazite U-Th-Pb electron microprobe chemical age dating at the University of Massachusetts (Williams and Jercinovic, 2002). Zones of similar composition and texture were first identified by X-ray elemental age- mapping (U, Th, Y) to preliminarily identify potential age populations. Four textural and compositional populations were identified. Each population was then analyzed on the CAMECA Ultrachron electron probe for determination of chemical ages. Six spots were analyzed within each age zone to compile an average age. Ages were then grouped into specific populations. These weighted mean populations are represented as Gaussian peaks in Figure 9.1.

2. Results

Figure 9.1 shows the weighted mean ages of the various age populations (Gaussian peaks), along with the age of the monazite standard determined during this study and its accepted age determined by U-Pb ID-TIMS analysis. Populations 1, 3, and 4 yield relatively tight clustered ages and have the following weighted mean ages: 1 = 345 $\pm$ 4 Ma; 3 =378 $\pm$ 4 Ma; 4 = 405 $\pm$ 4 Ma. Population 2 is divided into two subpopulations: 2b (~370 Ma) and 2a (~ 360 Ma).

B. U-Pb Zircon ages of the Hardwick tonalite and Nichewaug Sill.

U-Pb SIMS age analysis of samples of the Hardwick tonalite and Nichewaug quartz-diorite intrusion (Figs. 9.2 & 9.4) from the map area yielded ages of 357 ±4 and 362 ± 8 Ma respectively. Weighted mean ages for each analysis are represented in Figures 9.9 and 9.12. Both age populations demonstrate a high degree of concordancy as seen in the concordia diagrams (Figs. 9.8 and 9.11).

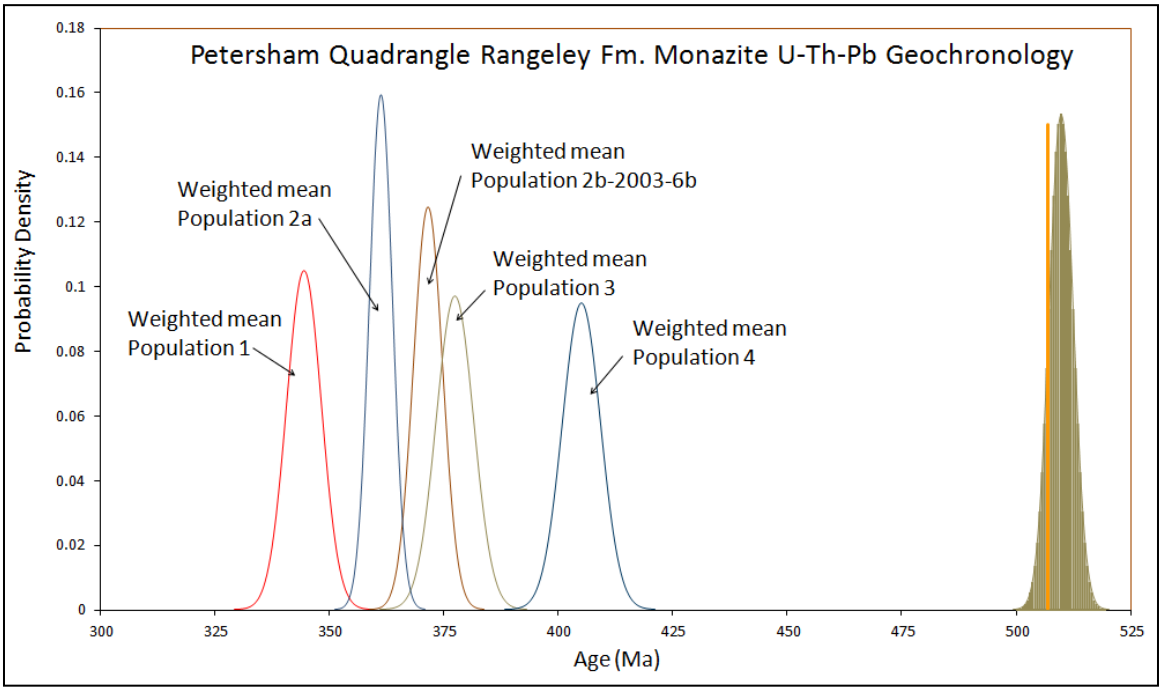

Figure 9.1. Probability age distribution function diagram that shows the weighted mean ages of the various age populations (Gaussian peaks) among monazite grains within selected samples of the Silurian Rangeley Fm. Peak at right shows ages obtained for the standard when treated as an unknown, and the accepted age for the monazite standard (gold bar) determined during this study and its accepted age determined by U-Pb ID-TIMS analysis.

Table 9.1. Table listing U-Pb ID-TIMS analysis dates with corresponding age spot locations and textural context.

Sample	Grain	Zone	Age	Textural Context
Population 1				
PE13-2001-6b	m1	low-Y core	340.5 ±6.2	Bt incl., aligned with foliation
PE13-2003-6b	m1	core3	343.6 ±3.3	Bt incl., small, equant
PE13-2003-6b	m9	core2	348.9 ±3.6	aligned with foliation
PE13-2002-5b	m3	low-Y core	349.7 ±2.0	insignificant, small, equant
Population 2a				
PE13-2002-5b	m11	low-Y core 3	355.4 ±3.1	Bt inclusion, unclear
PE13-2003-6b	m2	inner rim	355.7 ±2.2	aligned with foliation
PE13-2002-5b	m11	high-Y rim lower 3	355.7 ±2	Bt inclusion, unclear
PE13-2002-5b	m11	low-Y core	356.7 ±1.5	Bt inclusion, unclear
PE13-2001-6b	m3	low-Y core	356.7 ±3.9	aligned with foliation
PE13-2001-6b	m4	low-Y core	356.7 ±3.4	insignificant
PE13-2003-6b	m1	core 2	357.4 ±4.3	Small, equant, bt inclusion
PE13-2002-5b	m6	core	358.9 ±1.1	Grain boundary, insignificant
PE13-2001-6b	m5	high-Y rim south	359.4 ±2.0	Bt incl., aligned with foliation
PE13-2001-6b	m5	low-Y core	361.6 ±3.0	Bt incl., aligned with foliation
PE13-2003-6b	m9	II rim	362.4 ±1.5	aligned with foliation
PE13-2002-5b	m8	high-Y rim left	362.6 ±2.2	Equant, muscovite inclusion
PE13-2003-6b	m15	core	362.8 ±2.2	unknown
PE13-2001-6b	m4	high-Y rim left	363 ±2.2	insignificant
PE13-2002-5b	m6	core 3	364 ±4.1	Grain boundary, insignificant
PE13-2001-6b	m6	low-Y core	364 ±1.9	Bt inclusion
PE13-2001-6b	m1	high-Y rim left	364.6 ±3.7	Bt incl., aligned with foliation
PE13-2001-6b	m6	high-Y rim left	364.9 ±3.3	Bt inclusion, equant
PE13-2001-6b	m6	high-Y core	365.5 ±3.4	Bt inclusion
PE13-2002-5b	m11	high-Y bottom	365.7 ±5.3	Bt inclusion, unclear
Population 2b				
PE13-2003-6b	m11	core upper	367.2 ±3.2	Pfs inclusion, no fabric
PE13-2001-6b	m5	high-Y core	367.3 ±1.4	Bt inclusion, unclear
PE13-2003-6b	m2	low left rim	369 ±7.2	Aligned with foliation, bt inclusion
PE13-2003-6b	m15	low right rim	370.6 ±4.5	unknown
PE13-2001-6b	m3	high-Y rim	371.1 ±0.6	foliation
PE13-2003-6b	m11	up right rim	371.8 ±5.6	Pfs inclusion, no fabric
PE13-2003-6b	m5	upper	372.8 ±3.9	Grt inclusion
PE13-2003-6b	m6	lower	373.2 ±2.7	Grain boundary, no fabric
PE13-2002-5b	m3	upper rim	373.6 ±3.4	Bt inclusion, equant
Population 3				
PE13-2003-6b	m15	right spot	378.1 ±3.3	unknown

Table 9.1. (continued)

PE13-2002-5b	m6	low left rim	381.2 ±6.4	Grain boundary, insignificant
PE13-2002-5b	m13	low left rim	384 ±3.8	aligned with foliation
PE13-2002-5b	m8	high-Y core	388.3 ±5.9	Musc inclusion, equant
Population 4				
PE13-2002-5b	m13	low-Y core	396.2 ±5.5	aligned with foliation
PE13-2002-5b	m1	core	397.4 ±2.2	grain boundary, unclear
PE13-2001-6b	m4	high-Y core	398 ±10.1	grain boundary, equant
PE13-2001-6b	m7	high-Y core	409.2 ±3.3	Oblique to fabric
PE13-2002-5b	m13	high-Y core	415.7 ±3.5	aligned with foliation
PE13-2003-6b	m2	inner core	420.5 ±6.5	aligned with foliation

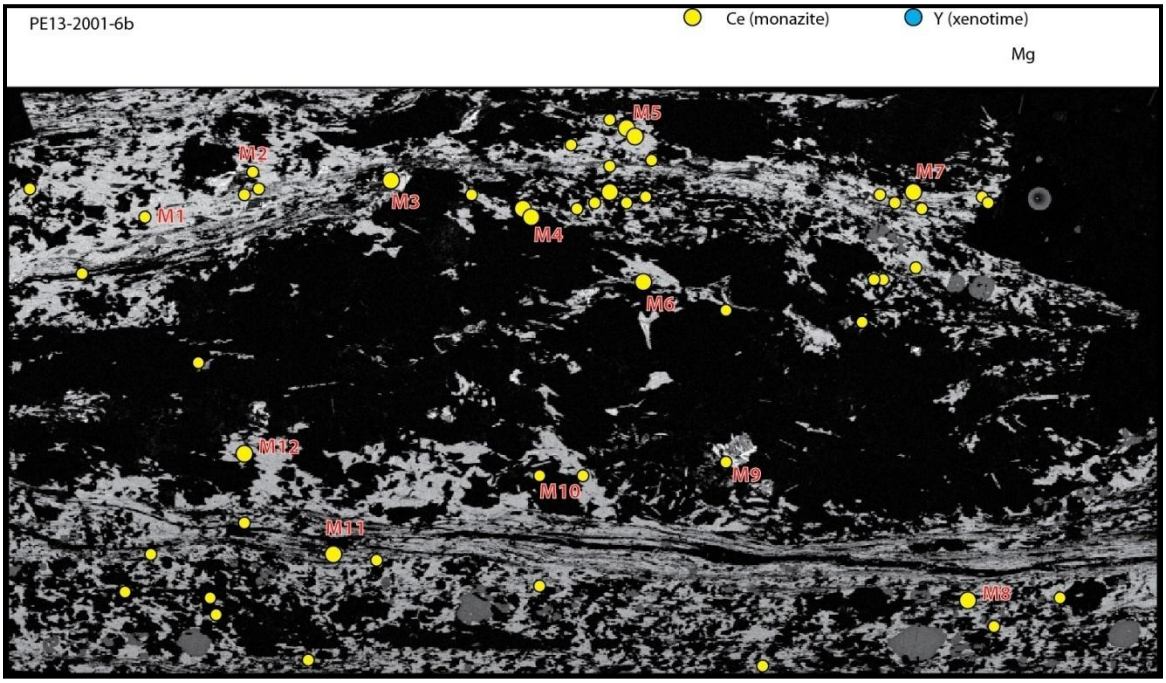

Figure 9.2. Mg X-Ray map of thin section PE13-2001-6b showing the location and textural context of dated monazite grains (yellow dots labeled with red letters). Brighter gray = biotite; medium gray = garnet, black = plagioclase or quartz.

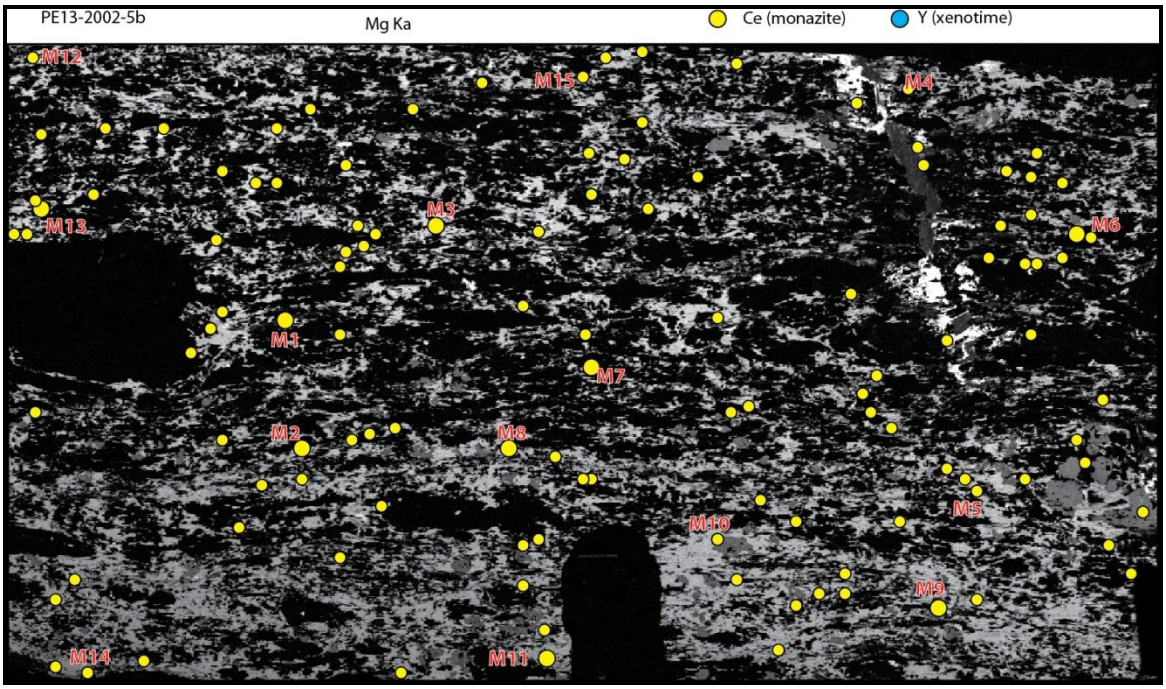

Figure 9.3. Mg X-Ray map of thin section PE13-2002-5b showing the location of dated monazite grains (yellow dots labeled with red letters).

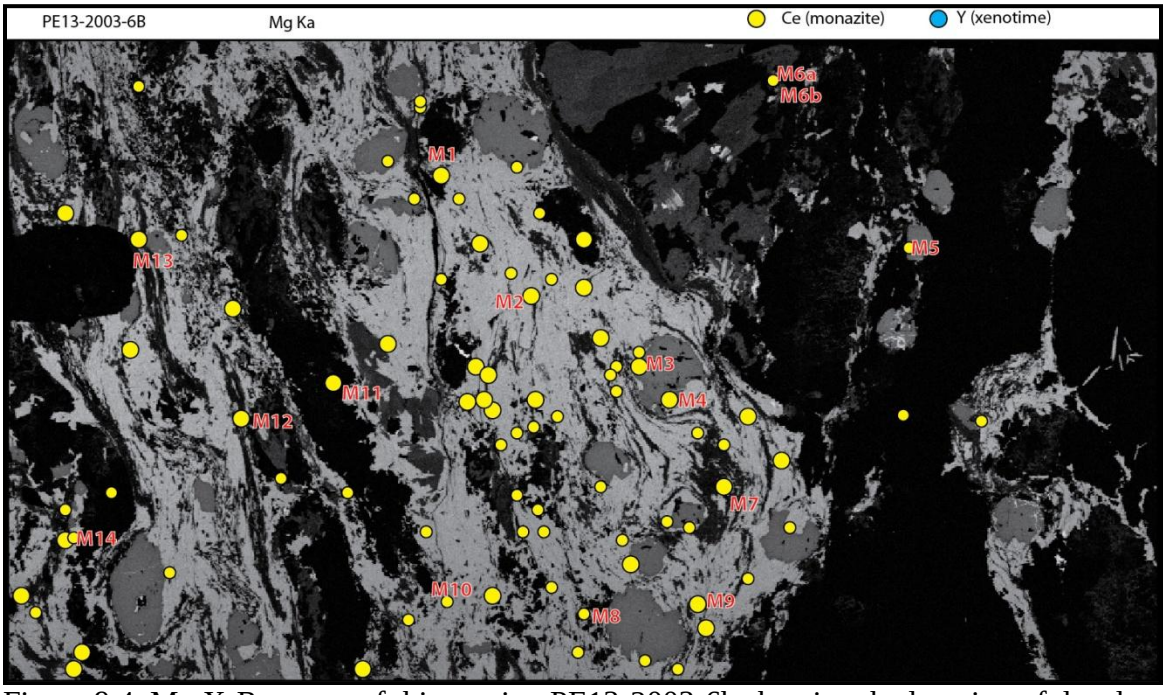

Figure 9.4. Mg X-Ray map of thin section PE13-2003-6b showing the location of dated monazite grains (yellow dots labeled with red letters).

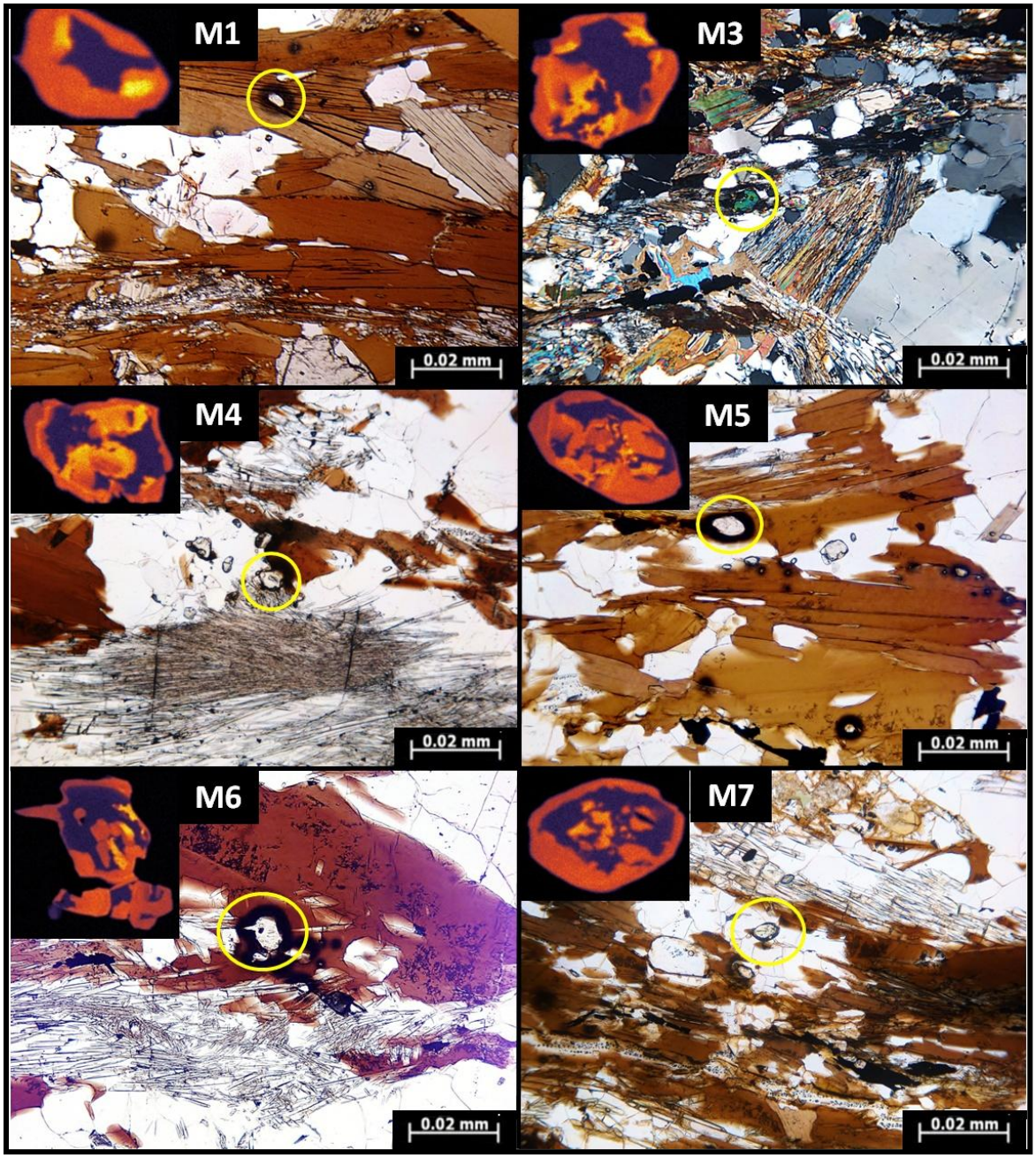

Figure 9.5. Figure showing Y maps of dated monazite grains from sample PE13-2001-6b and photomicrographs demonstrating their textural context. Monazite grains are circled in yellow.

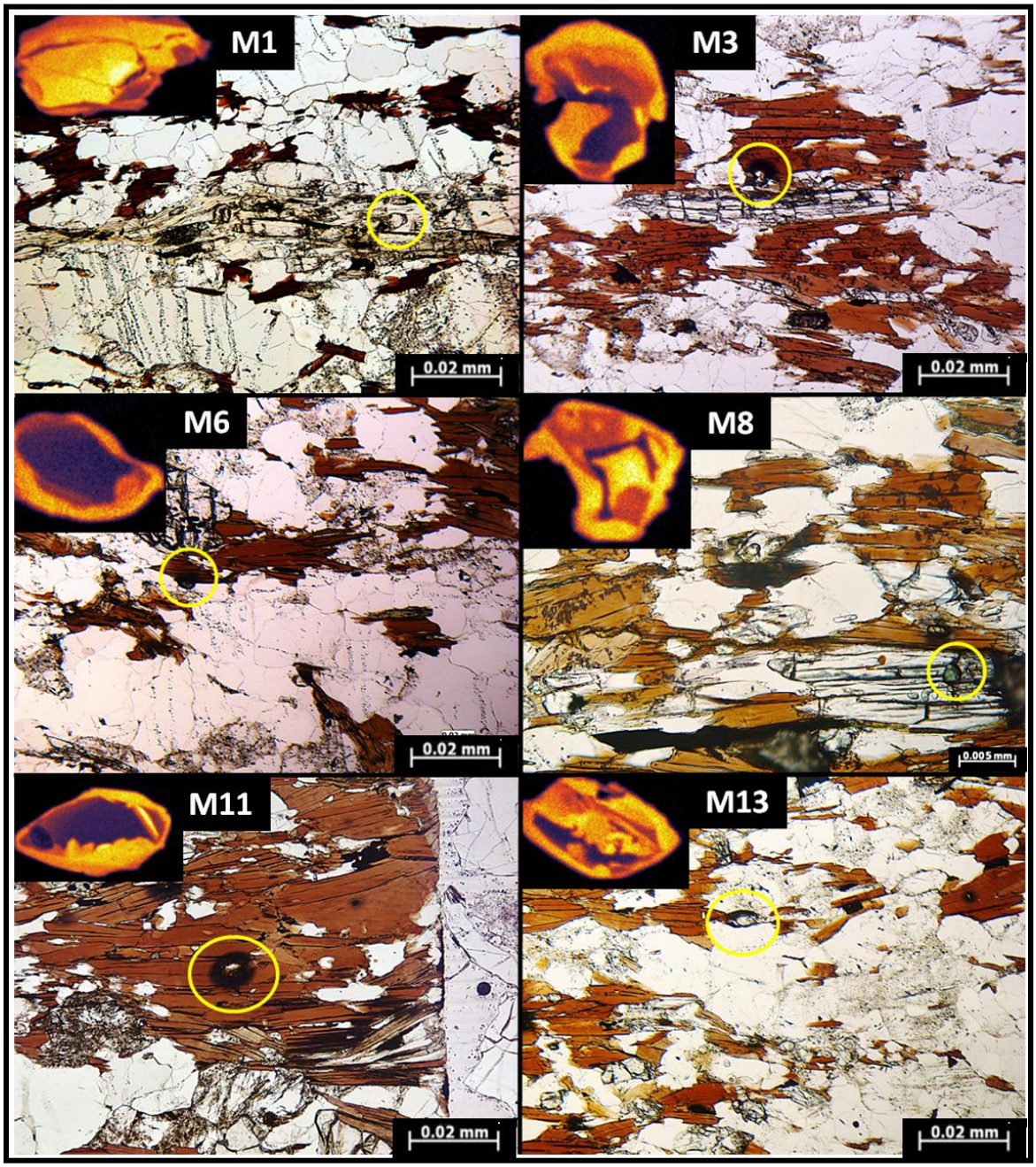

Figure 9.6. Figure showing Y maps of dated monazite grains from sample PE13-2002-5b and photomicrographs demonstrating their textural context. Monazite grains are circled in yellow.

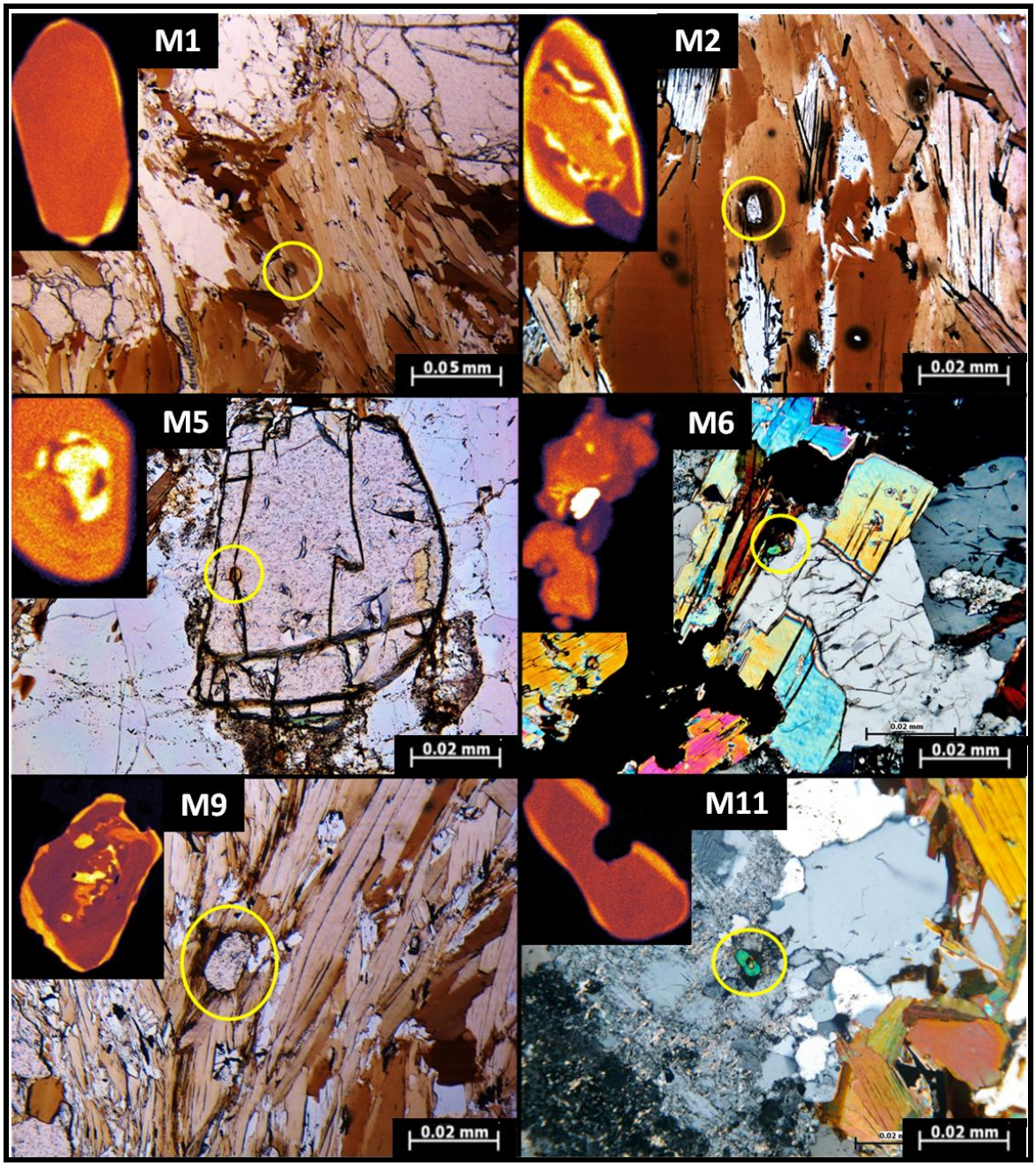

Figure 9.7. Figure showing Y maps of dated monazite grains from sample PE13-2003-6b and photomicrographs demonstrating their textural context. Monazite grains are circled in yellow.

Table 9.2. Table listing U-Pb zircon isotope analysis data for Nichewaug Sill.

Name	*206Pb/ 238U*	*207Pb/ 235U*	*207Pb/ 206Pb*	*206Pb*/ 238U*	*207Pb*/ 235U*	*207Pb*/ 206Pb**
2014_10_29Oct\ PE13-2004_Gr2.ais	351	348	326	5.59E-02	4.08E-01	5.29E-02
2014_10_29Oct\ PE13-2004_Gr3.ais	358	361	376	5.71E-02	4.26E-01	5.41E-02
2014_10_29Oct\ PE13-2004_Gr4.ais	372	362	297	5.94E-02	4.28E-01	5.23E-02
2014_10_29Oct\ PE13-2004_Gr5.ais	380	373	330	6.08E-02	4.44E-01	5.30E-02
2014_10_29Oct\ PE13-2004_Gr7.ais	345	366	495	5.50E-02	4.33E-01	5.71E-02
2014_10_29Oct\ PE13-2004_Gr11.ais	356	344	263	5.67E-02	4.03E-01	5.15E-02
2014_10_29Oct\ PE13-2004_Gr12.ais	352	352	348	5.62E-02	4.14E-01	5.35E-02
2014_10_29Oct\ PE13-2004_Gr13.ais	381	381	386	6.08E-02	4.56E-01	5.44E-02
2014_10_29Oct\ PE13-2004_Gr19.ais	359	336	180	5.73E-02	3.92E-01	4.97E-02

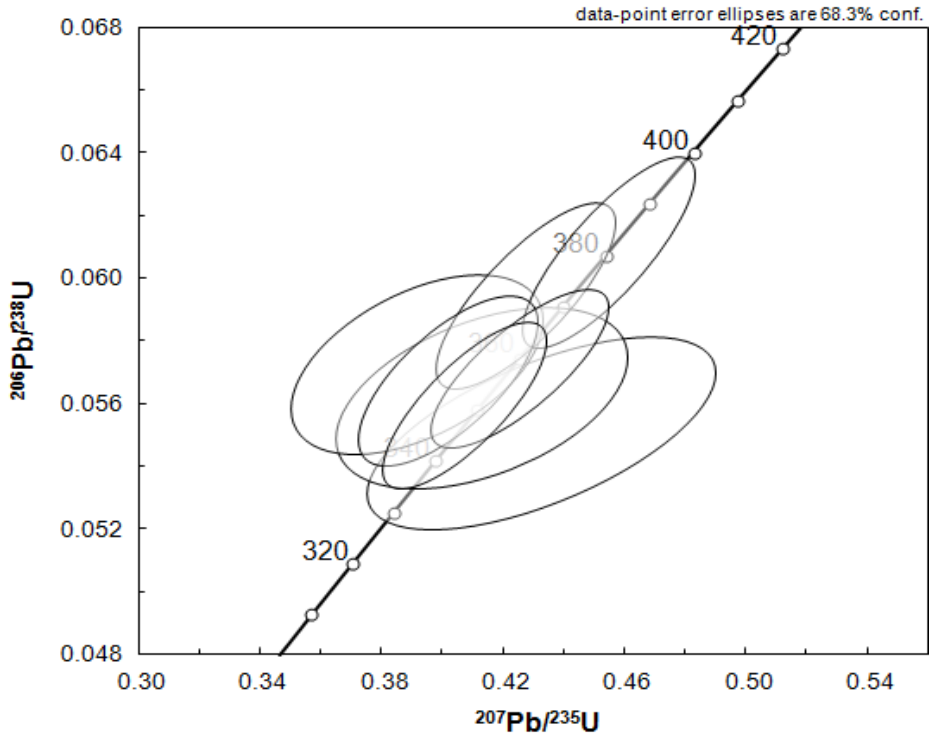

Figure 9.8. U-Pb Concordia diagram for Nichewaug Sill.

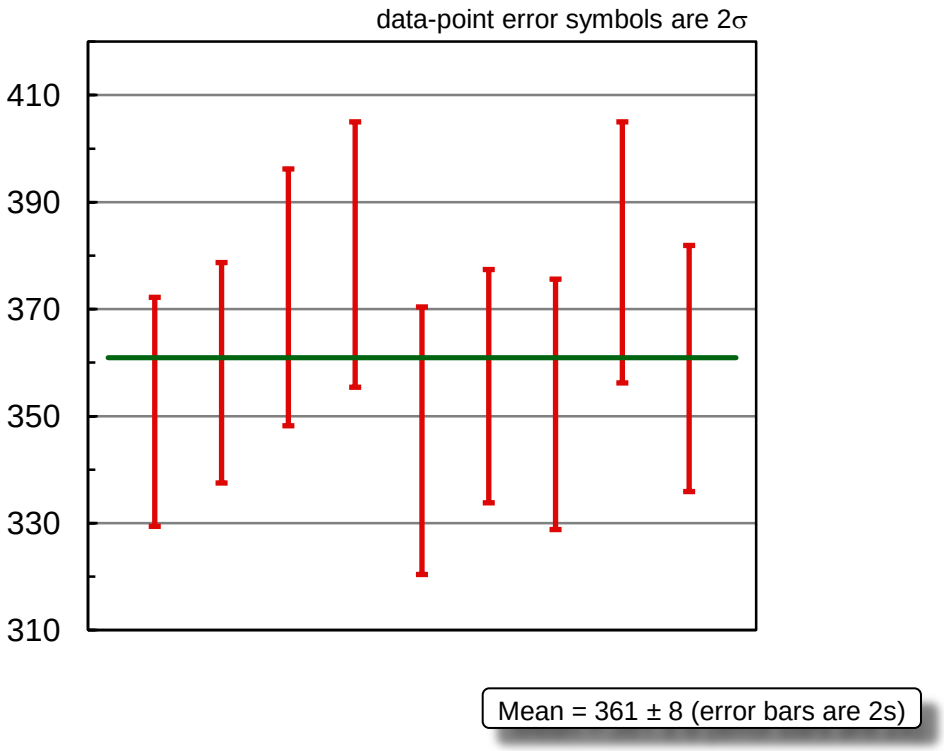

Figure 9.9.Weighted mean U-Pb zircon age from a sample of the Nichewaug Sill from a sample within the map area.

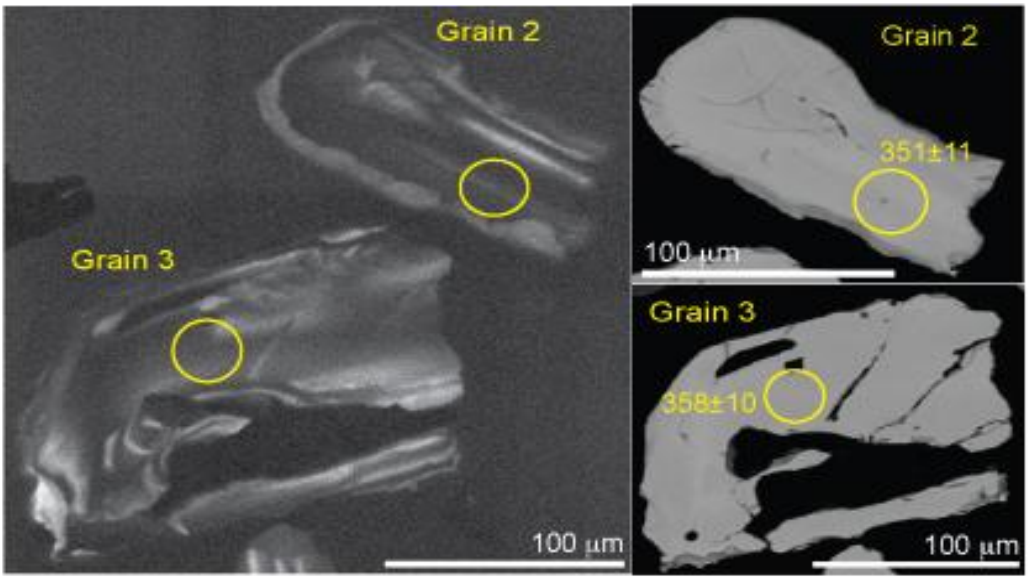

Figure 9.10. Cathodoluminescent (left) and backscattered electron (right) images of zircon grains separated from Nichewaug quartz-diorite sample PE13-2004. Yellow circles are location of beam spots selected for SIMS U-Pb geochronology.

Table 9.3. Table listing U-Pb zircon isotope analysis data for Hardwick Tonalite.

Name	Age (Ma) *206Pb/ 238U*	Age (Ma) *207Pb/ 235U*	Age (Ma) *207Pb/ 206Pb*	*206Pb*/ 238U*	*207Pb*/ 235U*	*207Pb*/ 206Pb**
2014_10_29Oct\ PE12-10A_Gr4.ais	472	457	381	7.60E-02	5.68E-01	5.42E-02
2014_10_29Oct\ PE12-10A_Gr6.ais	469	454	375	7.55E-02	5.63E-01	5.41E-02
2014_10_29Oct\ PE12-10A_Gr5.ais	466	463	448	7.50E-02	5.78E-01	5.59E-02
2014_10_29Oct\ PE12-10A_Gr10.ais	447	444	428	7.18E-02	5.48E-01	5.54E-02
2014_10_29Oct\ PE12-10A_Gr12.ais	488	474	408	7.86E-02	5.95E-01	5.49E-02
2014_10_29Oct\ PE12-10A_Gr9.ais	473	472	463	7.62E-02	5.91E-01	5.63E-02
2014_10_29Oct\ PE12-10A_Gr8.ais	476	474	467	7.66E-02	5.95E-01	5.64E-02

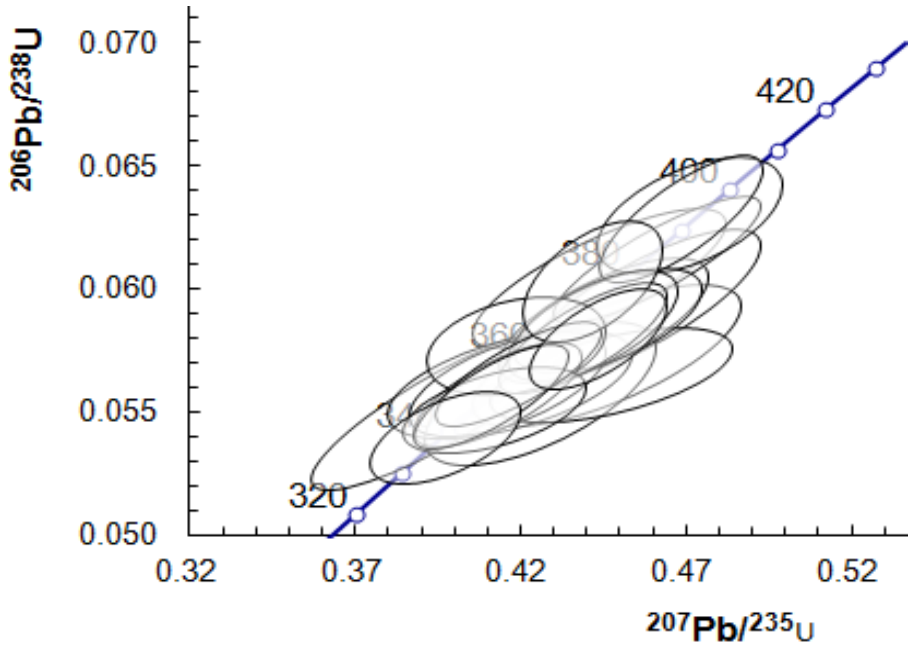

Figure 9.11. U-Pb concordia diagram for analyses of Hardwick tonalite.

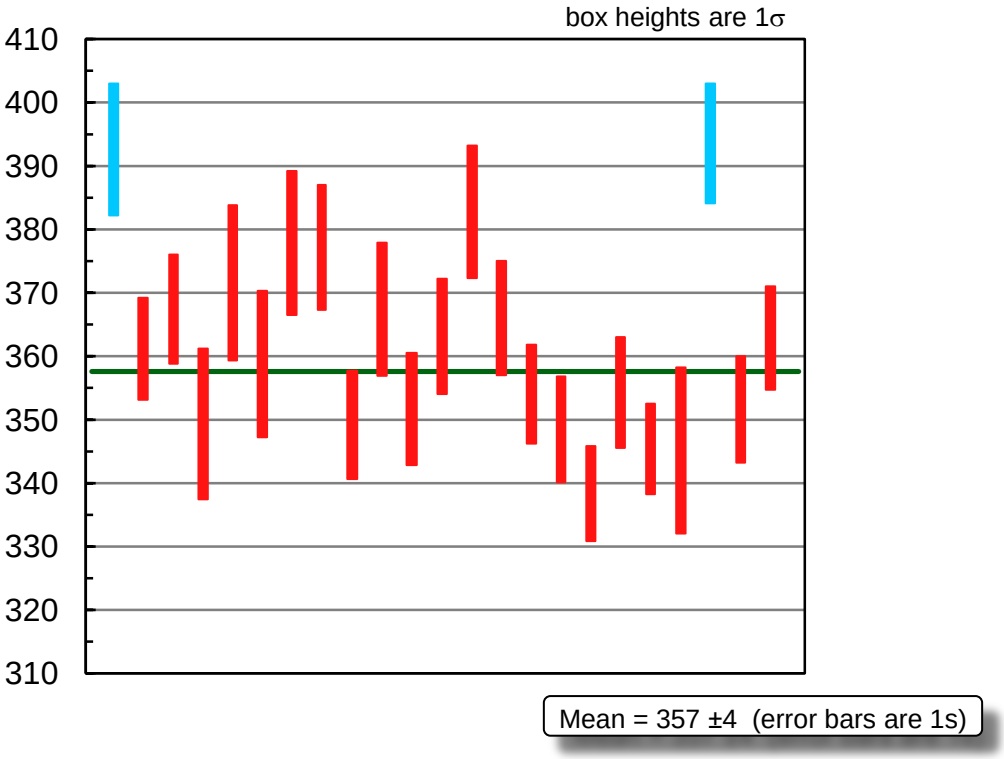

Figure 9.12.Weighted mean U-Pb zircon age from a sample of the Hardwick tonalite.

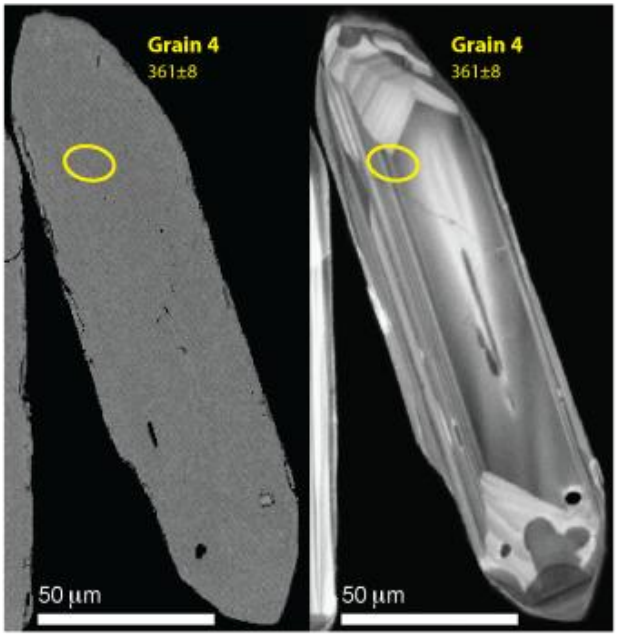

Figure 9.13. Backscattered electron and cathodoluminescent images of representative zircon grain separated from Hardwick Tonalite sample PE12-10A. Yellow circles are location of beam spots selected for SIMS U-Pb geochronology.

CHAPTER X. KINEMATIC INTERPRETATION

The general deformational pattern within the map area is pervasive strike-normal flattening with partitioned strike-parallel extension. Localized noncoaxial (sinistral) shear was observed locally along the Rangeley-Hardwick contact. Deformation is most intense in contact regions where thermally driven metamorphism resulted in partial melting and complex interfolding of lithologic units at multiple scales.

A. Flattening

Flattening strain (E-W shortening) is evident in all three of the main lithologic units. In the Monson, flattening is expressed in a pervasive moderately west-dipping foliation, planar bimodal layering of granitic gneiss and amphibolite (Fig. 5.1 and Fig. 5.2), and leucocratic banding and slabby appearance in the Monson amphibolite (Fig. 5.3, Fig. 7.2, and Fig. 7.3). A similar west-dipping foliation is almost as pervasive in the Rangeley (Fig. 5.4 and Fig. 5.5) as well as layering of paraschist and paragneiss with flattened leucosome (Fig. 7.4). The moderately west-dipping foliation is weakest in the younger Hardwick tonalite and is present in approximately half of the observed outcrops. This lack of intensity and occurrence is presumably because the Hardwick has endured fewer collisional orogenic events than the other two lithologies and is much more competent than the Rangeley Formation. Flattening is also evident in leucopegmatite which is occasionally foliated in a manner consistent with its surrounding lithologies.

B. Extension

North-south extension is more localized within the map area and is partitioned predominantly into the Rangeley formation as expressed by a sillimanite mineral stretching lineation and disaggregated leucosome (Fig. 7.7). In more rare cases, boudins of Monson amphibolite show a strong lineation defined by aligned hornblende needles and feldspar streaks (Fig. 7.8). This lineation in the Monson amphibolite is consistent in orientation with that in the Rangeley. Evidence of strike-parallel extension is absent in all other lithologies in the map area.

C. Noncoaxial Strain

In contrast to findings in the Palmer area, noncoaxial strain is largely absent within the Rangeley of the Petersham quadrangle. In fact, dextral shear is found nowhere within the map area. Sinistral (east to north) kinematics are constrained to contact regions between the Rangeley and Hardwick. Evidence for this includes asymmetrically folded leucosome (Fig. 7.6) and asymmetric porphyroclast tails (Fig. 8.3 and Fig. 8.4) which occur in both lithologies. Only two outcrops were discovered in the map area along this contact zone and sinistral kinematic indicators were present at both. Therefore, the extent to which this deformational style continues long strike to the north and south and whether it is a consistent or localized occurrence is inferred but not documentable.

D. Folding in Contact Regions

Deformation is most intense in contact regions between the Rangeley Formation and the two orthogneiss bodies. In contact regions, the two bounding lithologies were

complexly interfolded at various scales (outcrop to map: Fig. 6.2 and Fig. 7.5). Furthermore, the abundance of leucosome in outcrops closest to the Hardwick, and the contemporaneity of the Hardwick zircon crystallization ages and Rangeley monazite ages, is consistent with heating by the Hardick causing partial melting of the Rangeley Formation. At the Rangeley-Hardwick contact region in particular, intense deformation is demonstrated by a very strong foliation in both lithologies, a profusion of flattened leucosome, and two generations of folds in the Rangeley (Fig. 10.2 and Fig. 10.2). The widespread abundance of leucosome and intense deformation and metamorphism throughout the Rangeley lead to the inference that the Hardwick pluton was not the only source of heat. It is probable that heat various other magmatic intrusions, such as the Nichewaug Sill, contributed to this widespread metamorphism, deformation, and melting.

Figure 10.1. Field photo showing horizontal face of strongly foliated Hardwick tonalite with asymmetrically folded (east to north) leucosome at the Sr-Dh contact at Carter Road.

Figure 10.2. Field photo showing horizontal face of strongly foliated, migmatitic Rangeley with 1-2 cm garnets at the Sr-Dh contact at Carter Road.

CHAPTER XI. DISCUSSION

The purposes of this study were to: (1) to delineate the distribution of lithologic units within the study area, (2) to assess the significance of dominant fabrics and structures in the study area in the context of regional dextral transpression, (3) to determine the timing of metamorphism and deformation within the map area (geochronology), and (4) to relate the findings within the study area to those of previous studies in central Massachusetts, especially Massey and Moecher (2008, 2013).

A. Geochronology

Metamorphic ages of the Rangeley Fm. determined by U-Th-Pb electron microprobe chemical age dating of monazite grains reveal a protracted history of multiple metamorphic/deformational episodes defined by the various age populations that mostly cluster near 360 Ma. Population 3 (~378 Ma) corresponds to the time of late Acadian regional metamorphism in the Connecticut Valley Zone (Ayuso and Arth, 1990; Lanzirotti and Hanson, 1995). Population 4 (~405 Ma) corresponds to the age of extensive granite plutonism (New Hampshire Plutonic Suite) in the Central Maine Terrane (Solar et al., 1999; Dorais, 2003). Sub-population 2b (~370 Ma) probably corresponds to the same metamorphic event as population 3. The various ages of population 2a (~ 360 Ma) correspond to the age of the Hardwick tonalite, Petersham qtz-diorite sill, Walker Mtn. orthogneiss, and Diorite of West Warren in the western Central Maine terrane (Walker, 2012). The youngest population (1) (340 Ma) is taken as the time of retrograde metamorphism, garnet breakdown and sillimanite + biotite growth accompanying regional transpression as determined by Massey and Moecher (2013).

There is no textural evidence relating younger episodes of monazite growth with the generation of the most recent fabrics. It is apparent that nearly all elongate grains surrounded by a metamorphic fabric grew or rotated into alignment regardless of growth history (Table 9.1, Figs. 9.6-9.7).

The average U-Pb SIMS age of 361 ± 8 Ma for the Nichewaug quartz-diorite confirms its emplacement in the Devonian as previously mapped by Zen et al. (1983). The essentially identical ages of the Nichewaug and Hardwick (357 ± 4 Ma) plutons suggest that intrusion of the Hardwick and smaller intrusions of similar age were a major source of heat for the latest episodes of metamorphism and melting of the Rangeley. This is confirmed by the abundance of U-Th-Pb monazite ages at approximately 360 Ma.

B. Partitioned Flattening and Extension

The general pattern of deformation within the map area is of flattening and extension that are concentrated into the lesser competent Rangeley Fm. and the margins of the plutonic units. This is consistent with typical patterns in continental orogens where deformation tends to concentrate in complex zones that bound more resistant rheologies (e.g. Dewey et al., 1998).

The overall deformational patterns in the area show similarities to what is described as subdomain 7 from Massey and Moecher (2013), which is also in closest geographic proximity to the study area. This is evident in the relatively weak intensity of the foliation within the Monson coupled with its average orientation (181/39W) which has a much shallower dip than foliations found in other subdomains (5, 6, and 8) of Massey and Moecher (2013). This, coupled with the presence of only one lineation

(horizontal) within the Rangeley, suggests that the intensity of deformation is attenuating to the north. This trend continues at least as far as the Winchendon quadrangle (O'Brien, 2009). The fact that lateral escape tectonics attenuate so quickly away from the Palmer area is expected since kinematic/space requirements make this type of deformation possible only at smaller scales (Dewey et al., 1998).

C. Sinistral Kinematics

Sinistral deformation, though not necessarily expected in a dextral transpressive regime, is required for lateral extrusion/escape tectonics proposed for the Palmer area (Massey and Moecher, 2013). In this case, bounding zones of opposite shear sense accommodated northward escape of the Monson relative to its boundary zones. In this context, the possible implication for finding sinistral shear along the western margin of the Hardwick is a tectonic motif in which orthogneiss masses are escaping laterally relative to metastratified sequences to accommodate shortening across the transpressive tectonic regime of the Appalachian orogen. Since the region of highest E-W shortening of the Monson is farther to the south (Fig. 2.1), kinematic indicators of its lateral escape are evident in that area. The Hardwick, which is still highly attenuated in the Petersham area shows evidence that may be interpreted as northward escape as well.

D. Further Research

The geographic extent of sinistral kinematics along the western margin of the Hardwick needs to be investigated along strike to the north and south. Kinematic analysis of the eastern margin of the pluton is necessary in order to determine if dextral

asymmetries are present. Confirmation of dextral asymmetries along the eastern margin of the Hardwick would strongly suggest the northward escape of the Hardwick relative to bounding metasedimentary units. In contrast, a lack of dextral kinematics along the eastern margin of the Hardwick would mean that the sinistral asymmetries found in the Petersham quadrangle are a localized phenomenon caused by compatibility maintenance necessitated by heterogeneously deforming rocks. If the former case is established, it would be appropriate to establish additional deformational timing constraints to provide insight into temporal development of this system relative to that described in the Palmer area.

APPENDIX A

Table 1. Petersham outcrop, sample, structural data

Key
# = station #
x = longnitude
y = lattitude
Unit = map unit
s/s = strike of foliation
s/d = dip of foliation
s/dd = dip direction of foliation
l/t = trend of lineation
l/p = plunge of lineation
l/pd = plunge direction of lineation

#	x	y	Unit	s/s	s/d	s/dd	l/t	l/p	l/pd	sample
1a	-72.212	42.424	no outcrop	-	-	-	-	-	-	-
1b	-72.211	42.421	no outcrop	-	-	-	-	-	-	-
2	-72.207	42.427	Sr	-	-	-	-	-	-	-
3	-72.226	42.488	Om	-	-	-	-	-	-	-
4	-72.211	42.498	Sr	-	-	-	-	-	-	-
5	-72.205	42.498	Sr	-	-	-	-	-	-	-
6	-72.166	42.449	Dh	-	-	-	-	-	-	-
7a	-72.249	42.401	Om	-	-	-	-	-	-	-
7b	-72.249	42.402	Om	-	-	-	-	-	-	-
7c	-72.247	42.403	Om	-	-	-	-	-	-	-
7d	-72.243	42.403	Om	-	-	-	-	-	-	-
7e	-72.239	42.409	Om	-	-	-	-	-	-	-
7f	-72.241	42.407	Om	-	-	-	-	-	-	-
7g	-72.241	42.393	Om	-	-	-	-	-	-	-
8a	-72.138	42.384	rh	-	-	-	-	-	-	-
8b	-72.135	42.383	ch	-	-	-	-	-	-	-
9	-72.186	42.438	Dh	-	-	-	-	-	-	-
10a	-72.182	42.456	Dh	-	-	-	-	-	-	-
10b	-72.182	42.453	Dh	-	-	-	-	-	-	-
11	-72.204	42.435	Sr	-	-	-	-	-	-	-
12a	-72.196	42.418	Dh	-	-	-	-	-	-	-
12b	-72.197	42.417	Dh	-	-	-	-	-	-	-
12c	-72.197	42.414	Dh	-	-	-	-	-	-	-
13a	-72.216	42.465	Om	-	-	-	-	-	-	-
13b	-72.216	42.466	Sr	-	-	-	-	-	-	-
13c	-72.218	42.464	Sr	-	-	-	-	-	-	-

Table 1. (continued)

13d	-72.222	42.465	Om	-	-	-	-	-	-	-
13e	-72.222	42.466	Om	-	-	-	-	-	-	-
13f	-72.222	42.470	Om	-	-	-	-	-	-	-
13h	-72.221	42.471	Om	-	-	-	-	-	-	-
13i	-72.219	42.471	Om/Sr	-	-	-	-	-	-	-
13j	-72.218	42.471	Sr	-	-	-	-	-	-	-
14a	-72.225	42.461	Sr	-	-	-	-	-	-	-
15	-72.227	42.462	Om	-	-	-	-	-	-	-
16	-72.225	42.459	Sr	-	-	-	-	-	-	-
17	-72.225	42.458	Om	-	-	-	-	-	-	-
18	-72.140	42.389	Dh	-	-	-	-	-	-	-
19	-72.143	42.391	Dh	-	-	-	-	-	-	-
20	-72.129	42.393	rh	-	-	-	-	-	-	-
21	-72.126	42.390	ch	-	-	-	-	-	-	-
22a	-72.181	42.485	Dh	-	-	-	-	-	-	-
22b	-72.180	42.484	Dh	-	-	-	-	-	-	-
23a	-72.179	42.483	Sr	-	-	-	-	-	-	-
23b	-72.179	42.482	Sr	-	-	-	-	-	-	-
23c	-72.179	42.482	Sr	-	-	-	-	-	-	-
24	-72.217	42.471	Sr	-	-	-	-	-	-	-
25	-72.217	42.390	Sr	-	-	-	-	-	-	-
26a	-72.196	42.432	Sr	-	-	-	-	-	-	-
26b	-72.195	42.431	Dh	-	-	-	-	-	-	-
26c	-72.195	42.432	Dh w/Sr	-	-	-	-	-	-	-
27	-72.166	42.489	Dh	-	-	-	-	-	-	-
28	-72.165	42.488	Sr	-	-	-	-	-	-	-
29	-72.165	42.488	?	-	-	-	-	-	-	-
30	-72.165	42.487	Sr	-	-	-	-	-	-	-
31	-72.166	42.487	?	-	-	-	-	-	-	-
32	-72.128	42.491	Dh	-	-	-	-	-	-	-
33	-72.148	42.488	Dh	-	-	-	-	-	-	-
34	-72.168	42.496	Dh	-	-	-	-	-	-	-
35	-72.169	42.497	Dh	-	-	-	-	-	-	-
36	-72.169	42.496	Dh	-	-	-	-	-	-	-
37	-72.171	42.461	Dh	-	-	-	-	-	-	-
38a	-72.196	42.432	Sr	-	-	-	-	-	-	-
38b	-72.195	42.432	Dh	-	-	-	-	-	-	-
38c	-72.191	42.435	Dh	-	-	-	-	-	-	-
38d	-72.190	42.434	Dh	-	-	-	-	-	-	-
38e	-72.194	42.435	Dh	-	-	-	-	-	-	-
38f	-72.191	42.439	Dh	-	-	-	-	-	-	-
38g	-72.187	42.439	Dh	-	-	-	-	-	-	-

Table 1. (continued)

140	140303	915896	lp	-		-	-	-		-		-
141	140307	915940	lp	-		-	-	-		-		-
142	140337	916022	lp	-		-	-	-		-		-
143	140425	916057	lp	-		-	-	-		-		-
144	140431	916041	lp>Om	-		-	-	-		-		-
145	140465	916029	Om	-		-	-	-		-		-
146	140490	916008	lp	-		-	-	-		-		-
147	140510	916015	lp>Om	-		-	-	-		-		-
148	140560	916026	Sr		339		32	W	-		-	-
149	140600	916061	lp>Sr	-		-	-	-		-		-
150	140677	916109	lp>Sr	-		-	-	-		-		-
151	140742	916070	lp>Sr	-		-	-	-		-		-
152	140800	916096	lp>Sr	-		-	-	-		-		-
153	140805	915833	lp>Sr	-		-	-	-		-		-
155	140757	915904	lp>Sr	-		-	-	-		-		-
156	140366	915575	lp>Om	-		-	-	-		-		-
157	145043	916647	Dh	-		-	-	-		-		-
158	145013	916609	Dh	-		-	-	-		-		-
159	144972	916587	Dh	-		-	-	-		-		-
160	145034	916399	Dh	-		-	-	-		-		-
161	145079	916499	Dh		314		15	NW	-		-	-
162	144497	914843	Sr	-		-	-	-		-		-
163	144392	914862	Sr	-		-	-	-		-		-
164	144499	913911	Sr	-		-	-		10		25	SW	-
165	141891	908734	lp	-		-	-	-		-		-
166	141963	908714	lp	-		-	-	-		-		-
167	142042	908907	Sr	-		-	-	-		-		-
168	142085	908990	Ddi	-		-	-	-		-		-
169	142085	909083	Ddi	-		-	-	-		-		-
170	142134	909089	Ddi	-		-	-	-		-		-
171	142103	909255	Ddi	-		-	-	-		-		-
172	142104	909355	Ddi	-		-	-	-		-		-
173	142075	909356	Sr		9		90	-	-		-	-
174	142098	909637	Ddi	-		-	-	-		-		-
175	142087	909632	Sr	-		-	-	-		-		-
176	141566	916556	Ddi	-		-	-	-		-		-
177	141577	916470	Ddi	-		-	-	-		-		-
178	141526	916388	Ddi	-		-	-	-		-		-
179	141661	916409	Ddi	-		-	-	-		-		-
180	142239	908097	-	-		-	-	-		-		-
181	141367	916683	lp>Sr	-		-	-	-		-		-
182	141488	916617	lp>Sr	-		-	-	-		-		-

Table 1. (continued)

183	141519	916656	Sr		-	-	-	-	-	-	-	
184	141553	916622	Sr	-	-	-	-	-	-	-	-	
185	141554	916600	Sr	-	-	-		185		5	S	-
186	141552	916520	Ddi	-	-	-	-	-	-	-	-	
187	141532	916548	Sr	-	-	-	-	-	-	-	-	
188	141597	916462	Ddi	-	-	-	-	-	-	-	-	
189	141576	916379	Ddi.	-	-	-	-	-	-	-	-	
190	141523	916391	Ddi	-	-	-	-	-	-	-	-	
192	141526	916373	Sr	-	-	-	-	-	-	-	-	
193	141532	916374	Ddi.	-	-	-	-	-	-	-	-	
194	141569	916268	Sr	-	-	-	-	-	-	-	-	
194	141558	916214	Sr	-	-	-	-	-	-	-	-	
195	141568	916087	Sr	-	-	-	-	-	-	-	-	
196	141571	916089	Ddi	-	-	-	-	-	-	-	-	
197	141760	916045	Ddi	-	-	-	-	-	-	-	-	
198	141712	916162	-	-	-	-	-	-	-	-	-	
198	141672	916203	-	-	-	-	-	-	-	-	-	
199	141649	916223	Ddi	-	-	-	-	-	-	-	-	
199	141689	916308	-	-	-	-	-	-	-	-	-	
200	139006	904752	lp	-	-	-	-	-	-	-	-	
201	138993	904709	Om	-	-	-	-	-	-	-	-	
202	138949	904674	Om	-	-	-	-	-	-	-	-	
203	138945	904653	Om		170	36	W	-	-	-	-	
204	138915	904647	Om	-	-	-	-	-	-	-	-	
205	138841	904659	Om	-	-	-	-	-	-	-	-	
206	141693	910318	lp	-	-	-	-	-	-	-	-	
207	141727	910260	lp	-	-	-	-	-	-	-	-	
208	141798	910257	lp	-	-	-	-	-	-	-	-	
209	141916	910145	lp	-	-	-	-	-	-	-	-	
210	141920	910308	Sr	-	-	-	-	-	-	-	-	
211	141944	910260	-	-	-	-	-	-	-	-	-	
212	141950	910240	lp>Sr	-	-	-	-	-	-	-	-	
213	141926	910274	lp>Sr	-	-	-	-	-	-	-	-	
214	141993	910312	lp>Sr	-	-	-	-	-	-	-	-	
215	142057	910329	Ddi	-	-	-	-	-	-	-	-	
216	142047	910373	lp>Ddi	-	-	-	-	-	-	-	-	
217	142005	910435	lp>Sr	-	-	-	-	-	-	-	-	
218	141705	910698	lp	-	-	-	-	-	-	-	-	
219	141750	910617	Sr	-	-	-	-	-	-	-	-	
220	141603	906592	Ddi	-	-	-	-	-	-	-	-	
221	141563	906499	peg	-	-	-	-	-	-	-	-	
222	141557	906500	Ddi	-	-	-	-	-	-	-	-	

Table 1. (continued)

223	141627	906393	peg	-		-	-	-		-		-
224	141600	906347	peg	-		-	-	-		-		-
225	141617	906278	Ddi	-		-	-	-		-		-
226	141500	906236	lp>Sr	-		-	-	-		-		-
227	141526	906106	peg	-		-	-	-		-		-
228	141538	906073	Ddi	-		-	-	-		-		-
229	141522	906027	Ddi	-		-	-	-		-		PE13-229
230	141521	905932	Ddi	-		-	-	-		-		-
231	141504	905850	Ddi	-		-	-	-		-		-
232	141586	905611	peg	-		-	-	-		-		-
233	141526	905511	peg>Sr	-		-	-	-		-		-
234	141461	905475	Ddi	-		-	-	-		-		-
235	141428	905304	Ddi		44		35	W	-		-	-
236	141445	905258	Ddi	-		-	-	-		-		-
237	141467	905221	Sr	-		-	-	-		-		-
238	141459	905200	Sr	-		-	-		0		3	N -
239	141444	905196	Ddi	-		-	-	-		-		-
240	141423	905210	Ddi	-		-	-	-		-		-
241	141372	905210	Ddi	-		-	-	-		-		-
242	141326	905187	Ddi		2		90	-	-	-		-
243	141260	905118	Sr	-		-	-	-		-		-
244	141286	905101	Ddi	-		-	-	-		-		-
245	141290	904875	Ddi	-		-	-	-		-		-
246	138692	903036	Om	-		-	-	-		-		-
247	138670	903090	Om	-		-	-	-		-		-
248	138657	903149	Om	-		-	-	-		-		-
249	138676	903223	Om	-		-	-	-		-		-
250	138706	903266	Om		6		42	W	-		-	-
251	138748	903266	Om	-		-	-	-		-		-
253	138757	903482	Om	-		-	-	-		-		-
254	143807	911379	Dh		21		9	W	-		-	-
255	143751	911326	Dh		2		12	W	-		-	-
256	143693	911362	Dh	-		-	-	-		-		-
257	143667	911373	Dh	-		-	-	-		-		-
258	143671	911302	Dh	-		-	-	-		-		-
259	143630	911304	Dh	-		-	-	-		-		-
260	143663	911289	Dh	-		-	-	-		-		-
261	143680	911275	Dh	-		-	-	-		-		-
262	143689	911222	Dh	-		-	-	-		-		-
263	143657	911208	Dh	-		-	-	-		-		-
264	143638	911168	Dh	-		-	-	-		-		-

Table 1. (continued)

265	143599	911202	Dh	-	-	-	-	-	-	-
266	143565	911203	Dh	-	-	-	-	-	-	-
267	143568	911236	Dh	-	-	-	-	-	-	-
268	143588	911277	Dh	-	-	-	-	-	-	-
269	143631	911357	Dh	-	-	-	-	-	-	-
270	143568	911389	Dh	-	-	-	-	-	-	-
271	143531	911385	Dh	-	-	-	-	-	-	-
272	143411	911371	Dh	138	14	W	-	-	-	-
273	143358	911232	Dh	-	-	-	-	-	-	-
274	143267	911228	Dh	-	-	-	-	-	-	-
275	143244	911139	Dh	-	-	-	-	-	-	-
276	143308	910879	Dh	-	-	-	-	-	-	-
277	143353	910771	Dh	-	-	-	-	-	-	-
278	143334	910693	Dh	-	-	-	-	-	-	-
279	143279	910693	Dh	-	-	-	-	-	-	-
280	143254	910741	Dh	2	45	W	-	-	-	-
281	143288	910656	Dh	-	-	-	-	-	-	-
282	143372	910861	Dh	-	-	-	-	-	-	-
283	143402	910909	Dh	-	-	-	-	-	-	-
284	143383	910882	Dh	-	-	-	-	-	-	-
285	143393	910990	Dh	-	-	-	-	-	-	-
286	143582	911068	Dh	-	-	-	-	-	-	-
287	143603	911089	Dh	-	-	-	-	-	-	-
288	143598	911032	Dh	-	-	-	-	-	-	-
289	143609	911068	Dh	-	-	-	-	-	-	-
290	143644	910994	Dh	-	-	-	-	-	-	-
291	143635	911083	Dh	-	-	-	-	-	-	-
292	143666	911117	Dh	-	-	-	-	-	-	-
293	143665	911138	Dh	-	-	-	-	-	-	-
294	143687	911144	Dh	-	-	-	-	-	-	-
295	143677	911191	Dh	-	-	-	-	-	-	-
0	143722	911206	Dh							
0	143742	911204	Dh							
296	140711	912145	Om	-	-	-	-	-	-	-
297	140818	912162	Om	-	-	-	-	-	-	-
298	140885	912176	Om	-	-	-	-	-	-	-
299	140912	912202	Om	-	-	-	-	-	-	-
300	140742	912300	Om	-	-	-	-	-	-	-
301	140702	912277	Om	-	-	-	-	-	-	-
302	140700	912445	Om	-	-	-	-	-	-	-
303	140768	912535	Om	-	-	-	-	-	-	-
304	140814	912513	Om	-	-	-	-	-	-	-

Table 1. (continued)

305	140918	912296	Om	-		-	-	-	-	-	-
306	141045	912227	Om	-		-	-	-	-	-	-
307	141117	911889	Om	-		-	-	-	-	-	-
308	141147	911904	Sr		159		61	W	-	-	-
309	140971	911677	Om	-		-	-	-	-	-	-
310	140803	911567	Om	-		-	-	-	-	-	-
311	140714	911699	Om	-		-	-	-	-	-	-
312	140643	911631	Sr	-		-	-	-	-	-	-
313	140657	911598	Om	-		-	-	-	-	-	-
314	140652	911571	-	-		-	-	-	-	-	-
315	140664	911538	-	-		-	-	-	-	-	-
316	140651	911531	Om	-		-	-	-	-	-	-
317	140773	911298	Om	-		-	-	-	-	-	-
318	140769	911234	Om	-		-	-	-	-	-	-
319	140660	911303	Sr	-		-	-	-	-	-	-
320	140897	910871	Om	-		-	-	-	-	-	-
321	140953	910922	-	-		-	-	-	-	-	-
322	141012	910890	-	-		-	-	-	-	-	-
323	140996	910899	Om		33		28	SW	-	-	-
324	140973	910859	Om	-		-	-	-	-	-	-
325	141004	910768	Om	-		-	-	-	-	-	-
326	140977	910712	-	-		-	-	-	-	-	-
327	140936	910578	Om	-		-	-	-	-	-	-
328	141087	910422	-	-		-	-	-	-	-	-
329	141141	910387	Om	-		-	-	-	-	-	-
330	141225	910265	lp	-		-	-	-	-	-	-
331	141176	910191	Sr	-		-	-	-	-	-	-
332	141119	910219	-	-		-	-	-	-	-	-
333	141376	910385	lp>Sr	-		-	-	-	-	-	-
334	141377	910447	Sr	-		-	-	-	-	-	-
335	141251	910460	lp	-		-	-	-	-	-	-
336	141204	910546	lp	-		-	-	-	-	-	-
337	141169	910570	Om	-		-	-	-	-	-	-
338	141217	910630	lp	-		-	-	-	-	-	-
339	141160	910777	Om	-		-	-	-	-	-	-
340	141205	911001	Om-Sr	-		-	-	-	-	-	-
341	141136	910853	lp	-		-	-	-	-	-	-
342	141107	911058	lp	-		-	-	-	-	-	-
343	141169	911216	lp	-		-	-	-	-	-	-
344	141098	911259	Om	-		-	-	-	-	-	-
345	141062	911320	Om	-		-	-	-	-	-	-
346	141069	911399	lp	-		-	-	-	-	-	-

Table 1. (continued)

347	141011	911332	Om		167	65	W	-	-	-	-
348	140841	911754	lp>Om	-	-	-	-	-	-	-	-
377	138850	914211	Om	-	-	-	-	-	-	-	-
378	138938	914258	Om	-	-	-	-	-	-	-	-
379	139025	914304	Om	-	-	-	-	-	-	-	-
380	139020	914344	Om		154	35	SW	-	-	-	-
381	139137	914240	Om		145	66	SW	-	-	-	-
382	139124	914225	Om	-	-	-	-	-	-	-	-
383	139149	914119	Om	-	-	-	-	-	-	-	-
384	139160	914064	Om	-	-	-	-	-	-	-	-
385	139222	914044	Om	-	-	-	-	-	-	-	-
386	139261	914001	Om	-	-	-	-	-	-	-	-
387	139252	914123	Om	-	-	-	-	-	-	-	-
388	139194	914261	-	-	-	-	-	-	-	-	-
389	139209	914256	Om		130	27	W	-	-	-	-
390	139165	914381	Om	-	-	-	-	-	-	-	-
391	139115	914384	Om	-	-	-	-	-	-	-	-
392	138862	914349	Om	-	-	-	-	-	-	-	-
393	139039	914230	Om	-	-	-	-	-	-	-	-
394	139051	914198	Om	-	-	-	-	-	-	-	-
395	139021	914172	Om	-	-	-	-	-	-	-	-
396	138983	914116	Om	-	-	-	-	-	-	-	-
397	139059	914021	Om	-	-	-	-	-	-	-	-
398	139151	913944	Om	-	-	-	-	-	-	-	-
399	139131	913780	Om	-	-	-	-	-	-	-	-
400	138837	913491	Om	-	-	-	-	-	-	-	-
401	138742	913590	Om	-	-	-	-	-	-	-	-
402	138734	913591	Om	-	-	-	-	-	-	-	-
403	138566	913748	Om	-	-	-	-	-	-	-	-
404	138511	913607	Om	-	-	-	-	-	-	-	-
405	138430	913252	Om	-	-	-	-	-	-	-	-
406	138855	915795	Om	-	-	-	-	-	-	-	-
407	138756	915871	Om	-	-	-	-	-	-	-	-
408	138520	915901	Om	-	-	-	-	-	-	-	-
409	138505	915791	lp>Om	-	-	-	-	-	-	-	-
410	138744	915513	Om	-	-	-	-	-	-	-	-
411	138886	915309	Om	-	-	-	-	-	-	-	-
412	138886	915221	Om	-	-	-	-	-	-	-	-
413	138478	914617	Om	-	-	-	-	-	-	-	-
414	139461	915704	Om	-	-	-	-	-	-	-	-
415	139570	915467	Om	-	-	-	-	-	-	-	-
416	139533	915416	Om	-	-	-	-	-	-	-	-

Table 1. (continued)

417	139358	915350	Om	-	-	-	-	-	-	-	
418	139338	915248	Om	-	-	-	-	-	-	-	
419	139137	915814	Om	-	-	-	-	-	-	-	
420	139233	916057	Om	-	-	-	-	-	-	-	
421	139328	916162	Om	-	-	-	-	-	-	-	
422	139394	916298	Om	-	-	-	-	-	-	-	
423	139753	916509	Om	-	-	-	-	-	-	-	
424	139818	916591	?	-	-	-	-	-	-	-	
425	140068	916736	?	-	-	-	-	-	-	-	
426	139963	916775	Sr	-	-	-	-	-	-	-	
427	140005	916848	lp	-	-	-	-	-	-	-	
428	140072	916924	lp>Sr	-	-	-	-	-	-	-	
429	140102	916886	lp>Sr	-	-	-	-	-	-	-	
430	140056	916907	-	-	-	-	-	-	-	-	
431	140030	916892	Sr	-	-	-	-	-	-	-	
432	139865	916718	Om	-	-	-	-	-	-	-	
433	139782	916722	-	-	-	-	-	-	-	-	
434	139688	916698	Om	-	-	-	-	-	-	-	
435	139575	916413	Om	-	-	-	-	-	-	-	
436	139503	916562	Om	-	-	-	-	-	-	-	
437	140214	913950	?	-	-	-	-	-	-	-	
438	140190	913962	Om	-	-	-	-	-	-	-	
439	140059	914101	Om		182	35	W	-	-	-	-
440	140016	914070	Om		4	40	W	-	-	-	PE13-430
441	140016	914043	Om		4	27	W	200	10	S	PE13-431
442	139861	913948	Om	-	-	-	-	-	-	-	
443	139794	914164	-	-	-	-	-	-	-	-	
444	139475	914316	-	-	-	-	-	-	-	-	
445	139710	914735	Om	-	-	-	-	-	-	-	
446	139656	914932	Om	-	-	-	-	-	-	-	
447	139650	915013	Om	-	-	-	-	-	-	-	
448	139699	915177	Om	-	-	-	-	-	-	-	
449	139910	915158	Om	-	-	-	-	-	-	-	
450	139917	914888	-	-	-	-	-	-	-	-	
451	139957	914536	Om	-	-	-	-	-	-	-	
452	140003	914499	Om	-	-	-	-	-	-	-	
453	140013	914420	Om	-	-	-	-	-	-	-	
454	140010	914348	Om	-	-	-	-	-	-	-	
455	140016	914321	Om		215	30	NW	-	-	-	-
456	140079	914358	lp	-	-	-	-	-	-	-	
457	140051	914363	lp>Om	-	-	-	-	-	-	-	

Table 1. (continued)

458	140045	914270	Om		10	25	W	-	-		-	PE13-448
459	139959	914163	Om	-	-	-	-	-	-		-	PE13-449
460	139964	914112	Om	-	-	-		215		5	SW	-
461	140223	912982	Om	-	-	-	-	-	-		-	-
462	140385	914299	lp	-	-	-	-	-	-		-	-
463	140465	914550	Om	-	-	-	-	-	-		-	-
464	140487	914615	Om	-	-	-	-	-	-		-	-
465	140706	914963	lp	-	-	-	-	-	-		-	-
466	140702	915085	lp	-	-	-	-	-	-		-	-
467	140859	915145	lp	-	-	-	-	-	-		-	-
468	140873	915310	lp>Sr	-	-	-	-	-	-		-	-
469	140830	915300	Sr	-	-	-	-	-	-		-	-
470	140801	915291	lp	-	-	-	-	-	-		-	-
471	140641	915293	lp>Sr	-	-	-	-	-	-		-	-
472	140536	915295	-	-	-	-	-	-	-		-	-
473	140523	915330	Om	-	-	-	-	-	-		-	-
474	140500	915327	Om	-	-	-	-	-	-		-	-
475	140438	915338	lp>Om	-	-	-	-	-	-		-	-
476	140217	915126	Om	-	-	-	-	-	-		-	-
477	140246	915003	lp	-	-	-	-	-	-		-	-
478	140210	914892	Om		344	53	W	-	-		-	-
479	140195	914841	lp	-	-	-	-	-	-		-	-
480	140230	914753	lp	-	-	-	-	-	-		-	-
481	140226	914722	lp	-	-	-	-	-	-		-	-
482	140277	914699	lp	-	-	-	-	-	-		-	-
483	140394	914739	Sr?	-	-	-	-	-	-		-	-
484	140506	914975	Om	-	-	-	-	-	-		-	-
485	140718	912652	Om	-	-	-	-	-	-		-	-
486	140395	912511	lp	-	-	-	-	-	-		-	-
487	140368	912538	Sr	-	-	-		9		35	S	-
488	140331	912525	Om	-	-	-		7		4	S	-
489	140311	912621	lp	-	-	-	-	-	-		-	PE13-479
490	140248	912777	lp>Om	-	-	-	-	-	-		-	-
491	140281	912830	lp>Om	-	-	-	-	-	-		-	-
492	140275	912858	Om	-	-	-	-	-	-		-	-
493	140217	912961	Sr	-	-	-		17		2	S	-
494	140194	912953	Om	-	-	-	-	-	-		-	-
495	140178	912944	Om-Sr	-	-	-	-	-	-		-	-
496	140064	912939	Om-Sr	-	-	-		11		10	S	-
497	140026	913050	Om	-	-	-	-	-	-		-	-

Table 1. (continued)

498	139877	913240	lp	-	-	-	-	-	-	-
499	139911	913339	Om	-	-	-	-	-	-	-
500	139901	913398	Om	-	-	-	-	-	-	-
501	139792	913424	Om	-	-	-	-	-	-	-
502	139807	913877	Om	-	-	-	-	-	-	-
503	139926	913753	Om	-	-	-	-	-	-	-
504	140063	913765	Om	-	-	-	-	-	-	-
505	140193	913777	Om	-	-	-	-	-	-	-
506	140096	913978	-	-	-	-	-	-	-	-
507	140203	914218	Sr?	-	-	-	-	-	-	-
508	140152	914053	?	-	-	-	-	-	-	-
509	140481	912587	Sr	-	-	-	-	-	-	-
510	142345	916264	Sr	-	-	-	-	-	-	-
511	142207	916263	Sr	-	-	-	-	-	-	-
512	142144	916332	-	-	-	-	-	-	-	-
513	142074	916454	Sr	-	-	-	-	-	-	-
514	141981	916415	-	-	-	-	-	-	-	-
515	141752	915995	Ddi	-	-	-	-	-	-	-
516	141657	915948	Ddi	-	-	-	-	-	-	-
517	141627	915926	Sr-Ddi	-	-	-	-	-	-	-
518	141700	915868	Ddi	-	-	-	-	-	-	-
519	141674	915811	Ddi	-	-	-	-	-	-	-
520	141688	915768	Ddi	-	-	-	-	-	-	-
521	141705	915683	Ddi	-	-	-	-	-	-	-
522	141740	915627	Sr	-	-	-	-	-	-	-
523	141656	915484	Sr	-	-	-	-	-	-	-
524	141745	915487	Ddi	-	-	-	-	-	-	-
525	141713	915539	Ddi	-	-	-	-	-	-	-
526	141624	915608	Ddi	-	-	-	-	-	-	-
527	141677	915602	Ddi	-	-	-	-	-	-	-
528	141842	915595	Ddi	-	-	-	-	-	-	-
529	141864	915599	Ddi	-	-	-	-	-	-	-
530	141904	915659	Ddi	-	-	-	-	-	-	-
531	141930	915717	Sr	35	23	SW	-	-	-	-
532	141845	915836	Ddi	-	-	-	-	-	-	-
533	141806	915954	Ddi	-	-	-	-	-	-	-
534	142035	915686	lp	-	-	-	-	-	-	-
535	142196	915609	lp	-	-	-	-	-	-	-
536	142325	915597	lp	-	-	-	-	-	-	-
537	141392	913061	lp	-	-	-	-	-	-	-
538	141350	913101	Sr	-	-	-	-	-	-	-
539	141405	913162	Sr	-	-	-	-	-	-	-

Table 1. (continued)

540	141435	913229	-	-	-	-	-	-	-	-	-
541	141459	913314	Sr	-	-	-	-	-	-	-	-
542	141462	913448	?	-	-	-	-	-	-	-	-
543	141473	913341	lp	-	-	-	-	-	-	-	-
544	141619	913488	lp>Sr	-	-	-	-	-	-	-	-
545	141992	913341	Ddi	-	-	-	-	-	-	-	-
546	141846	913393	Ddi	-	-	-	-	-	-	-	-
547	141943	913620	-	-	-	-	-	-	-	-	-
548	141993	913661	Ddi	-	-	-	-	-	-	-	-
549	141994	913743	Sr	-	-	-	-	-	-	-	-
550	142083	913787	Ddi	-	-	-	-	-	-	-	-
551	142076	913807	Ddi	-	-	-	-	-	-	-	-
552	142119	913806	Ddi	-	-	-	-	-	-	-	-
553	142244	913877	Sr	-	-	-	-	-	-	-	-
554	142186	914068	Ddi	-	-	-	-	-	-	-	-
555	142244	914257	Ddi	-	-	-	-	-	-	-	-
556	142241	914412	Ddi	-	-	-	-	-	-	-	-
557	142091	914492	Ddi	-	-	-	-	-	-	-	-
558	141968	914689	Ddi	-	-	-	-	-	-	-	-
559	141928	914746	Ddi	-	-	-	-	-	-	-	-
560	141734	914731	Sr	-	-	-	-	-	-	-	-
561	141798	914772	Sr	-	-	-	-	-	-	-	-
562	141827	914851	Sr-Ddi	-	-	-	-	-	-	-	-
563	142164	914769	Ddi	-	-	-	-	-	-	-	-
564	142249	914785	Sr	-	-	-	-	-	-	-	-
565	142059	915090	Ddi	-	-	-	-	-	-	-	-
566	141944	915123	Ddi	-	-	-	-	-	-	-	-
567	141520	914688	Sr	-	-	-	-	-	-	-	-
568	141392	914604	Sr	-	-	-	-	-	-	-	-
569	141183	914447	-	-	-	-	-	-	-	-	-
570	141151	914458	lp	-	-	-	-	-	-	-	-
571	141128	914262	Sr		344	54	W	-	-	-	-
572	141068	914176	Sr	-	-	-	-	-	-	-	-
573	141110	914043	lp>Sr	-	-	-	-	-	-	-	-
574	141158	913874	lp	-	-	-	-	-	-	-	-
575	141319	914037	lp	-	-	-	-	-	-	-	-
576	141306	913724	lp	-	-	-	-	-	-	-	-
577	141369	913427	Sr	-	-	-	-	-	-	-	-
578	140223	912268	Om	-	-	-		185	10	S	-
579	139798	911855	lp	-	-	-	-	-	-	-	-
580	139896	911820	Om	-	-	-	-	-	-	-	-
581	139881	911686	lp	-	-	-	-	-	-	-	-

Table 1. (continued)

582	139899	911610	Om	-		-	-	-		-		-
583	139925	911531	-	-		-	-	-		-		-
584	139891	911457	Om	-		-	-	-		-		-
585	139946	911350	Om	-		-	-	-		-		-
586	140005	911349	Om	-		-	-	-		-		-
587	140038	911355	Om	-		-	-	-		-		-
588	140077	911349	Om		160		43	W	-		-	-
589	140110	911294	lp	-		-	-	-		-		-
590	140137	911271	Om	-		-	-	-		-		-
591	140151	911234	Sr	-		-	-	-		-		-
592	140177	911527	Sr	-		-	-	-		-		-
593	140103	911534	lp	-		-	-	-		-		-
594	140164	911695	Om	-		-	-	-		-		-
595	140054	911621	Om	-		-	-	-		-		-
596	140015	911582	Om	-		-	-	-		-		-
597	139978	911586	Om	-		-	-	-		-		-
598	139960	911536	Om	-		-	-	-		-		-
599	139777	911295	Om	-		-	-	-		-		-
600	139702	911372	Om	-		-	-	-		-		-
601	139684	911358	Om	-		-	-	-		-		-
602	139706	911540	Om	-		-	-	-		-		-
604	139970	915734	Om	-		-	-	-		-		-
605	140015	915715	Om	-		-	-	-		-		PE13-595
606	140054	915631	Om	-		-	-	-		-		-
607	139988	915595	Om	-		-	-	-		-		-
608	140066	915693	Om	-		-	-	-		-		-
609	140081	915721	Om	-		-	-	-		-		-
610	140109	915810	Om	-		-	-	-		-		-
611	140162	915854	Sr	-		-	-	-		-		-
612	140189	915819	lp>Sr	-		-	-	-		-		-
613	140250	915846	Om	-		-	-	-		-		PE13-603
614	140294	915829	lp	-		-	-	-		-		-
615	140402	915881	Om		182		27	W	-		-	-
616	140435	915860	Om	-		-	-	-		-		-
617	140465	915888	Sr	-		-	-	-		-		-
618	140484	915969	Om	-		-	-	-		-		-
619	140503	916027	Sr		1		19	W		1	4	S -
620	139945	915986	Om	-		-	-	-		-		PE13-610
621	140367	912740	Sr	-		-	-	-		-		-
622	140414	912747	Om	-		-	-	-		-		-

Table 1. (continued)

623	140452	912761	Om	-	-	-	-	-	-	-	
624	140481	912799	lp	-	-	-	-	-	-	-	
625	140687	912821	Om	-	-	-	-	-	-	-	
626	140705	912930	Om	-	-	-	-	-	-	-	
627	140774	912912	Om	-	-	-	-	-	-	-	
628	140717	913019	Om	-	-	-	-	-	-	-	
629	140799	913060	Om	-	-	-	-	-	-	-	
630	140817	913091	Om	-	-	-	-	-	-	-	
631	140873	912943	Sr	-	-	-	-	-	-	-	
632	140565	912970	Om	-	-	-	-	-	-	-	
633	140554	912977	Sr	-	-	-	-	-	-	-	
634	140509	912974	lp	-	-	-	-	-	-	-	
635	140450	913000	Sr	-	-	-	-	-	-	-	
636	140452	913079	lp>Sr	-	-	-	-	-	-	-	
637	140386	913096	Sr	-	-	-	-	-	-	-	
638	140380	913096	Om	-	-	-	-	-	-	-	
639	139607	911750	Om	-	-	-	-	-	-	-	
640	139062	911656	Om	-	-	-	-	-	-	-	
641	138943	911730	Om	-	-	-	-	-	-	-	
642	139200	912179	Om	192	47	W	-	-	-	-	
643	138994	912377	Om	-	-	-	-	-	-	-	
644	139239	912202	Om	5	33	W	-	-	-	-	
645	138994	911895	Om	-	-	-	-	-	-	-	
646	138888	911323	Om	-	-	-	-	-	-	-	
647	139252	911451	Om	-	-	-	-	-	-	-	
648	139306	911416	Om	-	-	-	-	-	-	-	
649	139344	911406	Om	7	67	W	-	-	-	-	
650	139554	911388	Om	85	51	W	-	-	-	-	
651	139494	911202	Om	-	-	-	-	-	-	-	
652	139511	911178	Om	-	-	-	-	-	-	-	
653	139389	911211	Om	-	-	-	-	-	-	-	
654	139339	911174	Om	-	-	-	-	-	-	-	
655	139390	911247	Om	-	-	-	-	-	-	-	
656	138885	911186	Om	-	-	-	-	-	-	-	
657	138749	911139	Om	-	-	-	-	-	-	-	
658	141458	906711	Sr	-	-	-	-	-	-	-	
659	141506	906743	Sr	-	-	-	-	-	-	-	
660	141507	906796	Sr	-	-	-	-	-	-	-	
661	141500	906841	Sr	-	-	-	-	-	-	-	
662	141409	906877	Sr	-	-	-	-	-	-	-	
663	141401	906945	Sr	-	-	-	30	10	S	-	
664	141335	907020	Sr	-	-	-	-	-	-	-	

Table 1. (continued)

665	141310	907175	Sr	-		-	-	-		-		-
666	141293	907250	lp	-		-	-	-		-		-
667	141416	907383	Sr	-		-	-	-		-		-
668	141629	907814	lp	-		-	-	-		-		-
669	141639	907806	lp	-		-	-	-		-		-
670	141667	907855	lp	-		-	-	-		-		-
671	141664	907860	Sr		184	76	W	190		15	N	PE13-662
672	141691	907490	lp	-		-	-	-		-		-
673	141743	907443	Ddi	-		-	-	-		-		-
674	141628	907227	lp	-		-	-	-		-		-
675	141457	907225	Sr	-		-	-	-		-		-
676	141304	907127	Sr	-		-	-	-		-		-
677	140485	913393	Sr		188	50	W	188		9	N	-
678	140535	913374	Sr	-		-	-	-		-		-
679	140599	913364	Om		180	14	W	-		-		-
680	140711	913378	Om	-		-	-	-		-		-
681	140744	913419	Om	-		-	-	-		-		-
682	140778	913400	Om		192	27	W	-		-		-
683	140838	913363	Sr	-		-	-	-		-		-
684	140808	913398	Sr	-		-	-	-		-		-
685	140810	913618	Om		182	27	W	-		-		-
686	140851	913610	Sr		175	24	W	-		-		-
687	140864	913841	Om	-		-	-	-		-		-
688	140870	913841	Sr	-		-	-	-		-		-
689	140802	914081	Sr	-		-	-	-		-		-
690	140782	914068	Om	-		-	-	-		-		-
691	139970	907497	Om	-		-	-	-		-		-
692	139895	907519	Om	-		-	-	-		-		-
693	139919	907458	Om	-		-	-	-		-		-
694	139894	907434	Om	-		-	-	-		-		-
695	139898	907377	Om	-		-	-	-		-		-
696	139822	907524	Om	-		-	-	-		-		-
697	139943	907193	Om	-		-	-	-		-		-
698	140027	907185	Om	-		-	-	-		-		-
699	140032	907354	Om	-		-	-	-		-		-
700	140081	907288	Om		156	32	W	-		-		-
701	140080	907047	Om	-		-	-	-		-		-
702	140072	906963	Om	-		-	-	-		-		-
703	140065	907105	Om	-		-	-	-		-		-
704	139447	903174	Om	-		-	-	-		-		-
705	139530	903755	Om	-		-	-	-		-		-

Table 1. (continued)

706	139508	903807	Om	-		-	-	-		-	-	
707	139964	904841	Om	-		-	-	-		-	-	
708	143081	915119	Dh	-		-	-	-		-	-	
709	143171	915178	lp	-		-	-	-		-	-	
710	143166	915164	lp	-		-	-	-		-	-	
711	143292	915144	lp	-		-	-	-		-	-	
712	143250	915032	Sr	-		-	-	-		-	-	
713	143103	915209	Dh	-		-	-	-		-	-	
714	143129	915199	Dh	-		-	-	-		-	-	
715	143398	904956	Dh	-		-	-	-		-	-	
716	143281	904606	Dh	-		-	-	-		-	-	
717	141267	912874	Sr		220	80	NE		220	50	SW	-
718	141515	912926	peg	-		-	-	-		-	-	
719	141654	912954	Dh?	-		-	-	-		-	-	
720	141715	912919	Dh?	-		-	-	-		-	-	
721	141791	912934	Sr	-		-	-	-		-	-	
722	141862	913006	Dh?	-		-	-	-		-	-	
723	141913	912995	Sr	-		-	-	-		-	-	
724	141915	912800	Sr	-		-	-	-		-	-	
725	141844	912600	Sr	-		-	-	-		-	-	
726	141751	912613	Dh	-		-	-	-		-	-	
727	141648	912715	lp	-		-	-	-		-	-	
728	141676	912516	Sr	-		-	-	-		-	-	
729	141584	912160	lp	-		-	-	-		-	-	
730	141724	911983	Dh?	-		-	-	-		-	-	
731	141736	911994	lp	-		-	-	-		-	-	
732	141745	912000	Sr	-		-	-	-		-	-	
733	141786	912215	Dh	-		-	-	-		-	-	
734	141822	912276	Dh	-		-	-	-		-	-	
735	141913	912281	lp	-		-	-	-		-	-	
736	141936	912329	lp	-		-	-	-		-	-	
737	141966	912374	lp	-		-	-	-		-	-	
738	141979	912436	lp	-		-	-	-		-	-	
739	141928	912486	lp	-		-	-	-		-	-	
740	142136	912391	lp	-		-	-	-		-	-	
741	142153	912378	Dh	-		-	-	-		-	-	
742	142179	912380	-	-		-	-	-		-	-	
743	142373	912516	-	-		-	-	-		-	-	
744	142426	912545	Dh	-		-	-	-		-	-	
745	142520	912611	Dh	-		-	-	-		-	-	
746	142637	912613	Dh	-		-	-	-		-	-	
747	142758	912586	Sr	-		-	-	-		-	-	

Table 1. (continued)

748	142818	912508	Dh	-	-	-	-	-	-	-
749	142920	912522	Sr	-	-	-	-	-	-	-
750	142866	912430	?	-	-	-	-	-	-	-
751	142807	912388	lp	-	-	-	-	-	-	-
752	142791	912306	Dh	-	-	-	-	-	-	-
753	142792	912266	Sr	-	-	-	-	-	-	-
754	142888	912240	Dh	-	-	-	-	-	-	-
755	142925	912251	Dh	-	-	-	-	-	-	-
756	143040	912300	Dh	-	-	-	-	-	-	-
757	143305	912270	Sr	-	-	-	-	-	-	-
758	143392	912292	Sr	-	-	-	-	-	-	-
759	143409	912316	Sr	-	-	-	198	29	S	-
760	143481	912473	Sr	-	-	-	-	-	-	-
761	143471	912703	Dh	-	-	-	-	-	-	-
762	143546	912743	Dh	-	-	-	-	-	-	-
763	143362	912703	Sr	-	-	-	-	-	-	-
764	143077	912749	Dh	-	-	-	-	-	-	-
765	142945	912895	Sr	-	-	-	-	-	-	-
766	142792	912962	Dh	-	-	-	-	-	-	-
767	142763	912952	Dh	-	-	-	-	-	-	-
768	142697	912989	Sr	-	-	-	-	-	-	-
769	142615	912985	Dh	-	-	-	-	-	-	-
770	142563	912980	Dh	-	-	-	-	-	-	-
771	142486	913007	Dh	-	-	-	-	-	-	-
772	142433	913253	Dh	-	-	-	-	-	-	-
773	142222	913055	Dh	-	-	-	-	-	-	-
774	142230	913191	Dh	-	-	-	-	-	-	-
775	142195	913092	Dh	-	-	-	-	-	-	-
776	142148	913163	Dh	-	-	-	-	-	-	-
777	142013	913192	lp	-	-	-	-	-	-	-
778	141840	913090	Sr	-	-	-	-	-	-	-
779	142989	914906	Sr	-	-	-	-	-	-	-
780	143034	914803	Sr	-	-	-	-	-	-	-
781	142936	914619	Sr	-	-	-	-	-	-	-
782	142907	914354	Dh	-	-	-	-	-	-	-
783	142977	914088	Dh	-	-	-	-	-	-	-
784	142810	914097	lp	-	-	-	-	-	-	-
785	142793	914052	lp	-	-	-	-	-	-	-
786	142742	914051	Dh	-	-	-	-	-	-	-
787	142806	913775	lp	-	-	-	-	-	-	-
788	142928	913777	Dh	-	-	-	-	-	-	PE13-775

Table 1. (continued)

789	143224	914405	Dh	-	-	-	-	-	-	PE13-776
790	139650	904683	Om	-	-	-	-	-	-	-
791	139572	904724	Om	-	-	-	-	-	-	-
792	139533	904697	Om	-	-	-	-	-	-	-
793	139334	904725	Om	-	-	-	-	-	-	-
794	139369	904800	Om	-	-	-	-	-	-	-
795	139601	905147	Om	-	-	-	-	-	-	-
796	140073	905187	Om	-	-	-	-	-	-	-
797	140108	905272	Om	-	-	-	-	-	-	PE13-784
798	140085	905357	Om	-	-	-	-	-	-	-
799	140134	905644	Om	-	-	-	-	-	-	-
800	140445	905265	Om	-	-	-	-	-	-	-
801	140590	905325	Om	-	-	-	-	-	-	-
802	140299	904963	Om	-	-	-	-	-	-	-
803	140228	904920	Om	27	50	W	-	-	-	-
804	140242	904813	Om	-	-	-	-	-	-	-
805	140278	904742	Om	-	-	-	-	-	-	-
806	140123	904463	Om	-	-	-	-	-	-	-
807	139644	903239	Om	-	-	-	-	-	-	-
808	139894	903102	Om	-	-	-	-	-	-	-
809	140029	903079	Om	-	-	-	-	-	-	-
810	140153	903162	Om	-	-	-	-	-	-	-
811	140251	903168	Om	-	-	-	-	-	-	-
812	140332	903235	Om	-	-	-	-	-	-	-
813	140504	903264	Om	-	-	-	-	-	-	-
814	140679	903200	Om	-	-	-	-	-	-	-
815	140795	903136	Sr	-	-	-	-	-	-	-
816	140890	903102	Ddi	-	-	-	-	-	-	-
817	140974	903043	Ddi	-	-	-	-	-	-	-
818	141030	903040	Ddi	-	-	-	-	-	-	-
819	141091	903091	Ddi	-	-	-	-	-	-	-
820	141119	903037	Ddi	-	-	-	-	-	-	-
821	141154	903080	Sr	-	-	-	-	-	-	-
822	141326	903159	lp	-	-	-	-	-	-	-
823	141404	903115	Sr-Dh	-	-	-	-	-	-	-
824	141479	903070	Dh	-	-	-	-	-	-	-
825	141569	903118	Dh	-	-	-	-	-	-	-
826	141461	903240	Dh	-	-	-	-	-	-	-
827	141414	903252	Dh	-	-	-	-	-	-	-
828	141325	903262	Dh	-	-	-	-	-	-	-
829	141206	903340	Dh	-	-	-	-	-	-	-

Table 1. (continued)

830	141413	903472	Dh	-	-	-	-	-	-	-
831	141540	903741	Om	-	-	-	-	-	-	-
832	141259	903781	Om	-	-	-	-	-	-	-
833	140415	903712	Om	-	-	-	-	-	-	-
834	140333	903641	-	-	-	-	-	-	-	-
835	140244	903546	-	-	-	-	-	-	-	-
836	139924	903622	-	-	-	-	-	-	-	-
837	139805	903665	-	-	-	-	-	-	-	-
838	142888	908140	Dh	-	-	-	-	-	-	-
839	142885	908052	Dh	-	-	-	-	-	-	-
840	143203	908220	Dh	-	-	-	-	-	-	-
841	143339	908198	Dh	-	-	-	-	-	-	-
842	143311	908156	Dh	-	-	-	-	-	-	-
843	143429	908018	Dh	-	-	-	-	-	-	-
844	143633	907598	Dh	-	-	-	-	-	-	-
845	143699	907594	Dh	-	-	-	-	-	-	-
846	143671	907502	Dh	-	-	-	-	-	-	-
847	143677	907262	Dh	-	-	-	-	-	-	-
848	143604	906873	Dh	-	-	-	-	-	-	-
849	143456	907055	Dh	-	-	-	-	-	-	-
850	143396	906808	Dh	-	-	-	-	-	-	-
851	143343	906839	Dh	-	-	-	-	-	-	-
852	143157	907024	Dh	-	-	-	-	-	-	-
853	143160	906885	Dh	-	-	-	-	-	-	-
854	143586	907313	Dh	-	-	-	-	-	-	-
855	143545	907442	Dh	-	-	-	-	-	-	-
856	143336	907506	Dh	-	-	-	-	-	-	-
857	143261	907476	Dh	-	-	-	-	-	-	-
858	143066	907890	Dh	-	-	-	-	-	-	-
859	143092	907960	Dh	-	-	-	-	-	-	-
860	142858	908272	Dh	-	-	-	-	-	-	-
861	142709	908429	Dh	-	-	-	-	-	-	-
862	142722	908513	Dh	-	-	-	-	-	-	-
863	142747	908675	Sr-Dh	-	-	-	-	-	-	-
864	142817	908777	Sr	-	-	-	-	-	-	-
865	142849	908845	Sr	-	-	-	-	-	-	-
866	142873	908881	?	-	-	-	-	-	-	-
867	142894	908984	Sr	-	-	-	-	-	-	-
868	142964	909045	Sr	-	-	-	-	-	-	-
869	143106	908977	?	-	-	-	-	-	-	-
870	143177	909007	Dh	-	-	-	-	-	-	-
871	143225	908896	Dh	-	-	-	-	-	-	-

Table 1. (continued)

872	143289	908633	Dh	-	-	-	-	-	-	-	
873	143187	908797	Dh	-	-	-	-	-	-	-	
874	143126	908788	Dh	-	-	-	-	-	-	-	
875	143092	908761	Dh	-	-	-	-	-	-	-	
876	142949	908767	Dh	-	-	-	-	-	-	-	
877	142946	908715	Dh	-	-	-	-	-	-	-	
878	142996	908693	?	-	-	-	-	-	-	-	
879	142997	908672	?	-	-	-	-	-	-	-	
880	143013	908633	?	-	-	-	-	-	-	-	
881	143061	908681	Dh	-	-	-	-	-	-	-	
882	143082	908679	Dh	-	-	-	-	-	-	-	
883	143162	908653	Dh	-	-	-	-	-	-	-	
884	143137	908545	Dh	-	-	-	-	-	-	-	
885	143097	908456	Dh	-	-	-	-	-	-	-	
886	143107	908414	Dh	-	-	-	-	-	-	-	
887	142996	908270	Dh	-	-	-	-	-	-	-	
888	141739	906612	Sr	-	-	-	-	-	-	-	
889	141861	906622	Sr	-	-	-	-	-	-	-	
890	141990	906735	Sr	-	-	-	-	-	-	-	
891	142410	906862	Dh	-	-	-	-	-	-	-	
892	142562	906945	Dh	-	-	-	-	-	-	-	
893	142549	906842	Dh	-	-	-	-	-	-	-	
894	142506	906756	Dh	-	-	-	-	-	-	-	
895	142763	906961	Dh	-	-	-	-	-	-	-	
896	142831	908089	Dh	-	-	-	-	-	-	-	
897	142851	908059	Dh	-	-	-	-	-	-	-	
898	142813	907869	Dh	-	-	-	-	-	-	-	
899	142786	907816	Dh	-	-	-	-	-	-	-	
900	142778	907767	Dh	-	-	-	-	-	-	-	
901	142786	907752	Dh	184	48	W	-	-	-	-	
902	142792	907751	Dh	355	31	W	-	-	-	-	
903	142779	907716	Dh	359	40	W	-	-	-	-	
904	142781	907695	Dh	-	-	-	-	-	-	-	
905	142781	907661	Dh	-	-	-	-	-	-	-	
906	142733	907709	Dh	178	72	W	-	-	-	-	
907	142731	907646	Dh	-	-	-	-	-	-	-	
908	142704	907557	Dh	-	-	-	-	-	-	-	
909	142690	907506	Dh	15	45	W	-	-	-	-	
910	142665	907495	Dh	-	-	-	-	-	-	-	
911	142637	907490	Dh	-	-	-	-	-	-	-	
912	142618	907473	Dh	-	-	-	-	-	-	-	
913	142621	907431	Dh	-	-	-	-	-	-	-	

Table 1. (continued)

914	142715	907364	Dh	-	-	-	-	-	-	-	
915	142696	907308	Dh	-	-	-	-	-	-	-	
916	142674	907240	Dh	-	-	-	-	-	-	-	
917	142650	907181	Dh	-	-	-	-	-	-	-	
918	142698	907058	Dh	-	-	-	-	-	-	-	
919	142698	907006	Dh	-	-	-	-	-	-	-	
920	142733	907001	Dh	-	-	--	-	-	-	-	
921	142792	907042	Dh	-	-	-	-	-	-	-	
922	142830	906993	Dh	-	-	-	-	-	-	-	
923	142930	907005	Dh	-	-	-	-	-	-	-	
924	142874	906982	Dh	-	-	-	-	-	-	-	
925	142965	906860	Dh	-	-	-	-	-	-	-	
926	142847	906644	Dh	-	-	-	-	-	-	-	
927	142755	906335	Dh	345	28	W	109	12	S	PE13-921	
928	142800	906263	Dh	-	-	-	-	-	-	-	
929	142778	906279	Sr	-	-	-	-	-	-	-	
930	142805	906288	Dh?	-	-	-	-	-	-	-	
931	142795	906307	Dh?	-	-	-	-	-	-	-	
932	142687	906259	Sr	-	-	-	-	-	-	-	
933	142723	906219	Sr	-	-	-	-	-	-	-	
934	142750	906246	Dh	-	-	-	-	-	-	-	
935	142820	906216	Sr	-	-	-	-	-	-	-	
936	142987	906136	Dh	-	-	-	-	-	-	-	
937	143050	906035	Sr	-	-	-	-	-	-	-	
938	142981	906038	Dh	-	-	-	-	-	-	-	
939	143029	906117	Dh	-	-	-	-	-	-	-	
940	143099	906214	Dh	-	-	-	-	-	-	-	
941	143060	905950	Dh	179	42	W	-	-	-	-	
942	143005	905937	Dh	-	-	-	-	-	-	-	
943	142996	905848	Sr	-	-	-	-	-	-	-	
944	142885	905911	Sr	-	-	-	-	-	-	-	
945	142810	905861	Sr	-	-	-	-	-	-	-	
946	142752	905925	Dh	-	-	-	-	-	-	-	
947	142725	905925	Sr	19	27	W	-	-	-	-	
948	142761	905760	Sr	-	-	-	-	-	-	-	
949	142758	905708	Dh	41	26	W	-	-	-	-	
950	142721	905677	Dh	40	30	W	-	-	-	-	
951	142742	905639	Dh	-	-	-	-	-	-	-	
952	142692	905604	Sr	-	-	-	-	-	-	-	
953	142618	905595	Dh	-	-	-	-	-	-	-	
954	142557	905499	Dh	-	-	-	-	-	-	-	

Table 1. (continued)

955	142558	905298	Dh	-		-	-	-		-	-	-
956	142588	905240	Dh	-		-	-	-		-	-	-
957	142719	905192	Dh	-		-	-	-		-	-	-
958	142621	905202	Dh	-		-	-	-		-	-	-
959	142536	905200	Dh	-		-	-	-		-	-	-
960	142511	905233	Dh	-		-	-	-		-	-	-
961	142459	905333	Dh	-		-	-	-		-	-	-
962	142531	905428	Dh	-		-	-	-		-	-	-
963	142607	905710	Dh	-		-	-	-		-	-	-
964	142519	905613	Dh	-		-	-	-		-	-	-
965	142312	905641	Dh	-		-	-	-		-	-	-
966	142258	905776	Dh	-		-	-	-		-	-	-
967	142359	905789	Dh	-		-	-	-		-	-	-
968	142330	905737	Dh	-		-	-	-		-	-	-
969	142600	905885	Dh	-		-	-	-		-	-	-
970	142654	905915	Dh		186		44	W	-		-	-
971	142679	906345	Dh	-		-	-	-		-	-	-
972	142674	906155	Dh	-		-	-	-		-	-	-
973	142569	906292	Dh	-		-	-	-		-	-	-
974	142527	906294	Dh	-		-	-	-		-	-	-
975	142474	906168	Dh	-		-	-	-		-	-	-
976	142445	906216	Dh	-		-	-	-		-	-	-
977	142402	906254	Dh	-		-	-	-		-	-	-
978	142515	906538	Dh	-		-	-	-		-	-	-
979	142644	906972	Dh	-		-	-	-		-	-	-
980	142580	907287	Dh	-		-	-	-		-	-	-
981	142559	907346	Dh	-		-	-	-		-	-	-
982	142583	907432	Dh	-		-	-	-		-	-	-
983	142551	907480	Dh	-		-	-	-		-	-	-
984	142538	907446	Dh	-		-	-	-		-	-	-
985	142534	907509	Dh	-		-	-	-		-	-	-
986	142536	907525	Dh	-		-	-	-		-	-	-
987	142563	907577	Dh	-		-	-	-		-	-	-
988	142563	907604	Dh	-		-	-	-		-	-	-
989	142603	907651	Dh	-		-	-	-		-	-	-
990	142597	907672	Dh	-		-	-	-		-	-	-
991	142612	907688	Dh	-		-	-	-		-	-	-
992	142595	907709	Dh	-		-	-	-		-	-	-
993	139934	904351	lp	-		-	-	-		-	-	-
994	139988	904262	Om		170		25	W	-		-	-
995	140029	904235	Om		188		36	W		35	0	-
996	140016	904182	Om	-		-	-	-		-	-	-

Table 1. (continued)

997	140007	904141	Om	-		-		-	-		-		-	-
998	139985	904138	Om	-		-		-	-		-		-	-
999	139971	904117	Om	-		-		-	-		-		-	-
1000	139954	904099	Om	-		-		-	-		-		-	-
1001	139917	904126	Om		11		35	W	-		-		-	-
1002	139909	904068	Om	-		-		-	-		-		-	-
1003	139929	904055	Om		15		24	W	-		-		-	-
1004	139958	904052	Om		17		16	S?		21		5	N	-
1005	140009	904076	Om	-		-		-	-		-		-	-
1006	140055	904103	Om	-		-		-	-		-		-	-
1007	140032	904041	Om	-		-		-	-		-		-	-
1008	140028	903947	Om	-		-		-	-		-		-	PE13-1000
1009	140220	903685	Om	-		-		-	-		-		-	-
1010	140250	903992	Om	-		-		-	-		-		-	-
1011	140674	903955	Om	-		-		-	-		-		-	-
1012	140942	903974	Sr	-		-		-	-		-		-	-
1013	140766	903932	Om	-		-		-	-		-		-	-
1014	141033	904122	Sr	-		-		-	-		-		-	-
1015	141117	904245	lp	-		-		-	-		-		-	-
1016	141092	904303	Sr	-		-		-	-		-		-	-
1017	141209	904327	Ddi	-		-		-	-		-		-	PE13-1009
1018	141270	904408	Ddi	-		-		-	-		-		-	-
1019	141418	904502	Dh?	-		-		-	-		-		-	-
1020	141483	904938	Sr	-		-		-	-		-		-	-
1021	141562	905140	Sr	-		-		-	-		-		-	-
1022	141909	905130	Sr	-		-		-	-		-		-	-
1023	141451	904767	Sr	-		-		-	-		-		-	-
1024	141338	904616	Sr	-		-		-	-		-		-	-
1025	141422	904608	Sr	-		-		-	-		-		-	-
1026	141356	904509	Sr	-		-		-	-		-		-	-
1027	141269	904495	Sr	-		-		-	-		-		-	-
1028	140991	904561	Sr	-		-		-	-		-		-	-
1029	140968	904441	Sr	-		-		-	-		-		-	-
1030	140972	904657	lp	-		-		-	-		-		-	-
1031	141095	904699	lp>Sr	-		-		-	-		-		-	-
1032	141109	904709	lp	-		-		-	-		-		-	-
1033	141206	904948	Sr	-		-		-	-		-		-	-
1034	141154	905059	Sr	-		-		-	-		-		-	-
1035	140796	904537	Om	-		-		-	-		-		-	-
1036	140935	904559	Sr	-		-		-	-		-		-	-
1037	140727	904446	Om	-		-		-	-		-		-	-

Table 1. (continued)

1038	140532	904547	Om	-	-	-	-	-	-	-
1039	140604	904619	Om	-	-	-	-	-	-	-
1040	140473	904451	Om	-	-	-	-	-	-	-
1041	140412	904235	Om	-	-	-	-	-	-	-
1042	142438	907897	Dh	-	-	-	-	-	-	-
1043	142778	908098	Dh	-	-	-	-	-	-	-
1044	142352	907903	Dh	-	-	-	-	-	-	-
1045	142347	907951	Sr	-	-	-	-	-	-	-
1046	142289	907640	Dh	-	-	-	-	-	-	-
1047	142177	907625	Dh	-	-	-	-	-	-	-
1048	142128	907444	Sr	-	-	-	-	-	-	-
1049	142198	907459	Sr	-	-	-	-	-	-	-
1050	142225	907464	Dh	-	-	-	-	-	-	-
1051	142186	907297	Sr	-	-	-	-	-	-	-
1052	142206	907254	Dh	-	-	-	-	-	-	-
1053	142190	907169	Dh	-	-	-	-	-	-	-
1054	142249	907158	Dh	-	-	-	-	-	-	-
1055	142125	907066	Sr	-	-	-	-	-	-	-
1056	142145	907100	Dh	-	-	-	-	-	-	-
1057	142150	907025	?	-	-	-	-	-	-	-
1058	142034	906944	Sr	-	-	-	-	-	-	-
1059	142060	907005	Sr	-	-	-	-	-	-	-
1060	142005	906976	Sr	-	-	-	-	-	-	-
1061	142004	907257	Sr	-	-	-	-	-	-	-
1062	141994	907150	Sr	-	-	-	-	-	-	-
1063	142029	907347	Sr	-	-	-	-	-	-	-
1064	142045	907424	Sr	-	-	-	-	-	-	-
1065	142034	907461	Sr	-	-	-	-	-	-	-
1066	141983	907632	Sr	-	-	-	-	-	-	-
1067	141678	906628	?	-	-	-	-	-	-	-
1068	141504	906547	Sr	-	-	-	-	-	-	-
1069	141485	906524	Om?	-	-	-	-	-	-	-
1070	141363	906500	lp	-	-	-	-	-	-	-
1071	141329	906418	Om?	-	-	-	-	-	-	-
1072	141297	906386	?	-	-	-	-	-	-	-
1073	141321	906325	Sr	-	-	-	-	-	-	-
1074	141251	906348	Om?	-	-	-	-	-	-	-
1075	141040	906269	Om	-	-	-	-	-	-	-
1076	141005	906193	-	-	-	-	-	-	-	-
1077	140956	906142	Om	-	-	-	-	-	-	-
1078	141101	906093	Om-Sr	-	-	-	-	-	-	-
1079	141130	906137	Sr	-	-	-	177	12	N	-

Table 1. (continued)

1080	141125	906193	Om	-	-	-	-	-	-	-	
1081	141224	906177	Sr	-	-	-	-	-	-	-	
1082	141332	906203	lp	-	-	-	-	-	-	-	
1083	141355	906199	lp	-	-	-	-	-	-	-	
1084	141397	906199	lp	-	-	-	-	-	-	-	
1085	141475	906227	lp	-	-	-	-	-	-	-	
1086	141468	906143	lp	-	-	-	-	-	-	-	
1087	138958	910831	Om	-	-	-	-	-	-	-	
1088	138580	910786	Om	-	-	-	-	-	-	-	
1089	138390	910132	Om	-	-	-	-	-	-	-	
1090	138550	909850	Om	-	-	-	-	-	-	-	
1091	138684	910094	Om	4	52	W	-	-	-	-	
1092	138688	910192	Om	-	-	-	-	-	-	-	
1093	138935	910264	Om	-	-	-	-	-	-	-	
1094	138954	910161	Om	-	-	-	-	-	-	-	
1095	138879	909944	Om	-	-	-	-	-	-	-	
1096	139135	910036	Om	-	-	-	-	-	-	-	
1097	139215	909964	Om	-	-	-	-	-	-	-	
1098	139200	909975	Om	-	-	-	-	-	-	-	
1099	139354	910191	Om	-	-	-	-	-	-	-	
1100	139350	910256	Om	-	-	-	-	-	-	-	
1101	139358	910270	Om	-	-	-	-	-	-	-	
1102	139344	910274	Om	-	-	-	-	-	-	-	
1103	139303	910295	Om	-	-	-	-	-	-	-	
1104	139316	910369	Om	-	-	-	-	-	-	-	
1105	139420	910396	Om	181	51	W	-	-	-	-	
1106	139461	910289	Om	-	-	-	-	-	-	-	
1107	139559	910285	Om	-	-	-	-	-	-	-	
1108	139564	910305	Om	-	-	-	-	-	-	-	
1109	139581	910362	Om	-	-	-	-	-	-	-	
1110	139586	910405	Om	-	-	-	-	-	-	-	
1111	139695	911184	Om	-	-	-	-	-	-	-	
1112	139687	910990	Om	-	-	-	-	-	-	-	
1113	138867	907765	Om	-	-	-	-	-	-	-	
1114	138593	907738	Om	-	-	-	-	-	-	-	
1115	138539	907771	Om	-	-	-	-	-	-	-	
1116	138542	907850	Om	-	-	-	-	-	-	-	
1117	138551	907930	Om	-	-	-	-	-	-	-	
1118	138516	908061	Om	-	-	-	-	-	-	-	
1119	138500	908059	Om	-	-	-	-	-	-	-	
1120	138480	908100	Om	168	19	W	-	-	-	-	
1121	138492	908127	Om	-	-	-	-	-	-	-	

Table 1. (continued)

1122	138541	908159	Om		177		15	W	-	-	-
1123	138538	908181	Om	-		-		-	-	-	-
1124	138509	908147	Om		174		24	W	-	-	-
1125	138512	908269	Om	-		-		-	-	-	-
1126	138499	908346	Om	-		-		-	-	-	-
1127	138503	908369	Om	-		-		-	-	-	-
1128	138519	908404	Om	-		-		-	-	-	-
1129	138505	908470	Om	-		-		-	-	-	-
1130	138688	908449	Om	-		-		-	-	-	-
1131	138734	908395	Om		171		33	W	-	-	-
1132	138745	908244	Om		160		40	W	-	-	-
1133	138561	908185	Om	-		-		-	-	-	-
1134	138472	908169	Om		42		34	W	-	-	-
1135	138453	908222	Om	-		-		-	-	-	-
1136	138425	908011	Om	-		-		-	-	-	-
1137	138515	907693	Om	-		-		-	-	-	-
1138	138533	907723	Om	-		-		-	-	-	-
1139	142035	908319	Sr	-		-		-	-	-	-
1140	142228	908542	?	-		-		-	-	-	-
1141	142288	908456	?	-		-		-	-	-	-
1142	142197	908684	?	-		-		-	-	-	-
1143	142172	908719	lp	-		-		-	-	-	-
1144	142085	908745	Sr	-		-		-	-	-	-
1145	142080	908982	lp	-		-		-	-	-	-
1146	142092	909007	Ddi	-		-		-	-	-	-
1147	142101	909002	Sr	-		-		-	-	-	-
1148	142163	909195	?	-		-		-	-	-	-
1149	142150	909238	Ddi	-		-		-	-	-	-
1150	142137	909291	Sr	-		-		-	-	-	-
1151	142142	909348	Sr	-		-		-	-	-	-
1152	142177	909567	Sr	-		-		-	-	-	-
1153	142169	909638	Sr	-		-		-	-	-	-
1154	142162	909674	Sr	-		-		-	-	-	-
1155	142147	909718	Sr	-		-		-	-	-	-
1156	142132	909659	Sr	-		-		-	-	-	-
1157	142049	909680	Sr	-		-		-	-	-	-
1158	142013	909640	Sr	-		-		-	-	-	-
1159	142016	909734	Sr	-		-		-	-	-	-
1160	142081	909282	Ddi	-		-		-	-	-	-
1161	142751	909163	Dh	-		-		-	-	-	-
1162	142804	909127	Dh	-		-		-	-	-	-
1163	142789	909112	Dh	-		-		-	-	-	-

Table 1. (continued)

1164	142816	909138	Dh	-	-	-	-	-	-	-
1165	142834	909172	Sr	-	-	-	-	-	-	-
1166	142836	909177	Dh	-	-	-	-	-	-	-
1167	142858	909172	Sr	-	-	-	-	-	-	-
1168	142862	909170	Dh	-	-	-	-	-	-	-
1169	142863	909175	Sr	-	-	-	-	-	-	-
1170	142881	909189	Dh	-	-	-	-	-	-	-
1171	142881	909196	Dh	-	-	-	-	-	-	-
1172	142884	909198	Dh	-	-	-	-	-	-	-
1173	142904	909214	Dh	-	-	-	-	-	-	-
1174	142929	909213	Dh	-	-	-	-	-	-	-
1175	142927	909223	Dh	-	-	-	-	-	-	-
1176	142939	909223	Dh	-	-	-	-	-	-	-
1177	142940	909241	Dh	-	-	-	-	-	-	-
1178	142946	909267	Dh	-	-	-	-	-	-	-
1179	142963	909256	Dh	-	-	-	-	-	-	-
1180	142930	909289	Dh	-	-	-	-	-	-	-
1181	142920	909275	Dh	-	-	-	-	-	-	-
1182	142916	909295	Dh	-	-	-	-	-	-	-
1183	142913	909308	Dh	-	-	-	-	-	-	-
1184	142925	909281	Dh	-	-	-	-	-	-	-
1185	142923	909245	Dh	-	-	-	-	-	-	-
1186	142900	909253	Dh	-	-	-	-	-	-	-
1187	142869	909285	Dh	-	-	-	-	-	-	PE13-1189
1188	142919	909355	Sr	-	-	-	-	-	-	-
1189	142873	909401	Sr	-	-	-	-	-	-	-
1190	142829	909433	Sr	-	-	-	-	-	-	-
1191	142678	909483								
1192	142622	909375								
1193	142571	909300	Sr	-	-	-	-	-	-	-
1194	142701	909277	Dh	-	-	-	-	-	-	-
1195	142737	909264	Dh	-	-	-	-	-	-	-
1196	142749	909260	Dh	-	-	-	-	-	-	-
1197	142754	909271	Dh	-	-	-	-	-	-	-
1198	142810	909299	Dh	-	-	-	-	-	-	-
1199	142835	909313	Dh	-	-	-	-	-	-	-
1200	142842	909294	Dh	-	-	-	-	-	-	-
1201	142848	909247	Dh	-	-	-	-	-	-	-
1202	142767	909210	Dh	-	-	-	-	-	-	-
1203	142705	909212	Sr	-	-	-	-	-	-	-
1204	142681	909201	Sr	-	-	-	-	-	-	-

Table 1. (continued)

1205	142678	909199	Sr	-	-	-	-	-	-	-
1206	142653	909223	Dh-Sr	-	-	-	-	-	-	-
1207	142725	909234	Dh	-	-	-	-	-	-	-
1208	142724	909199	Dh	-	-	-	-	-	-	-
1209	142705	909197	Sr	-	-	-	-	-	-	-
1210	142725	909180	Dh	-	-	-	-	-	-	-
1211	138533	909368	Om	-	-	-	-	-	-	-
1212	138595	909262	Om	-	-	-	-	-	-	-
1213	138585	909321	Om	-	-	-	-	-	-	-
1214	138630	909246	Om	-	-	-	-	-	-	-
1215	138657	909225	Om	-	-	-	-	-	-	-
1216	138673	909237	Om	-	-	-	-	-	-	-
1217	138689	909263	Om	-	-	-	-	-	-	-
1218	138667	909290	Om	-	-	-	-	-	-	-
1219	138838	909319	Om	-	-	-	-	-	-	-
1220	138836	909281	Om	156	23	W	-	-	-	-
1221	138841	909244	Om	-	-	-	-	-	-	-
1222	138875	909235	Om	-	-	-	-	-	-	-
1223	138888	909214	Om	-	-	-	-	-	-	-
1224	138890	909230	Om	-	-	-	-	-	-	-
1225	138870	909236	Om	188	49	W	-	-	-	-
1226	138881	909275	Om	-	-	-	-	-	-	-
1227	138882	909309	Om	205	35	W	-	-	-	-
1228	138888	909326	Om	-	-	-	-	-	-	-
1229	138885	909384	Om	-	-	-	-	-	-	-
1230	138912	909340	Om	153	38	W	-	-	-	-
1231	138901	909261	Om	-	-	-	-	-	-	-
1232	138900	909267	Om	-	-	-	-	-	-	-
1233	138967	909306	Om	-	-	-	-	-	-	-
1234	138995	909302	Om	-	-	-	-	-	-	-
1235	139072	909301	Om	-	-	-	-	-	-	-
1236	139143	909219	Om	-	-	-	-	-	-	-
1237	139213	909293	Om	-	-	-	-	-	-	-
1238	139353	909360	Om	-	-	-	-	-	-	-
1239	139461	909426	Om	-	-	-	-	-	-	-
1240	139489	909388	Om	-	-	-	-	-	-	-
1241	139486	909361	Om	170	16	W	-	-	-	-
1242	139535	909317	Om	-	-	-	-	-	-	-
1243	139525	909302	Om	-	-	-	-	-	-	-
1244	139509	909273	Om	-	-	-	-	-	-	-
1245	139497	909249	Om	-	-	-	-	-	-	-
1246	139562	909395	Om	-	-	-	-	-	-	-

Table 1. (continued)

1247	139310	908896	Om	-	-	-	-	-	-	-
1248	139313	909158	Om	-	-	-	-	-	-	-
1249	139426	909202	Om	-	-	-	-	-	-	-
1250	139236	909178	Om	-	-	-	-	-	-	-
1251	139225	909198	Om	-	-	-	-	-	-	-
1252	139169	909143	Om	-	-	-	-	-	-	-
1253	139009	909140	Om	-	-	-	-	-	-	-
1254	138851	909170	Om	-	-	-	-	-	-	-
1255	138810	909074	Om	-	-	-	-	-	-	-
1256	138785	909024	Om	-	-	-	-	-	-	-
1257	141616	910394	Sr	-	-	-	-	-	-	-
1258	141663	910445	Sr	-	-	-	-	-	-	-
1259	141650	910518	Sr	-	-	-	-	-	-	-
1260	141674	910581	Sr	-	-	-	-	-	-	-
1261	141679	910670	Sr	-	-	-	-	-	-	-
1262	141685	910699	Sr	-	-	-	-	-	-	-
1263	141692	910712	Sr	-	-	-	-	-	-	-
1264	141698	910917	Sr	-	-	-	-	-	-	-
1265	141654	910983	Sr	-	-	-	-	-	-	-
1266	141670	911013	Sr	-	-	-	-	-	-	-
1267	141741	911110	Sr	-	-	-	-	-	-	-
1268	141787	911118	Sr	-	-	-	-	-	-	-
1269	141791	911208	Sr	-	-	-	-	-	-	-
1270	141759	911455	Sr	-	-	-	-	-	-	-
1271	141805	911481	Sr	-	-	-	-	-	-	-
1272	141777	911532	Sr	-	-	-	-	-	-	-
1273	141692	911577	Sr	-	-	-	-	-	-	-
1274	141683	911856	Sr	-	-	-	-	-	-	-
1275	141771	911914	Sr	-	-	-	-	-	-	-
1276	141763	910625	lp	-	-	-	-	-	-	-
1277	141323	906792	Sr	-	-	-	-	-	-	-
1278	141251	906732	Sr	-	-	-	-	-	-	-
1279	141074	906587	Sr	-	-	-	-	-	-	-
1280	141049	906540	Om	-	-	-	-	-	-	-
1281	140907	906157	Om	-	-	-	-	-	-	-
1282	140915	906028	Om	-	-	-	-	-	-	-
1283	140901	905882	Om	-	-	-	-	-	-	-
1284	140981	905742	Sr	-	-	-	-	-	-	-
1285	140985	905748	Sr	-	-	-	-	-	-	-
1286	141047	905722	Sr	-	-	-	-	-	-	-
1287	141039	905686	Sr	-	-	-	-	-	-	-
1288	141143	905734	Sr	-	-	-	-	-	-	-

Table 1. (continued)

1289	141435	905428	Ddi	-	-	-	-	-	-	-	
1290	141336	905046	Ddi	-	-	-	-	-	-	-	
1291	141139	905068	?	-	-	-	-	-	-	-	
1292	141163	905165	Sr	-	-	-	-	-	-	-	
1293	141264	905391	Sr	-	-	-	-	-	-	-	
1294	141149	905438	Sr	-	-	-	-	-	-	-	
1295	140996	905530	Sr	-	-	-	-	-	-	-	
1296	140874	905491	Om	-	-	-	-	-	-	-	
1297	141003	905632	Sr	-	-	-	-	-	-	-	
1298	141162	905880	Sr	-	-	-	-	-	-	-	
1299	141167	905918	Sr	-	-	-	-	-	-	-	
1300	141138	906040	Sr	-	-	-	-	-	-	-	
1301	141050	906022	Sr	-	-	-	181	27	S	-	
1302	141041	906021	Om	-	-	-	-	-	-	-	
1303	142681	910279	Sr	-	-	-	-	-	-	-	
1304	142678	910354	-	-	-	-	-	-	-	-	
1305	142728	910456	-	-	-	-	-	-	-	-	
1306	142662	910575	-	-	-	-	-	-	-	-	
1307	142709	910597	-	-	-	-	-	-	-	-	
1308	142713	910644	-	-	-	-	-	-	-	-	
1309	142686	910685	-	-	-	-	63	42	W	-	
1310	142615	910843	-	-	-	-	73	35	W	-	
1311	142620	910929	-	-	-	-	36	38	SW	PE13-1311	
1312	142553	910946	-	-	-	-	44	13	SW	-	
1313	142654	910714	-	-	-	-	165	2	N	-	
1314	142568	910731	-	-	-	-	-	-	-	-	
1315	142518	910774	-	-	-	-	-	-	-	-	
1316	142530	910827	-	-	-	-	45	43	SW	-	
1317	142391	910887	-	-	-	-	-	-	-	PE13-1317	
1318	142357	911005	-	-	-	-	-	-	-	-	
1319	142388	911091	-	-	-	-	-	-	-	-	
1320	142558	911155	-	-	-	-	-	-	-	-	
1321	142496	911274	-	-	-	-	34	8	SW	-	
1322	142604	911581	-	-	-	-	-	-	-	-	
1323	142440	911654	-	-	-	-	-	-	-	-	
1324	142543	911544	-	-	-	-	-	-	-	-	
1325	142448	911459	-	-	-	-	-	-	-	-	
1326	142446	911675	-	-	-	-	-	-	-	-	
1327	142574	911676	-	-	-	-	-	-	-	-	
1328	142661	911543	-	-	-	-	-	-	-	-	
1329	142574	911510	-	-	-	-	-	-	-	-	

Table 1. (continued)

1330	142612	911430	-	-	-	-	-	-	-		
1331	142502	911306	-	-	-	-	-	-	-	-	
1332	142433	911303	-	-	-	-	-	-	-	-	
1333	142402	911293	-	-	-	-	-	-	-	PE13-1333	
1334	142457	911321	-	-	-	-	-	-	-	-	
1335	142246	911359	-	-	-	-	-	-	-	-	
1336	142199	911363	-	-	-	-	-	-	-	-	
1337	142204	911287	-	-	-	-	-	-	-	-	
1338	142168	911310	-	-	-	-	-	-	-	-	
1339	142250	911153	-	-	-	-	-	-	-	-	
1340	142134	911120	-	-	-	-	-	-	-	-	
1341	142057	911240	-	-	-	-	-	-	-	-	
1342	141931	911517	-	-	-	-	-	-	-	-	
1343	142015	911302	-	-	-	-	-	-	-	-	
1344	142050	911184	-	-	-	-	-	-	-	-	
1345	142052	911062	-	-	-	-	-	-	-	-	
1346	141994	910933	-	-	-	-	-	-	-	-	
1347	142126	910957	-	-	-	-	-	-	-	-	
1348	142221	910904	-	-	-	-	-	-	-	-	
1349	142341	910903	-	-	-	-	-	-	-	PE13-1349	
1350	142358	910850	-	-	-	-	-	-	-	-	
1351	142424	910746	-	-	-	-	-	-	-	-	
1352	142514	910650	-	-	-	-	-	-	-	-	
1353	142566	910483	-	-	-	-	-	-	-	-	
1354	142614	910426	-	-	-	-	149	5	S	-	
1355	142742	910456	-	-	-	-	-	-	-	-	
1356	142730	910650	Sr	-	-	-	-	-	-	-	
1357	142768	910649	Sr	-	-	-	-	-	-	-	
1358	142825	910619	Sr	-	-	-	-	-	-	-	
1359	142930	910564	Sr	-	-	-	-	-	-	-	
1360	142827	910794	Dh	-	-	-	-	-	-	-	
1361	142628	911396	Sr	-	-	-	-	-	-	-	
1362	142811	911458	Sr	-	-	-	-	-	-	-	
1363	142920	911448	Dh	-	-	-	-	-	-	-	
1364	142872	911588	Dh	-	-	-	-	-	-	-	
1365	142830	911607	Dh	-	-	-	-	-	-	-	
1366	142622	911811	Sr	-	-	-	-	-	-	-	
1367	142563	911810	-	-	-	-	-	-	-	-	
1368	142436	911781	Dh	-	-	-	-	-	-	-	
1369	142304	911776	Dh	-	-	-	-	-	-	-	
1370	142226	911781	Sr	-	-	-	-	-	-	-	

Table 1. (continued)

1371	142177	911878	Sr	-	-	-	-	-	-	-
1372	142232	912061	Sr	-	-	-	-	-	-	-
1373	142207	912076	Dh	-	-	-	-	-	-	-
1374	142236	912204	Sr	-	-	-	-	-	-	-
1375	142268	912198	Sr	-	-	-	-	-	-	-
1376	142339	912279	Dh	-	-	-	-	-	-	-
1377	142570	912309	Dh	-	-	-	-	-	-	-
1378	142689	912379	Dh	-	-	-	-	-	-	-
1379	143037	912283	Dh	-	-	-	-	-	-	-
1380	142969	912218	Dh	-	-	-	-	-	-	-
1381	143053	912027	Dh	-	-	-	-	-	-	-
1382	143074	911886	Dh	-	-	-	-	-	-	-
1383	143042	911847	-	-	-	-	-	-	-	-
1384	143093	911877	-	-	-	-	-	-	-	-
1385	143270	911842	-	-	-	-	-	-	-	-
1386	143339	911721	-	-	-	-	-	-	-	-
1387	143381	911703	-	-	-	-	-	-	-	-
1388	143387	911616	-	-	-	-	-	-	-	-
1389	143388	911588	Dh	-	-	-	-	-	-	-
1390	143283	911447	-	-	-	-	-	-	-	-
1391	143410	911470	-	-	-	-	-	-	-	-
1392	143486	911598	Dh	-	-	-	-	-	-	-
1393	143204	911852	Dh	-	-	-	-	-	-	-
1394	141005	909447	Om	-	-	-	-	-	-	-
1395	140644	909450	Om	-	-	-	-	-	-	-
1396	140539	909449	Om	-	-	-	-	-	-	-
1397	140355	909476	Om	-	-	-	-	-	-	-
1398	140101	909516	Om	-	-	-	-	-	-	-
1399	140176	909733	Om	-	-	-	-	-	-	-
1400	140170	909959	Om	-	-	-	-	-	-	-
1401	140111	910310	Om	-	-	-	-	-	-	-
1402	140748	910393	Om	-	-	-	-	-	-	-
1403	140348	910460	Om	-	-	-	-	-	-	-
1404	140475	910710	Om	-	-	-	-	-	-	-
1405	140445	910567	Om	-	-	-	-	-	-	-
1406	140811	910541	Om	-	-	-	-	-	-	-
1407	140621	910284	Sr?	-	-	-	-	-	-	-
1408	140604	910200	?	-	-	-	-	-	-	-
1409	140545	910185	?	-	-	-	-	-	-	-
1410	140528	910192	Sr	140	51	W	-	-	-	-
1411	140582	910145	Om	-	-	-	-	-	-	-
1412	140632	910155	Om	-	-	-	-	-	-	-

Table 1. (continued)

1413	140867	910097	?	-		-	-	-	-	-	-
1414	140789	910086	Om	-		-	-	-	-	-	-
1415	140876	909926	Om	-		-	-	-	-	-	-
1416	140863	909759	Om	-		-	-	-	-	-	-
1417	140579	910073	Om	-		-	-	-	-	-	-
1418	140573	910072	Om	-		-	-	-	-	-	-
1419	140551	910076	Om	-		-	-	-	-	-	-
1420	140524	910082	Om	-		-	-	-	-	-	-
1421	140460	910093	Om	-		-	-	-	-	-	-
1422	140280	910258	Om	-		-	-	-	-	-	-
1423	140388	909622	Om	-		-	-	-	-	-	-
1424	140431	909311	Om	-		-	-	-	-	-	-
1425	140456	909141	Om	-		-	-	-	-	-	-
1426	140261	909101	Om	-		-	-	-	-	-	-
1427	140501	908975	Om	-		-	-	-	-	-	-
1428	140629	908673	Om	-		-	-	-	-	-	-
1429	140600	908672	Om	-		-	-	-	-	-	-
1430	140569	908628	Om	-		-	-	-	-	-	-
1431	140550	908608	Om	-		-	-	-	-	-	-
1432	140565	908525	Om	-		-	-	-	-	-	-
1433	140573	908557	Om	-		-	-	-	-	-	-
1434	140627	908544	Om		9		30	W	-	-	-	-
1435	140660	908603	Om	-		-	-	-	-	-	-	-
1436	140641	908629	Om	-		-	-	-	-	-	-	-
1437	140676	908632	Om	-		-	-	-	-	-	-	-
1438	140698	908638	Om	-		-	-	-	-	-	-	-
1439	140753	908629	Om	-		-	-	-	-	-	-	-
1440	140833	908676	Om	-		-	-	-	-	-	-	-
1441	140921	908574	Om	-		-	-	-	-	-	-	-
1442	140951	908600	Om	-		-	-	-	-	-	-	-
1443	140946	908617	Om	-		-	-	-	-	-	-	-
1444	140947	908631	Om	-		-	-	-	-	-	-	-
1445	140950	908653	Om	-		-	-	-	-	-	-	-
1446	140961	908643	Om		157		22	W	-	-	-	-
1447	140959	908658	Om	-		-	-	-	-	-	-	-
1448	140961	908682	Om	-		-	-	-	-	-	-	-
1449	140969	908729	Om	-		-	-	-	-	-	-	-
1450	140672	908946	Om	-		-	-	-	-	-	-	-
1451	140701	909078	-	-		-	-	-	-	-	-	-
1452	140557	909230	Om	-		-	-	-	-	-	-	-
1453	140499	909559	Om	-		-	-					
1454	140521	909663	Om		325		20	W	-	-	-	-

Table 1. (continued)

1455	140547	909666	Sr	-	-	-	-	-	-	-	
1456	140621	909758	Om	-	-	-	-	-	-	-	
1457	140592	909756	Om	-	-	-	-	-	-	-	
1458	140682	909757	Sr	-	-	-	-	-	-	-	
1459	140717	909767	Sr-Om	-	-	-	-	-	-	-	
1460	140736	909774	Om	-	-	-	-	-	-	-	
1461	142720	909168	Sr	-	-	-	-	-	-	-	
1462	142753	909318	Dh	-	-	-	-	-	-	-	
1463	142762	909342	Dh	-	-	-	-	-	-	-	
1464	142724	909379	Sr	-	-	-	-	-	-	-	
1465	142722	909393	Sr	-	-	-		26	16	S	-
1466	142797	909492	Dh	-	-	-	-	-	-	-	
1467	142852	909582	-	-	-	-	-	-	-	-	
1468	142938	909624	Dh	-	-	-	-	-	-	-	
1469	143076	909649	Dh	-	-	-	-	-	-	-	
1470	143137	909620	Dh	-	-	-	-	-	-	-	PE13-1471
1471	143182	909503	Dh	-	-	-	-	-	-	-	PE13-1472
1472	143289	909708	Dh	-	-	-	-	-	-	-	-
1473	143286	909904	Dh	-	-	-	-	-	-	-	-
1474	143310	909969	Dh	-	-	-	-	-	-	-	-
1475	143330	910002	Dh	-	-	-	-	-	-	-	-
1476	143397	910241	Dh	-	-	-	-	-	-	-	-
1477	143298	910211	Dh	-	-	-	-	-	-	-	-
1478	143201	910152	Dh	-	-	-	-	-	-	-	-
1479	143171	910140	Dh	-	-	-	-	-	-	-	-
1480	143151	910002	Dh	-	-	-	-	-	-	-	-
1481	143137	909899	Dh	-	-	-	-	-	-	-	-
1482	143017	909859	Dh	-	-	-	-	-	-	-	-
1483	142997	909754	Dh	-	-	-	-	-	-	-	-
1484	142883	909718	Sr-Dh	-	-	-		359	4	S	-
1485	142822	909596	-	-	-	-	-	-	-	-	-
1486	142987	909316	Dh	-	-	-	-	-	-	-	-
1487	141984	904683	Sr	-	-	-		151	5	S	-
1488	141982	904662	Sr	-	-	-	-	-	-	-	-
1489	142101	904561	Sr	-	-	-	-	-	-	-	-
1490	142196	904587	Dh	-	-	-	-	-	-	-	-
1491	142394	904587	Dh	-	-	-	-	-	-	-	-
1492	142451	904487	Dh	-	-	-	-	-	-	-	-
1493	142946	904519	Dh	-	-	-	-	-	-	-	-
1494	142950	904657	Dh		351	74	W	-	-	-	-
1495	142940	904480	Dh		345	67	W	-	-	-	-

Table 1. (continued)

1496	142943	904457	Dh		11	65	W	-	-	-	-
1497	142883	904195	Dh	-	-	-	-	-	-	-	-
1498	142830	904082	Dh	-	-	-	-	-	-	-	-
1499	142872	904038	Dh	-	-	-	-	-	-	-	-
1500	142839	903995	Dh		30	56	W	-	-	-	PE13-1501
1501	142766	904015	Dh		179	25	W	-	-	-	-
1502	142783	903640	Dh		182	45	W	-	-	-	-
1503	142771	903378	Dh	-	-	-	-	-	-	-	-
1504	142390	903349	Dh	-	-	-	-	-	-	-	-
1505	142361	903537	Dh	-	-	-	-	-	-	-	-
1506	142360	903741	Dh	-	-	-	-	-	-	-	-
1507	142315	903737	Dh		355	47	W	-	-	-	-
1508	142319	903771	Dh	-	-	-	-	-	-	-	-
1509	142338	903793	Dh	-	-	-	-	-	-	-	-
1510	142251	903895	Dh	-	-	-	-	-	-	-	-
1511	142106	903108	Dh	-	-	-	-	-	-	-	-
1512	141950	903184	Dh	-	-	-	-	-	-	-	-
1513	142031	903377	Dh	-	-	-	-	-	-	-	-
1514	142177	903509	Dh	-	-	-	-	-	-	-	-
1515	142219	904089	Dh	-	-	-	-	-	-	-	-
1516	142274	904349	Dh	-	-	-	-	-	-	-	-
1517	141955	904208	-	-	-	-	-	-	-	-	-
1518	141932	904311	Dh	-	-	-	-	-	-	-	-
1519	141965	904434	Sr	-	-	-	-	-	-	-	-
1520	141878	904441	Dh	-	-	-	-	-	-	-	-
1521	141995	904586	Dh	-	-	-	-	-	-	-	-
1522	143679	911355	Dh	-	-	-	-	-	-	-	-
1523	143629	911297	Dh	-	-	-	-	-	-	-	-
1524	143619	911248	Dh	-	-	-	-	-	-	-	-
1525	143595	911249	Dh	-	-	-	-	-	-	-	-
1526	143562	911243	Dh	-	-	-	-	-	-	-	-
1527	143522	911231	Dh	-	-	-	-	-	-	-	-
1528	143391	910894	Dh	-	-	-	-	-	-	-	-
1529	143423	910878	Dh	-	-	-	-	-	-	-	-
1530	143307	910717	Dh	-	-	-	-	-	-	-	-
1531	143177	910726	Dh	-	-	-	-	-	-	-	-
1532	143314	911107	Dh	-	-	-	-	-	-	-	-
1533	143350	911278	Dh	-	-	-	-	-	-	-	-
1534	143384	911401	Dh	-	-	-	-	-	-	-	-
1535	143404	911422	Dh	-	-	-	-	-	-	-	PE13-1536
1536	143400	911479	Dh	-	-	-	-	-	-	-	-

Table 1. (continued)

1537	143402	911578	Dh	-	-	-	-	-	-	-
1538	143364	911601	Sr	-	-	-	-	-	-	-
1539	143310	911595	Dh	-	-	-	-	-	-	-
1540	143282	911610	Dh	-	-	-	-	-	-	-

REFERENCES

Ayuso, R.A., Arth, J.G., 1990. The Northeast Kingdom batholith, Vermont: magmatic evolution and geochemical constraints of the origin of Acadian granitic rocks. *Contrib. Mineral Petrol.*, 111, 1-23.

Barreiro, B., Aleinikoff, J.N., 1985. Sm-Nd and U-Pb isotopic relationships in the Kinsman quartz monzonite, New Hampshire: Geological Society of America, Abstracts with Programs, 17, p.3.

Berry, H.N, IV, 1989. A new stratigraphic and structural interpretation of granulite-facies metamorphic rocks in the Brimfield-Sturbridge area, Massachusetts and Connecticut: Ph.D. dissertation, University of Massachusetts, Amherst, 330, pp, 4 plates.

Billings, M.P., 1937. Regional metamorphism of the Littleton Moosilauke area, New Hampshire: Geological Society of America Bulletin, v. 46, p. 463-566.

Billings, M.P., 1956. Bedrock Geologic Map of New Hampshire.

Bradley, D.C., Tucker, R.D., Lux, D.R., Harris, A.G., and McGregor, D.C., 2000. Migration of the Acadian orogen and foreland basin across the northern Appalachians of Maine and adjacent areas: U.S. Geological Survey Professional Paper 1624, 48, pp.

Dewey, J.F., Holdsworth, R.E., Strachan, R.A., 1998. Transpression and transtension zones. In: Holdsworth, R.E., Strachan, R.A., Dewey, J.F. (Eds.), Continental Transpressional and Transtensional Tectonics, vol. 135. Special Publication of the Geological Society, London, pp. 1e14.

Dorais, M. J., 2003. The petrogenesis and emplacement of the New Hampshire plutonic suite, *Am J Sci*. 303, 447-487.

Eusden, J.D., Bothner, W.A., and Hussey, A.M., 1987. The Kearsarge-Central Maine Synclinorium of Southeastern New Hampshire and Southwestern Maine: Stratigraphic and Structural Relations of an Inverted Section, *Am J Sci.* 287, 242-264.

Goodwin, L.B., Tikoff, B., 2002. Competency contrast, kinematics, and the development of foliations and lineations in the crust. *Journal of structural Geology*. 24, 1065-1085.

Hall L.M., Robinson, P., 1982. Stratigraphic-tectonic subdivisions of southern New England: Major Structural Zones and Faults of the Northern Appalachians. *Geological Association of Canada Special Paper*. 24. 15-41.

Hatch, N.L. Jr., Moench, R.H., Lyons, J.B., 1983. Silurian-Lower Devonian stratigraphy of eastern and south-central New Hampshire, extensions from western Maine.*American Journal of Science*. 283, 739-761.

Hibbard, J.P., van Staal, C.R., Rankin, D.W., 2007. A comparative analysis of pre-Silurian crustal building blocks of the northern and the southern Appalachian orogen. *American Journal of Science*. 307, 23-45.

Hollocher, K., Bull, J., Robinson, P., 2002. Geochemistry of the metamorphosed Ordovician Taconian magmatic arc, Bronson Hill anticlinorium, western New England. *Physics and Chemistry of the Earth*. 27, 5-45.

Lanzirotti, A., and Hanson, G.N., 1995. U-Pb dating of major and accessory minerals formed during metamophism and deformation of metapelites. *Geochimica et Cosmochimica acta* ,v. 59, 2513-2526.

Leo, G.W., Zartman, R.E., and Brookins, D.G., 1984. Glastonbury Gneiss and mantling rocks (a modified Oliverian dome) in south-central Massachusetts and north-central Connecticut: Geochemistry, petrogenesis, and radiometric age: *U.S. Geological Survey Professional Paper* 1295, 45 p.

Massey, M.A., and Moecher, D.P., 2006. Heterogeneous flow of an extruded granitic dome in the Bronson Hill terrane, Massachusetts, USA: Evidence for oblique convergence and indentation, and the Alleghanian orogeny: AGU Eos Transactions, Fall Meeting Supplement Abstract T23B-0495.

Massey, M.A., and Moecher, D.P., 2008a. Bedrock geologic map of the Palmer 7.5 minute quadrangle, south central Massachusetts: Open file report, Office of Massachusetts State Geologist, 1:25000 map.

Massey, M.A.*, and Moecher, D.P., 2008b. Deep crustal partitioned transpression and ductile extrusion of the Monson orthogneiss, Bronson Hill-Central Maine boundary zone, south-central Massachusetts, in, Van Balen, M.R. (ed.), Guidebook to field trips in the Massachusetts and adjacent regions of Connecticut and New York: New England Intercollegiate Geological Conference 100th Annual Meeting, Trip A2, 29 pp.

Massey, M.A., 2011. Transpression, deformation partitioning, and extrusion in the Appalachian orogen, southern New England, U.S.A. Ph. D. Dissertation, University of Kentucky, Lexington, KY, 255 pp.

Massey, M.A., and Moecher, D.P., 2013. Transpression, extrusion, partitioning, and lateral escape in the middle crust: Significance of structures, fabrics, and kinematics in the Bronson Hill zone, southern New England, U.S.A. *J. Struct. Geo.*

Moecher, D.P., and Massey, M.A., 2007. Late Paleozoic partitioned transpression and heterogeneous extrusion of granitic Monson orthogneiss, Appalachian orogen, southern New England, USA: Eos Transactions, Fall Meeting Supplement, Abstract T23E-03.

Moecher, D.P., 1999. The distribution, style, and intensity of Alleghanian metamorphism in south-central New England: Petrologic evidence from the Pelham and Willimantic domes. *Journal of Geology*, v. 107, 449-471.

Moench, R.H., 1971. Geologic Map of the Rangeley and Phillips Quadrangles, Franklin and Oxford Counties, Maine. U.S.G.S. Miscellaneous Geologic Investigations Map I-605.

Moench R.H., and Aleinikoff, J.N.; 2002. Stratigraphy, geochronology, and accretionary terrane settings of two Bronson-Hill arc sequences, northern New England. *Physics and Chemistry of the Earth*. 27, 47-95.

Moench, R.H., Boone, G.M., Bothner, W.A., Boudette, E.L., Hatch, Jr., N.L., Hussey II, A.M., and Marvinney, R.G., 1995. Geologic map of the Sherbrooke–Lewiston area, Maine, New Hampshire, Vermont, United States, and Quebec, Canada, with contributions togeochronology by J.N. Aleinikoff, US Geological Survey Miscellaneous Series Investigations Map I-1898-D; scale 1:250,000, pamphlet, 56 p.

O'Brien, T.M., 2009. Bedrock mapping of the Winchendon (1:25,000) quadrangle (MA-NH): Evidence for discontinuous deformation along the Bronson Hill-Central Maine Boundary Zone: M.S. thesis, University of Kentucky, Lexington, KY.

Osberg, P.H., Tull, J.F., Robinson, P., Hon, R.; and Butler, J.R., Jr., 1989. The Acadian orogeny. In Hatcher, R.D., Jr.; Thomas, W.A.; Viele, G.W. (eds.): The Appalachian-Ouachita orogen in the United States; The Geology of North America, Geological Society of America, Boulder, CO, v.F-2, 179-232.

Pease, M.H. 1982. The Bonemill Brook fault zone, eastern Connecticut, in: Guidebook for field trips in Connecticut and south-central Massachusetts, New England Intercollegiate Geological Conference, 74th Annual Meeting, University of Connecticut, Storrs, CT. p. 263-287.

Peterson, V.L., 1992. Structure, petrology, and tectonic implications of highly strained rocks along the west margin of the Acadian granulite-facies high, south-central Massachusetts, Ph.D. thesis, University of Massachusetts, Amherst, Massachusetts pp. 283.

Peterson, V.L., and Robinson, P., 1993. Progressive evolution from uplift to orogen-parallel transport in a late Acadian, upper amphibolite – to granulite – facies shear zone, South-Central Massachusetts. *Tectonics*. 12, 550-567.

Rankin, D.W., Coish, R.A., Tucker, R.D., Peng, Z.X., Wilson, S.A., And Rouff A.A., 2007. Silurian extension in the upper Connecticut Valley, United States and the origin of Middle Paleozoic basins in the Quebec Embayment. *Am. J. Sci.* v. 307, 216-264.

Robin, P.F., and Cruden, A.R.; 1994, Strain and vorticity patterns in ideally ductile transpression zones.*Journal of Structural Geology*.16, 447-466.

Robinson, P., Thomspson, P.J., and Elbert, D.C. 1991. The nappe theory in the Connecticut Valley region: Thirty-five years since Jim Thompson's first proposal. American Minerologist, v. 76, p. 689-712.

Robinson, P., 2003. Tectonic-Stratigraphic-Metamorphic Perspective of the New England Caledonides, west-central Massachusetts. In: Guidebook for field trips in the Five College Region,*95th Annual meeting NEIGC*, A1-1 – A1-54.

Robinson, P.; and Goldsmith, R., 1991. Stratigraphy of the Merrimack Belt, Central Massachusetts, in: The Bedrock Geology of Massachusetts, U.S. Geological Survey Professional Paper, 1366-E-J, p. G1-G37.

Robinson, P., Field, M.T., and Tucker, R.D., 1982. Stratigraphy and structure of the Ware-Barre area, central Massachusetts.In Joeston, Raymond, and Quarrier, S.S., eds., Guidebook for fieldtrips in Connecticut and south central Massachusetts.NEIGC 74th Annual Meeting, the University of Connecticut, Storrs. 341-374.

Robinson, P., and Tucker R.D., 1981. Discussion: The Merrimack synclinorium in northeastern Connecticut, *American Journal of Science*, 281, 1735-1744.

Robinson, P., Tucker, R.D., Bradley, D., Berry, H.N. IV., and Osberg, P.H., 1998. Paleozoic orogens in New England, USA, *GFF. Journal of the Geological Society of Sweden*, 120, 119-148.

Sanderson, D.J., Marchini, W.R.D., 1984. Transpression. Journal of Structural Geology 6, 449-458.

Seiders, V.M., 1976. Bedrock Geologic Map of the Wales Quadrangle, Massachusetts and Connecticut. U.S.G.S. GQ-1320.

Shearer, C.K., 1983, Petrography, mineral chemistry, and geochemistry of the Hardwick Tonalite and associated igneous rocks, central Massachusetts: Ph.D. thesis, University of Massachusetts, Amherst, 265p.

Solar, G.S., Brown, M., 2001. Deformation partitioning during transpression in response to Early Devonian oblique convergence, northern Appalachian orogen, USA. *Journal of Structural Geology*. 23, 1043-1065.

Solar, G.S.; Brown, M.; 1999. The classic high-T – low-p metamorphism of west-central Maine: Is it post-tectonic or syntectonic? Evidence from porphyroblast - matrix relations.*The Canadian Mineralogist*. 37, 311-333.

Teyssier, C.; Tikoff, B.; 1999. Fabric stability in oblique convergence and divergence.*Journal of Structural Geology*. 21, 969-974.

Thompson, J.B., Jr. 1954. Structural Geology of the Skitchewaug Mountain area, Claremont quadrangle, Vermont-New Hampshire. New England Intercollegiate Geological Conference, 46th Annual Meeting, Hanover, New Hampshire, Guidbook, 93-174.

Thompson, J.B. Jr., Robinson, P., Clifford, T.N., Trask, N.J., Jr., 1969. Nappes and gneiss domes in west-central New England. In: Zen, E-an; White, W.S.; Hadley, J.B.; and Thompson J.B., Jr., eds. Studies of Appalachian geology: northern and maritime. 203-218.

Thompson, P.J., 1985. Stratigraphy, structure, and metamorphism in the 7.5' Monadnock quadrangle, New Hampshire. Ph.D. thesis, University of Massachusetts, Amherst, Massachusetts.

Thomson, J.A., 1992. Petrology of high-grade schists, gneisses and cordierite pegmatites in south-central Massachusetts: Ph.D. thesis, University of Massachusetts, Amherst, Mass.

Thomson, J.A.; Peterson, V.L., Berry, H.N., Barreiro, B., 1992. Recent studies in the Acadian metamorphic high, south-central Massachusetts. In: Guidebook for field trips in the Connecticut Valley region of Massachusetts and adjacent states, Vol.1,*84th Annual meeting NEIGC*,229-255.

Tucker, R.D., 1977. Bedrock geology of the Bare area, central Massachusetts. Contribution No. 30 (M.S. thesis), Department of Geology and Geography, University of Massachusetts, Amherst, 132 p.

Tucker, R.D., Bradley, D.C., VerStraeten, C.A., Harris, A.G., Ebert, J.R., McCutcheon, S.R., 1998. New U-Pb zircon ages and the duration and division of Devonian time. *Earth and Planetary Science Letters*. 158, 175-186.

Tucker, R. D., and Robinson, P., 1990. Age and setting of the Bronson Hill magmatic arc: A re-evaluation based on U-Pb zircon ages in southern New England. *GSA Bulletin*, 102,1404-1419.

Tucker, R.D., Osberg, P.H., Berry, H.N. IV, 2001. The geology of a part of Acadia and the nature of the Acadian orogeny across central and eastern Maine. *American Journal of Science*. 301, 205-260.

Tucker, R.D. & Robinson, P., 1995. U-Pb Age of the Hardwick Pluton and Pre "Dome-Stage" Pegmatite, Quabbin Reservoir, and their Bearing on the "Acadian" Orogeny in Central Massachusetts and Adjacent New Hampshire. *Geological Society of America Abstracts with Programs. 27*, A-223–224.

van Staal, C.R., 2006. Pre-Carboniferous metallogeny of the Canadian Appalachians; Mineral Deposits of Canada, Natural Resources of Canada http://gsc.nrcan.gc.ca/mindep/synth_prov/appalachian/index_e.php).

Walker, T.B., 2011. Bedrock Geology and Tectonic Evolution of The Western Central Maine Zone, South Central Massachusetts: M.S. thesis, University of Kentucky, Lexington, KY.

Wintsch, R.P., Kunk, M.J., Boyd, J.L., and Aleinikoff, J.N., 2003. P-T-t paths and differentialAlleghanian loading and uplift of the Bronson Hill terrane south central New England: *American Journal of Science*. v. 303, p. 410-446.

Wintsch, R.P., Sutter, J.F.; 1986. A tectonic model for the late Paleozoic of southern New England. *The Journal of Geology*. 94, 459-472.

Wintsch, R.P., 1985. Bedrock geology of the Deep River area, Connecticut. In: Tracy R.J., ed. Guidebook for field trips in Connecticut and adjacent areas of New York and Rhode Island, *77th annual meeting NEIGC*, Yale University, New Haven Connecticut, 115-128.

Wintsch, R.P., Sutter, J.F., Kunk, M.J., Aleinikoff, J.N., Dorais, M.J., 1992. Contrasting P-T-t paths: Thermochronologic evidence for a Late Paleozoic final assembly of the Avalonian Composite Terrane in the New England Appalachians. *Tectonics*. 11, 672-689.

Zartman, R.E., and Leo, G.W., 1985. New radiometric ages on Oliverian core gneisses, New Hampshire and Massachusetts, *American Journal of Science*. v. 285, p. 267-280.

Zartman, R.E., 1988. Three decades of geochronologic studies in the New England Appalachians. *Geological Society of America Bulletin*. 100, 1168-1180.

Zen, E, Goldsmith, R., Ratcliffe, N.M., Robinson, P., Stanley, R.S., Hatch, N.L., Shride, A.F., Weed, E.G.A., Wones, D.R., 1983. Bedrock Geologic Map of Massachusetts. *U.S.G.S.*

Figure References:

Figure 1.1-

Moecher, D.P., 1999. The distribution, style, and intensity of Alleghanian metamorphism in south-central New England: Petrologic evidence from the Pelham and Willimantic domes. *Journal of Geology*, v. 107, 449-471.

Figure 1.2-

Robinson, P., Tucker, R.D., Bradley, D., Berry, H.N. IV., and Osberg, P.H., 1998. Paleozoic orogens in New England, USA, *GFF. Journal of the Geological Society of Sweden*, 120, 119-148.

Figure 2.1-

Shearer, C.K., 1983, Petrography, mineral chemistry, and geochemistry of the Hardwick Tonalite and associated igneous rocks, central Massachusetts: Ph.D. thesis, University of Massachusetts, Amherst, 265p.

Figure 2.2-

Rankin, D.W., Coish, R.A., Tucker, R.D., Peng, Z.X., Wilson, S.A., And Rouff A.A., 2007. Silurian extension in the upper Connecticut Valley, United States and the origin of Middle Paleozoic basins in the Quebec Embayment. *Am. J. Sci.* v. 307, 216-264.

Figure 3.1-

Massey, M.A.*, and Moecher, D.P., 2008b. Deep crustal partitioned transpression and ductile extrusion of the Monson orthogneiss, Bronson Hill-Central Maine boundary zone, south-central Massachusetts, in, Van Balen, M.R. (ed.), Guidebook to field trips in the Massachusetts and adjacent regions of Connecticut and New York: New England Intercollegiate Geological Conference 100th Annual Meeting, Trip A2, 29 pp.

Figure 3.2-

Dewey, J.F., Holdsworth, R.E., Strachan, R.A., 1998. Transpression and transtension zones. In: Holdsworth, R.E., Strachan, R.A., Dewey, J.F. (Eds.), Continental Transpressional and Transtensional Tectonics, vol. 135. Special Publication of the Geological Society, London, pp. 1e14.

Figure 4.1-

Zen, E, Goldsmith, R., Ratcliffe, N.M., Robinson, P., Stanley, R.S., Hatch, N.L., Shride, A.F., Weed, E.G.A., Wones, D.R., 1983. Bedrock Geologic Map of Massachusetts.

Figure 4.2-

Zen, E, Goldsmith, R., Ratcliffe, N.M., Robinson, P., Stanley, R.S., Hatch, N.L., Shride, A.F., Weed, E.G.A., Wones, D.R., 1983. Bedrock Geologic Map of Massachusetts.

Figure 4.3-

Massey, M.A., and Moecher, D.P., 2013. Transpression, extrusion, partitioning, and lateral escape in the middle crust: Significance of structures, fabrics, and kinematics in the Bronson Hill zone, southern New England, U.S.A. *J. Struct. Geo.*

Figure 5.6-

Shearer, C.K., 1983, Petrography, mineral chemistry, and geochemistry of the Hardwick Tonalite and associated igneous rocks, central Massachusetts: Ph.D. thesis, University of Massachusetts, Amherst, 265p.

Curriculum Vita

Lucas P. Rohrer
lucas.rohrer@caldwell.kyschools.us

Education
M.S. 2015 (Earth Sciences) University of Kentucky
Thesis: Bedrock Geologic Mapping and Structural Analysis of the Western Half of the Petersham Quadrangle, Central Massachusetts: Further Tests of the Model for Middle to Late Paleozoic Ductile Transpression, Vertical Extrusion, and Lateral Escape in the Northern Appalachians

B.A. 2010 (Chemistry) Asbury University

Professional Experience
7/14-present High School Science Teacher, Caldwell County High School
7/11-5/14 Teaching Assistant, University of Kentucky

Awards
USGS EdMap Grant
GSA Grant
Ferm Fund Grant, UK Department of Earth and Environmental Sciences
Pirtle Fund, UK Department of Earth and Environmental Sciences

PLATE 1 - 2011 EDMAP Poster

Explanation

The poster to follow presents the full 1:24,000 scale bedrock geologic map of the western half of the Petersham quadrangle with legend and supporting documentation, submitted to the U.S. Geological Survey EDMAP component of the National Cooperative Geologic Mapping Program. Support from EDMAP allowed this project to be completed. The map and poster reproduce many of the figures presented and data discussed in the thesis. The thesis document does not permit inclusion of a large-format geologic map, so the EDMAP poster is included here for the interested reader.

GEOLOGIC BEDROCK MAPPING AND STRUCTURAL ANALYSIS OF THE WESTERN HALF OF THE PETERSHAM 7.5-MINUTE QUADRANGLE, CENTRAL MASSACHUSETTS: EVIDENCE FOR TRANSPRESSION ALONG THE BRONSON HILL-CENTRAL MAINE BOUNDARY

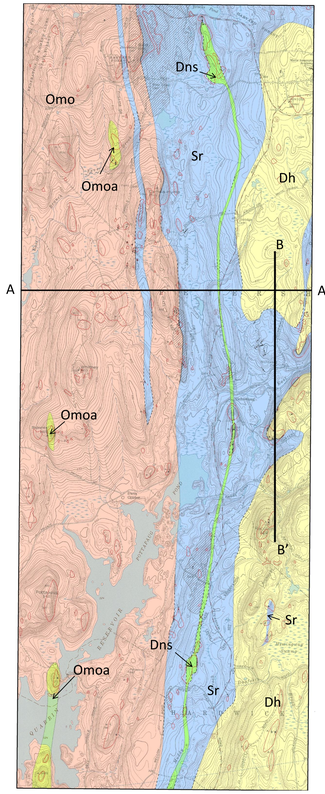

DESCRIPTION OF MAP UNITS

Dh — HARDWICK TONALITE (LATE DEVONIAN) - Dark, strongly foliated plagioclase-quartz-biotite-hornblende tonalitic mylonite and ultramylonite. Exposures, contacts, and description from Peterson (1992); not observed by authors.

Dns — QUARTZ DIORITE (DEVONIAN) - Massive to mildly foliated (minerals) quartz diorite sheet intruded into metasedimentary sequence within the Central Maine Zone.

Sr — RANGELEY FORMATION (SILURIAN) - Gray- to rusty-weathering, medium-grained, mildly to strongly foliated or complexly folded, quartz-plagioclase-biotite ± garnet ± sillimanite ± muscovite paragneiss or paraschist. Strong mineral lineations and a mylonite to ultramylonite texture develop in highly deformed zones associated with contacts with the other lithologies. Layered or irregular (often heavily deformed) leucosomes and coarse grained plagioclase and k-feldspar porphyroclasts are common.

Omo — ORTHOGNEISS – Mildly to moderately foliated, leucocratic, equigranular or porphyritic, fine- to medium-grained, plagioclase-quartz-biotite ± muscovite ± garnet orthogneiss interlayered with 1 cm to meter-scale, massive to moderately foliated or strongly lineated hornblende-plagioclase ± garnet amphibolite.

Omoa — AMPHIBOLITE - Map-scale bodies of massive to moderately foliated (slabby) hornblende-plagioclase±garnet amphibolite, interpreted as identical to but thicker than layers present with in Omo.

STRUCTURAL FEATURES

Located Contact
Approximate Contact
Inferred Contact

Foliation
Lineation

Areas where rock mass is dominated by leucopegmatite.
Area with an individual or multiple outcrops.

SCALE 1:24 000
1 MILE
1000 0 1000 2000 3000 4000 5000 6000 7000 FEET
1 KILOMETER
CONTOUR INTERVAL 10 FEET
NATIONAL GEODETIC VERTICAL DATUM OF 1929

QUADRANGLE LOCATION

Bedrock Geologic Map of the Western Half of the Petersham Quadrangle, Massachusetts

University of Kentucky
Department of Earth and Enviromental Sciences

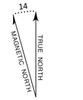

APPROXIMATE MEAN DECLINATION, 2013

Topographic base modified from U.S. Geological Survey, <1969>

Polyconic projection. 1983 North American Datum.

10,000-foot grid ticks based on Massachusetts state plane coordinate system, mainland zone, 1927 North American Datum.

1000-meter Universal Transverse Mercator grid ticks from 1927 North American Datum, zone 19.

ABSTRACT

Bedrock geologic mapping and structural analysis reveal the distribution of lithologic units and the orientation of tectonic fabrics and structures in the western half of the Petersham 7.5' quadrangle, western Mass. The area is underlain by three main lithologic units (W to E: Ordovician Monson granitic orthogneiss, Silurian Rangeley migmattitic paragneiss, and Devonian Hardwick tonalitic orthogneiss). Their tightly folded contact zones strike north to south through the entire quadrangle. An undated (Devonian?), generally unfoliated qtz diorite (10-100 m wide) intrusion occurs within the Rangeley along strike through the entire map area. The dominant fabric present in both orthogneisses is a shallow to moderately west-dipping foliation defined by quartzofeldspathic streaks, Bt and/or Hbl mineral grain orientation, and planar amphibolite layers in the Monson. In the strongly migmattitic Sil-Grt-Bt-Pl -Kfs Rangeley paragneiss, a subvertical foliation and a subhorizontal lineation (both striking north to south) are present. The foliation is defined by parallelism of leucosomes and mica grain orientation; the lineation is defined by the orientation of acicular Sil grains. Recumbent isoclinal outcrop-scale folds (axes parallel to Sil lineation) within the Rangeley near lithologic contacts, have been refolded on the cm to m scale, and are visible in vertical east to west striking faces. Asymmetric structures are only visible in one location in the map area (near the Rangeley-Hardwick contact), include asymmetric folds and S-C and S-C-C' fabrics, and are most prominent on horizontal faces. They indicate localized sinistral displacement along a north to south striking axis parallel to unit boundaries and tectonic fabrics in the area. Evidence for vertical and lateral extrusion of the Monson Orthogneiss as observed in the Palmer area (Massey and Moecher, 2013) is absent in the Petersham area. Instead, the primary strains are E-W shortening and N-S boundary compatible extension. Shortening is expressed in the planar foliation fabrics present in all three units; elongation is expressed in the lineation most prevalent in the Rangeley formation. The abundance of leucosome and large garnet porphyroblasts in the Rangeley adjacent to the Hardwick and diorite suggest regional metamorphism was driven by magmatic heat.

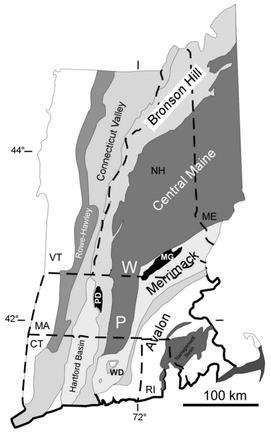

Figure 1: Regional geologic summary of the major lithotectonic units underlying New England.

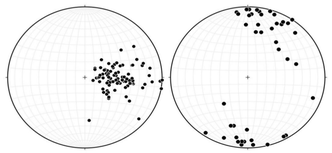

Figure 2: Structural Data. **Left:** Poles to foliation show a slightly to near vertical west-dipping foliation. **Right:** Mineral lineations recorded within the map area are subhorizontal or dip slightly to the northeast or southwest.

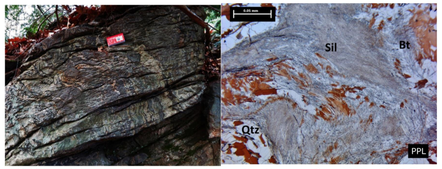

Left: Outcrop of Rangeley Fm. with leucosomes showing at least two generations of folding. **Right:** Thin section showing a similar micros-scale complex folding pattern within the Rangeley Fm.

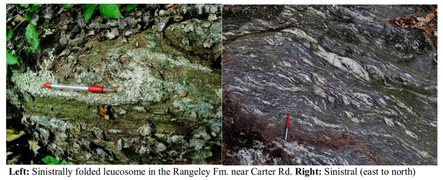

Left: Sinistrally folded leucosome in the Rangeley Fm. near Carter Rd. **Right:** Sinistral (east to north) asymmetries in a horizontal face of a Rangeley outcrop next to Carter Rd.

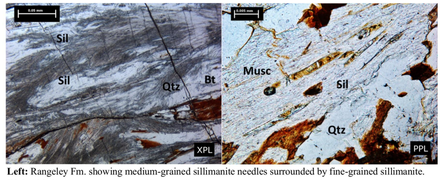

Left: Rangeley Fm. showing medium-grained sillimanite needles surrounded by fine-grained sillimanite. **Right:** Medium grained remnant sillimanite fragments surrounded by retrograde muscovite that has replaced the fine grained sillimanite.

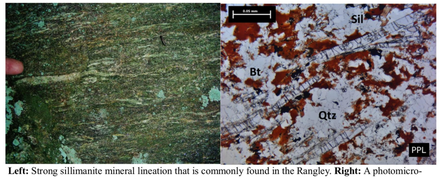

Left: Strong sillimanite mineral lineation that is commonly found in the Rangley. **Right:** A photomicrograph showing the same mineral lineation on the microscopic scale.

Left: Foliated Rangeley granofels from Trot Hill. **Right:** A vertical face of Rangeley granofels created by a fracture along the vertical foliation 10 meters from the contact with the quartz diorite intrusion.

Left: Hand sample of undeformed (Devonian?) quartz diorite (Ddi). **Center:** Cliff face of leucopegmatite that includes rafts and wispy bands of the Rangeley Fm. **Right:** Outcrop of leucopegmatite with 1-cm garnet.

Left: Strongly foliated Hardwick Fm. with feldspar porphyroclasts in a fine grained mica + qtz matrix. **Center:** Medium grained, undeformed Hardwick Fm. **Right:** Foliated and refolded Hardwick with folded leucosomes on horizontal face of outcrop next to Carter Rd.

Left: Outcrop of Monson Gneiss with 10-cm, amphibolite layers. **Right:** An example of strongly interlayered Monson Gneiss and amphibolite.

Examples of two different fabrics that occur in the Monson amphibolite. **Left:** Moderate west-dipping foliation with parallel fractures "slabby amphibolite". **Right:** Strong mineral lineations in the Monson amphibolite defined by hbl orientation and feldspar streaks.

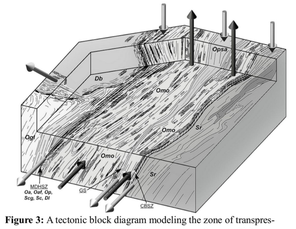

Figure 3: A tectonic block diagram modeling the zone of transpression and extrusion studied in the Palmer area, south-central Massachusetts from Massey and Moecher, (2008).

Regional Context

Part of the study was a comparison of the tectonic history of the map area with that of other quadrangles that have been studied nearby. Quadrangles along strike of the Bronson Hill-Central Maine Zone boundary such as the Palmer quadrangle show evidence for a zone of transpression and extrusion (Fig. 3) in which the Monson orthogneiss is simultaneously flattened and extruded upward and to the north while opposite sense, lateral simple shear is accommodated by two bounding zones of high strain, the Mount Dumplin High Strain Zone to the West and the Connant Brook Shear Zone to the East.

SUMMARY

The western half of the Petersham quadrangle records a tectonic history of strain partitioning between the Monson and Hardwick orthogneiss masses and the Rangeley metasedimentary unit of the Central Maine Trough. The Rangeley Fm. records north-south elongation and constriction recorded in subhorizotnal north- to south-trending mineral lineations and complex folding patterns respectively. The Hardwick and especially the Monson orthogneisses record primarily flattening strain via mildly to moderately west-dipping foliation. A subhorizontal north to south trending mineral lineation is also recorded in the Monson amphibolite.

The Devonian? quartz diorite instrusive sheet shows virtually no deformation in spite of the fact that this age would place its intrusion during Acadian orogenesis. Thus, it is proposed that this intrusive body is likely much younger than it has been suggested.

The outcrop next to Carter Rd. displays sinistral east to north asymmetries in horizontal exposures suggesting that the pattern of deformation demonstrated in the Palmer area may be repeated to the east, centered around the Hardwick Fm.

REFERENCE:

Massey, M.A., 2010, transpression, deformation partitioning, and extrusion in the Appalachian orogen, southern New England, U.S.A.: Ph.D. dissertation, University of Kentucky.